

Investigations on Ultra-Wideband (UWB) Monopole Antennas for Spectrum Monitoring

A Thesis Submitted to
Nirma University
In Partial Fulfilment of the Requirements for
the Degree of
Doctor of Philosophy
in
Technology & Engineering

By
Ravindra Kumar Singh
(14EXTPHDE127)



Department of Electronics and Communication Engineering,
Institute of Technology, Nirma University,
Ahmedabad, Gujarat, India

November 2018

Nirma University
Institute of Technology

CERTIFICATE

This is to certify that the thesis entitled 'Investigations on Ultra-Wideband (UWB) Monopole Antennas for Spectrum Monitoring' has been prepared by Mr. Ravindra Kumar Singh (14EXTPHDE127) under my supervision and guidance. The thesis is his own original work completed after careful research and investigation. The work of the thesis is of the standard expected of a candidate for the Ph.D. Programme in Electronics and Communication Engineering and I recommend that it be sent for evaluation.

Date: 12 NOV 18

Handwritten signature
12-11-2018

Signature of Guide

Forwarded through:

Handwritten signature

(i) Head, Electronics and Communication Engineering Department

Handwritten signature

(ii) Dean, Faculty of Technology and Engineering

Handwritten signature

(iii) Dean, Faculty of Doctoral Studies and Research

To:

Handwritten signature
Executive Registrar,
Nirma University

Nirma University
Institute of Technology
DECLARATION

I, Ravindra Kumar Singh, registered as Research Scholar, bearing Registration No. 14EXTPHDE127 for Doctoral Programme under the Faculty of Technology and Engineering of Nirma University do hereby declare that I have completed the course work, pre-synopsis seminar and my research work as prescribed under R. Ph.D. 3.5.

I do hereby declare that the thesis submitted is original and is the outcome of the independent investigations / research carried out by me and contains no plagiarism. The research is leading to the discovery of techniques. This work has not been submitted to any other University or body in quest of a degree, diploma or any other kind of academic award.

I do hereby further declare that the text, diagrams or any other material taken from other sources (including but not limited to books, journals and web) have been acknowledged, referred and cited to the best of my knowledge and understanding.

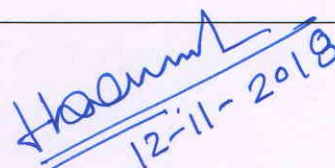
Date: 12 Nov 2018



Ravindra Kumar Singh
14 EXTPHDE127

I endorse the above declaration made by the student.

Date: 12 Nov 2018


12-11-2018

Dr. Dhaval Pujara
Guide

ACKNOWLEDGMENTS

First and the foremost, I thank the almighty GOD who has given me good health and ample blessings to complete my doctoral studies.

It is my profound privilege to express sense of gratitude to my guide Prof. Dhaval Pujara for his constant guidance, inspiration and encouragement throughout this research work and for their critical reviews during the compilation of this thesis. Without their valuable support, I could not have envisaged the successful completion of the thesis. The guidance provided by him has helped me in understanding the subject and associated research elements.

My sincere thanks to my research progress committee members Dr. S. K. Pathak, Institute of Plasma Research (IPR), Gandhinagar and Dr. K. K. Sood, Space Applications Centre (ISRO), Ahmedabad for providing valuable and rewarding feedback throughout my research work.

My Sincere thanks to Dr. S.V.Kulkarni, Scientist-SG, IPR, Gandhinagar, for helping me to carry out measurements of all proto type fabricated antennas during my Ph.D. work.

I would also thankful Dr. Alka Mahajan, Director, Institute of Technology, Nirma University for her support and cooperation.

I wish to express my sincere gratitude to Nirma University and Institute of Technology, Nirma University for allowing me to join Ph.D. programme and providing support during my doctoral studies.

It is a great pleasure to acknowledge the constant support and encouragement from my wife Dr. Rinku Singh and my brother Prof. H.K. Singh, BHU Varansi for their consistent

support and motivation at every stage during my research work. I am much indebted to my daughter “Rhythm” and son “Raunak” for their patience and endless love and support to me during this research work.

Thank you one and all for encouraging and motivating me.

Ravindra Kumar Singh

(14EXTPHDE127)

ABSTRACT

Electro Magnetic Spectrum (EMS) is a precious natural resource that is getting consumed fast and every Hertz of frequency is being grabbed. Recycling, harmonisation and allotment of whatever is left has become a management challenge for regulatory bodies around the world. Spectrum monitoring is a vital part of spectrum management to keep a check on interference, EIRP compliance and proper utilisation of this limited resource.

Effective spectrum monitoring requires sophisticated equipment like Automated Frequency Management System (AFMS). The acquisition of AFMS is difficult to most of the developing countries due to the high cost and non-availability of technology. Thus, there is a compelling need to design an UWB antenna, light in weight with moderate gain to match up with commonly available spectrum analysers, to detect and monitor frequency spectrum.

Microstrip antennas were first conceptualised by Deschamps in 1953 before Munson and Howell practically demonstrated it in 1970s. A microstrip patch antenna is fabricated by etching the antenna element pattern in metal trace, bonded to an insulating dielectric substrate with radiating elements and the feeding mechanism. A single UWB antenna would also avoid the requirement of deploying multiple antennas for the spectrum range. The onerous task of spectrum management can thus be facilitated to a great extent by the proposed single UWB microstrip antenna.

The design feasibility of a microstrip patch antenna capable of operating from a few GHz to 40 GHz and above, with omni-directional radiation patterns and moderate gain to utilise it for spectrum management was explored. Ten (10) different UWB microstrip monopole patch antennas with different radiating patch shapes and sizes have been studied using the finite-element method (FEM) based high-frequency simulation software –HFSS V13. All the designs have been simulated and specially optimised for compact size and maximum bandwidth using the HFSS. While the ideal omni-directional monopole characteristics were recorded at lower frequencies of the spectrum, the radiation patterns gradually become directional at the higher frequencies (size of antenna becomes large relative to

wavelength). Different techniques to improve the bandwidth have been used. These include, change in shapes of a radiating patch, multi-stepped feed network, narrow slot of different shapes into the radiating patch of an antenna and ground plane below the feed network. Comparative performance of the CPW-fed patch antenna and microstrip feed patch antenna was examined in terms of the bandwidth and the radiation patterns at high frequencies. The CPW-fed antenna performed better at higher frequencies despite limitations in copper-etching accuracy.

Simulations were validated with actual measurements recorded. Variations in recorded measurements are attributable to the factors such as manufacturing tolerances, undercuts while etching copper at sharp corners, effect of SMA connector at different frequencies and the limitations of the simulation software. Research work carried out during the Ph.D. course has been presented in total of five chapters.

Chapter 1 covers the objectives with a brief description of the thesis content. The literature survey carried out on design of printed monopole antennas with emphasis on achieving higher bandwidth has been laid out.

Chapter 2 deals with the simulation and design of printed antennas operating up to 20 GHz covering the entire FCC-authorized frequency band. The simulated and measured return-loss and parametric analysis of the antennas under consideration are discussed in this chapter.

Chapter 3 presents the design and development of printed monopole antennas able to operate satisfactorily from 3 to 30 GHz. In this chapter, design methodology, simulation and parametric analysis are discussed. Simulated and experimental results of a few prototype antennas are recorded.

Chapter 4 elaborates the design of a few ultra-wideband printed antennas suitable for spectrum monitoring from 3 to 40 GHz and beyond along with recorded parameters.

Chapter 5 concludes the investigation and research findings of the design of UWB antennas. It also outlines the scope for future research in this domain.

CONTENTS

ACKNOWLEDGMENTS	III
ABSTRACT	V
LIST OF FIGURES	XII
LIST OF TABLES	XVII
LIST OF ABBREVIATIONS.....	XVIII
PUBLICATIONS / PRESENTATIONS RELATED TO THE THESIS WORK.....	XIX

CHAPTER-1: Introduction and Literature Review 1

1.1 Background.....	1
1.2 Spectrum Monitoring.....	2
1.3 UWB Antennas	4
1.4 Feasibility Study of the Microstrip Monopole for Spectrum Monitoring	4
1.5 Early Works on Patch Antennas	5
1.6 Literature Survey	6
1.7 Problem Statement.....	13
1.8 Organization of the Thesis.....	14
1.9 Summary.....	15

CHAPTER-2: UWB Patch Antennas–Class I 17

2.1 Rectangular Printed Monopole Antenna-1	17
2.1.1 Design of the Proposed UWB Patch Antenna-1	18
2.1.2 Return-Loss Performance of UWB Antenna-1	19
2.1.3 Parametric Study of the Proposed UWB Antenna-1	19

2.1.4	Radiation Patterns of the Proposed UWB Antenna-1	24
2.2	Hexagonal and Circular-Shaped Printed Monopole Antenna-2	25
2.2.1	Design of the Proposed UWB Patch Antenna-2	25
2.2.2	Return-Loss Performance of the UWB Antenna-2	27
2.2.3	Parametric Study of the Proposed UWB Antenna-2	27
2.2.4	Radiation Patterns of the Proposed UWB Antenna-2	30
2.3	Quarter Circular Printed Monopole Antenna-3	31
2.3.1	Design of the Proposed UWB Patch Antenna-3	31
2.3.2	Return-Loss Performance of the UWB Antenna-3	32
2.3.3	Parametric Study of the Proposed UWB Antenna -3	33
2.3.4	Radiation Patterns of the Proposed UWB Antenna-3	36
2.4	Goblet-Shaped Printed Monopole Antenna-4	37
2.4.1	Design of the Proposed UWB Patch Antenna-4	37
2.4.2	Return-Loss Performance of the UWB Antenna-4	39
2.4.3	Parametric Study of the Proposed UWB Antenna-4	39
2.4.4	Radiation Patterns of the Proposed UWB Antenna-4	43
2.5	Summary	44
 CHAPTER-3: UWB Patch Antennas –Class II.....		45
3.1	Truncated Circular Printed Monopole Antenna-5	45
3.1.1	Design of the Proposed UWB Patch Antenna-5	45
3.1.2	Return-Loss Performance of the UWB Antenna-5	47
3.1.3	Parametric Study of the Proposed UWB Antenna-5	47
3.1.4	Radiation Patterns of the Proposed UWB Antenna-5	51
3.2	CPW-Fed Truncated Circular-Shaped Printed Monopole Antenna-6	52
3.2.1	Design of the Proposed UWB Patch Antenna-6	53

3.2.2	Return-Loss Performance of the UWB Antenna-6.....	54
3.2.3	Parametric Study of the Proposed UWB Antenna-6	55
3.2.4	Radiation Patterns of the Proposed UWB Antenna-6.....	57
3.3	Summary.....	59
 CHAPTER-4: UWB Patch Antennas –Class III		61
4.1	Tri-Circular Printed Monopole Antenna-7	61
4.1.1	Design of the Proposed UWB Patch Antenna-7	61
4.1.2.	Return-Loss Performance of the UWB Antenna-7	63
4.1.3	Parametric Study of the Proposed UWB Antenna-7	63
4.1.4	Radiation Patterns of the Proposed UWB Antenna-7.....	66
4.2	Circular Printed Monopole Antenna-8	68
4.2.1	Design of the Proposed UWB Patch Antenna-8A.....	68
4.2.2	Layout of a Stepped Circular Monopole with a Notch in Ground Plane (Antenna-8B)	70
4.2.3	Stepped Circular Monopole with a Notch in Ground Plane and Slot in Radiating Patch (Antenna-8C).....	72
4.3	Truncated Annular Printed Monopole Antenna-9	76
4.3.1	Design of the Proposed UWB Patch Antenna-9.....	77
4.3.2	Return-Loss Performance of the UWB Antenna-9.....	78
4.3.3	Parametric Study of the Proposed UWB Antenna-9	79
4.3.4	Radiation Patterns of the Proposed UWB Antenna-9.....	83
4.4	Elliptical Shape Printed Monopole Antenna-10.....	84
4.4.1	Design of the Proposed UWB Patch Antenna-10.....	84
4.4.2	Return-loss performance of the UWB antenna-10	85
4.4.3.	Parametric Study of the Proposed UWB Antenna-10	86

4.4.4 Radiation Pattern of the Proposed UWB Antenna-10	88
4.5. Summary.....	89
 CHAPTER-5: Summary and Scope of Future Work	91
5.1 Summary and Conclusion.....	91
5.2 Future Scope of Works	94
 References... ..	97

LIST OF FIGURES

Fig. 2. 1	Design of the proposed UWB antenna-1 under consideration.....	18
Fig. 2. 2	Return-loss performance of the proposed UWB antenna-1.	19
Fig. 2. 3	Effect of change in substrate material on the return-loss performance of the proposed UWB antenna-1.	20
Fig. 2. 4	Effect of change in patch dimension (l_1) on the return-loss performance of the proposed UWB antenna-1.	21
Fig. 2. 5	Effect of change in patch dimension (w_1) on the return-loss performance of the proposed UWB antenna-1.	21
Fig. 2. 6	Effect of change in length (l_g) of the ground plane on the return-loss performance of the proposed UWB antenna-1.	22
Fig. 2. 7	Effect of change in the notch dimension (l_2) of the ground plane on the return-loss performance of the proposed UWB antenna-1.....	23
Fig. 2. 8	Effect of change in the notch dimensions (w_2) of the ground plane on the return-loss performance of the proposed UWB antenna-1.....	23
Fig. 2. 9	Radiation patterns of the proposed UWB antenna-1.....	24
Fig. 2.10	Peak Gain of the proposed UWB antenna-1.	24
Fig. 2. 11	Layout of the proposed UWB antenna-2 under consideration.....	25
Fig. 2. 12	Photograph of the proposed UWB antenna-2 under consideration.....	26
Fig. 2. 13	Measured and simulated return-loss performance of the proposed UWB antenna-2.	27
Fig. 2. 14	Effect of change in substrate material on the return-loss performance of the proposed UWB antenna-2.	28
Fig. 2. 15	Effect of change in feed width dimension (w_f) on the return-loss performance of the proposed UWB antenna-2.	29
Fig. 2. 16	Effect of change in length (l_g) of the ground plane on the return-loss performance of the proposed UWB antenna-2.....	30
Fig. 2. 17	Radiation patterns of the proposed UWB antenna-2.....	30
Fig. 2. 18	Variations in peak gain for the proposed UWB antenna-2.	31
Fig. 2. 19	Design of the proposed UWB antenna-3 under consideration	32

Fig. 2. 20	Measured and simulated return-loss performance of the proposed UWB antenna-3.	33
Fig. 2. 21	Effect of change in substrate material on the return-loss performance of the proposed UWB antenna-3.	34
Fig. 2. 22	Effect of change in length (l_g) of the ground plane on the return-loss performance of the proposed UWB antenna-3.	35
Fig. 2. 23	Effect of change in feed width dimension (w_f) on the return-loss performance of the proposed UWB antenna-3.	35
Fig. 2. 24	Radiation patterns of the proposed UWB antenna-3.....	36
Fig. 2. 25	Peak gain of the proposed UWB antenna-3.	37
Fig. 2. 26	Design of the proposed UWB antenna-4 under consideration	38
Fig. 2. 27	Measured and simulated return-loss performance of the proposed UWB antenna-4.	39
Fig. 2. 28	Effect of change in substrate material on the return-loss performance of the proposed UWB antenna-4.	40
Fig. 2. 29	Effect of change in length (l_g) of the ground plane on the return-loss performance of the proposed UWB antenna-4.	41
Fig. 2. 30	Effect of change in patch dimension (r_1) on the return-loss performance of the proposed UWB antenna-4.	42
Fig. 2. 31	Effect of change in slot dimension (r_2) on the return-loss performance of the proposed UWB antenna-4.	42
Fig. 2. 32	Radiation patterns of the proposed UWB antenna-4.....	43
Fig. 2. 33	Peak gain of the proposed UWB antenna-4.	43
Fig. 3. 1	Layout of the proposed UWB antenna-5 under consideration.	46
Fig. 3. 2	Return-loss performance of the proposed UWB antenna-5.	47
Fig. 3. 3	Effect of change in the substrate material on return-loss performance on the proposed UWB antenna-5.	48
Fig. 3. 4	Effect of change in the patch dimension (r_1) on the return-loss performance of the proposed UWB antenna-5.	49
Fig. 3. 5	Effect of change in the main feed width (w_f) on the return-loss performance of the proposed UWB antenna-5.	50

Fig. 3. 6	Effect of change in length (l_g) of the ground plane on the return-loss performance of the proposed UWB antenna-5.	50
Fig. 3. 7	Radiation patterns of the proposed UWB antenna-5.	51
Fig. 3. 8	Peak gain of the proposed UWB antenna-5.	52
Fig. 3. 9	Layout of the proposed UWB antenna-6 under consideration.	53
Fig. 3. 10	Simulated and measured return-loss performance of the proposed UWB antenna-6.	54
Fig. 3. 11	Effect of change in the substrate material on the return-loss performance of the proposed UWB antenna-6.	55
Fig. 3. 12	Effect of change in feed gap (g) on the return-loss performance of the proposed UWB antenna-6.	56
Fig. 3. 13	Effect of change in the length (l_g) of the ground plane on the return-loss performance of the proposed UWB antenna-6.	57
Fig. 3. 14	Radiation patterns of proposed UWB antenna-6.	58
Fig. 3. 15	Peak gain of the proposed UWB antenna-6.	58
Fig. 4.1	Design of the proposed UWB antenna-7 under consideration.	62
Fig. 4.2	Return-loss Performance of the Proposed UWB Antenna-7.	63
Fig. 4.3	Effect of change in substrate material on the return-loss performance of the proposed UWB antenna-7.	64
Fig. 4.4	Effect of change in patch dimension (r_1) on the return-loss performance of the proposed UWB antenna-7.	65
Fig. 4.5	Effect of change in patch dimension (r_2) on the return-loss performance of the proposed UWB antenna-7.	65
Fig. 4.6	Effect of change in length (l_g) of the ground plane on the return-loss performance of the proposed UWB antenna-7.	66
Fig. 4.7	Radiation patterns of the proposed UWB antenna-7.	67
Fig. 4.8	Peak gain of the proposed UWB antenna-7.	68
Fig. 4.9	Layout of the proposed UWB antenna-8A under consideration.	69
Fig. 4.10	Simulated return-loss performance of the proposed UWB antenna-8A.	70
Fig. 4.11	Layout of the proposed UWB antenna-8B under consideration with stepped feedline and notch in the ground plane.	71

Fig. 4.12	Simulated return-loss performance of the proposed UWB antenna-8B.....	71
Fig. 4.13	Layout of the proposed UWB antenna-8C under consideration with stepped feedline, notch in the ground plane and slot in the radiating patch.....	72
Fig. 4.14	Measured and simulated return-loss performance of the proposed UWB antenna-8C.....	73
Fig. 4.15	Effect of change in feed width dimension (w_f) on the return-loss performance of the proposed UWB antenna-8C.....	74
Fig. 4.16	Effect of ground height (l_g) on the antenna performance. of the proposed UWB antenna-8C.....	74
Fig. 4.17	Radiation patterns of the proposed UWB antenna-8C	75
Fig. 4.18	Peak gain of the proposed UWB antenna-8C.....	76
Fig. 4.19	Design of the proposed UWB antenna-9 under consideration.	77
Fig. 4.20	Return-loss performance of the proposed UWB antenna-9.	78
Fig. 4.21	Effect of change in patch dimension (r_1) on the return-loss performance of the proposed UWB antenna-9.	80
Fig. 4.22	Effect of change in patch dimension (r_2) on the return-loss performance of the proposed UWB antenna-9.	80
Fig. 4.23	Effect of change in patch dimension (r_3) on the return-loss performance of the proposed UWB antenna-9.	81
Fig. 4.24	Effect of change in length (l_g) of the ground plane on the return-loss performance of the proposed UWB antenna-9	82
Fig. 4.25	Effect of change in feed width (w_f) on the return-loss performance of the proposed UWB antenna-9.....	82
Fig. 4.26	Radiation patterns of the proposed UWB antenna-9.....	83
Fig. 4.27	Peak gain of the proposed UWB antenna-9.	83
Fig. 4.28	Design of the proposed UWB antenna-10 under consideration.	84
Fig. 4.29	Return-loss performance of the proposed UWB antenna-10.	85
Fig. 4.30	Effect of change in the substrate material on the return-loss performance of the proposed UWB antenna-10.	86
Fig. 4.31	Effect of change in major axis (a) on the return-loss performance of the proposed UWB antenna-10.....	87

Fig. 4.32	Effect of change in length (l_g) of the ground plane on the return-loss performance of the proposed UWB antenna-10.	88
Fig. 4.33	Radiation patterns of the proposed UWB antenna-10.....	88
Fig. 4.34	Peak gain of the proposed UWB antenna-10.	89

LIST OF TABLES

Table 2.1	Design Parameters of UWB Antenna-1	18
Table 2.2	Design Parameters of UWB Antenna-2	26
Table 2.3	Design Parameters of UWB Antenna-3	26
Table 2.4	Design Parameters of UWB Antenna-4	32
Table 2.5	Summary of the Proto Type Patch Antennas: Class I	44
Table 3.1	Design Parameters of UWB antenna-1	46
Table 3.2	Design Parameters of UWB Antenna-2	54
Table 3.3	Summary of the Proto Type Patch Antennas: Class II	59
Table 4.1	Design Parameters of UWB Antenna-1	62
Table 4.2	Design Parameters of UWB Antenna-2A	69
Table 4.3	Design Parameters of UWB Antenna-3	78
Table 4.4	Design Parameters of UWB Antenna-4	85
Table 4.5	Summary of the Proto Type Patch Antennas: Class III	90
Table 5.1	Summary of the Proposed Microstrip Monopole UWB Patch Antennas	92

LIST OF ABBREVIATIONS

AFMS	Automated Frequency Management System
BW	Bandwidth
CPW	Co-Planar Waveguide
dB	Decibel
dBi	Decibel Isotropic
EIRP	Equivalent Isotropically Radiated Power
EMI	Electro-Magnetic Interference
EMC	Electro-Magnetic Compatibility
EMS	Electro-Magnetic Spectrum
ESM	Electronic Support Measures
FCC	Federal Communications Commission
FR-4	Flame Retardant-4
GHz	Giga Hertz
HFSS	High Frequency Simulation Software
MoC	Ministry of Communications
ITU	International Telecommunication Union
RADAR	Radio Detection and Ranging
RF	Radio Frequency
SMA	Sub Miniature Version A
S/N	Signal to Noise
UWB	Ultra-Wide Band
VSWR	Voltage Standing Wave Ratio
WPC	Wireless Planning Commission

PUBLICATIONS / PRESENTATIONS RELATED TO THE THESIS WORK

- [1]. Singh, R. K. and Dhaval A. Pujara. “A Novel Design of Ultra-wideband Quarter Circular Microstrip Monopole Antenna.” *Microw. Opt. Technol. Lett.* 59.2 (2016): 225-29.
- [2] Singh, R. K. and Dhaval A. Pujara. “Design of an UWB (2.1–38.6 GHz) Circular Microstrip Aantenna.” *Microw. Opt. Technol. Lett.* 59 (2017): 2757-62.
- [3] Singh, R. K. and Dhaval A. Pujara. “Design and Development of UWB (3.0–42.8 GHz) Truncated Annular Microstrip Monopole Antenna.” *Microw. Opt. Technol. Lett.* 60 (2018): 1581-84.
- [4] Singh, R. K. and Dhaval A. Pujara. “Design of Goblet Shape UWB Microstrip Monopole Antenna.” *Proceedings of International Symposium on Antennas and Propagation (APSYM 2016)*. 179-182.
- [5] Singh, R. K. and Dhaval A. Pujara. “A Novel Circular Ultra-Wide Band Microstrip Antenna Design using Slots, Stepped Microstrip Feed and Partial Ground.” *International Symposium on Antennas and Propagation (APSYM 2016)*. 15-17 Dec 2016, Cochin, India.

INTRODUCTION AND LITERATURE REVIEW

The primary objective of this chapter is to discuss the requirements of an Ultra-Wide Band (UWB) patch antenna for spectrum monitoring application. Literature on compact UWB patch antennas has been thoroughly surveyed. The major research areas in the field of patch antennas and the corresponding challenges, scope for new research, etc. are discussed in this chapter. A feasibility study was also conducted to understand whether a compact size patch antenna will be able to detect unknown signals up to 200 km. The outline of the thesis and its organisation are presented towards the end of the chapter.

1.1 Background

Electro Magnetic Spectrum (EMS) is a precious natural resource that is fast getting consumed and every Hertz of frequency is being grabbed. The trend is likely to continue in future too. However, several challenges are encountered in the field due to liberalisation in the telecommunications field globally. Due to new market entrants along with existing competitive wireless operators, the assignment of EM spectrum to a particular service and ensuring interference-free operations to spectrum users is a difficult task.

Proper utilisation of the EMS can increase efficiency and productivity of a nation's work force and improve their quality of life. Various uses of the RF spectrum include personal and corporate communications, radio navigation, aeronautical and maritime radio, broadcasting, public safety and distress operations, radio location, amateur radio, etc.

To avoid interference, the allotment of the spectrum needs to be well coordinated. Two radio-communication devices operating at the same time and frequency in close locations will interfere with the receivers. As the uses of wireless applications are wide and varied, it is crucial to ensure that the spectrum is efficiently and effectively managed to optimally benefit the society and the economy.

1.2 Spectrum Monitoring

Spectrum monitoring is one of the key processes in spectrum management, besides spectrum planning and licensing. It deals with:

- Proper utilisation of the licensed parameters, like bandwidth and field strength
- Identifies illegal uses of the spectrum
- Electromagnetic Interference/Electromagnetic Compatibility (EMI/EMC) compliance
- Equivalent Isotropically Radiated Power (EIRP) compliance
- Analysis of interference
- Immunity tests
- High-power microwave detection
- Health-related testing
- Detecting white spaces, etc.

Thus, the overall aim of spectrum monitoring is to support proper functioning of the spectrum management process. The core objectives of spectrum management are:

- Estimate the spectrum efficiency in determining the planned and actual frequency usage and its occupancy,
- Assess the availability of spectrum for future uses,
- Ensure compliance with the existing spectrum regulations and maximise the benefit of the spectrum resource to the society by resolving interference problems for existing and potential users.

Frequency planning and licensing provide the theoretical occupancy of spectrum, while monitoring provides its actual utilisation. The difference between theoretical and real occupancy should be as small as possible for better quality of overall spectrum management process (Pozar, 1987).

Globally, the radio spectrum is being regulated by the International Telecommunication Union (ITU). The ITU Radio Regulations form the international framework within which member nations allocate and manage spectrum at a more detailed level (Spectrum

Monitoring and Compliance, 2017). India is also a member of the ITU. As a signatory to the ITU Constitution and Convention, India has the obligation to ensure that the spectrum management activities comply with its regulations.

Spectrum management in India is the responsibility of the Wireless Planning Commission (WPC), a branch of the Ministry of Communications (MoC). The MoC routinely monitors frequency and traces unauthorised transmissions. When a radio service is licensed, the WPC conducts radio monitoring to ensure that the licensee complies with the licensed operating conditions in terms of RF output power, modulation, frequency accuracy, etc. The spectrum managers need to work in the two following scenarios:

Scenario 1: Prior information on emitters like approximate frequency, modulation and transmitted power, etc. are to be ascertained by tracking or testing. In this case, the traditional spectrum analysis techniques and equipment can be used to monitor the signal in a limited band.

Scenario 2: There is no prior knowledge about the emitters and hence complete frequency scan is made in the band of interest.

The equipment required to monitor the RF spectrum include spectrum analysers, radio receivers, direction-finding equipment and antenna designed to operate in a band of interest. Presently, highly sophisticated Automated Frequency Management System (AFMS) and Electronic Support Measures (ESM) receivers are available that can scan frequencies ranging from a few KHz up to 40 GHz (R&S®ESMD Wideband Monitoring Receiver, 2017). Designing such receivers is very challenging due to stringent requirements and specifications.

For any ESM receiver, the antenna is a key element. The antenna is linked to either radio receivers or signal generators of direction-finding equipment to detect or monitor any interfering signal. For this purpose, several antennas are needed for different applications and bands ranging from a few MHz to 40 GHz. In many cases, it is essential to design

compact antennas having bandwidth of the order of a few octaves to several decades. Only the UWB antennas can satisfy the requirements of such high bandwidth.

1.3 UWB Antennas

The UWB antenna is not a new concept and it has been in commercial use since the invention of the AM Radio. However, over the last three decades, many researchers have worked on it. Most of the UWB-designed antennas are in the operating range of a few MHz to 3 GHz, as most of the wireless products operate in this range. In the open literature, many microstrip patch antenna geometries are reported covering the FCC authorised band from 3.1 to 10.6 GHz.

Amongst the various UWB antenna configurations, the planar microstrip monopole antenna (printed/patch) has been the preferred choice due to its attractive features like light weight, low volume, thin profile configuration, multiband operations, etc. However, microstrip antennas suffer from limitations such as narrow impedance bandwidth (typically around 2–5%) and low power-handling capability. However, comparatively the microstrip monopole configuration has a capability to operate with very large bandwidth (Kumar and Ray, 2003). Thus, it was decided to study the feasibility of the microstrip monopole antenna for spectrum monitoring application.

1.4 Feasibility Study of the Microstrip Monopole for Spectrum Monitoring

A Spectrum Monitoring Receiver will receive any intentional/unintentional signal transmitted by any of the RF systems. If P_t is peak transmitted power by the source and antenna gain of transmitting antenna is G_t , then at a distance of R , the power density will be

$$U_t = \frac{P_t G_t}{4\pi R^2} \text{-----} (1.1)$$

In a worst-case scenario, let the receiver antenna is an isotropic with cross-section area A_e , then the received power (P_r) will be

$$P_r = \frac{P_t G_t}{4\pi R^2} A_e \text{-----} (1.2)$$

Let the transmitter be transmitting with peak power of the order of 10 watts with an isotropic antenna (worst case with unity gain). Let the receiver antenna design be with the physical area of $40 \times 30 \text{ mm}^2$. In this case, at distance of 200 km, $Pr = 2.388 \times 10^{-14} \text{ Watt}$ or $Pr = -106 \text{ dBm}$.

Commercial-grade low-noise RF amplifiers are available with sensitivity better than -110 dBm. Hence, an antenna with $40 \times 30 \text{ mm}^2$ physical size with unity gain is also sufficient to detect any RF signal in 200 km radius. Based on this study, it can be concluded that for spectrum-monitoring application, a small-sized antenna even with unity gain will be sufficient. However, it should offer ultra-wide bandwidth.

1.5 Early Works on Patch Antennas

Deschamps was the first to propose the concept of microstrip antenna in 1953, while Gutton and Baissinot patented it in France in 1955 (Deschamps, 1953; Gutton and Baissinot, 1955). Munson and Howell were the first to practically develop and demonstrate it and it happened only in 1970s (Munson, 1974; Howell, 1974). Since then, the researchers have been engaged in reducing the size of the antenna and improve its performance in terms of bandwidth, gain and radiation patterns. A microstrip antenna consists of four essential parts:

- a main radiating patch of very thin flat metallic region
- a thin dielectric substrate
- a ground plane, usually much larger than the patch, and
- a feed network to pump the power from source (Richards, 1998)

A microstrip patch antenna is fabricated by etching the antenna element in metal trace, bonded to an insulating dielectric substrate such as a printed circuit board with a continuous metal layer bonded to the opposite side of the substrate which forms a ground plane. Its performance is highly dependent on the shape and size of the radiating patch and ground plane, substrate permittivity and feed techniques. Common microstrip antenna shapes are square, rectangular, circular and elliptical, but any continuous shape is possible. Most of the time, radiating elements and the feeding mechanism are etched together on the substrate

(Garg, 2001). The direction of maximum radiation is found to be normal to the plane of the antenna.

The typical size of the radiating patch is about half free space wavelength, while the thickness of the substrate is about 0.002 to $0.005 \lambda_o$ (λ_o is free space wavelength). The dielectric permittivity used for the microstrip antenna is usually in the range of 2 to 12. As the dielectric constant of the substrate increases, the antenna bandwidth decreases which increases the quality factor of the antenna and therefore decreases the impedance bandwidth. The same is verified using the cavity model by Lo in the late 1970s (Lo, 1979). To achieve low dielectric constant, sometimes a low-density honeycomb material is also used as substrate material which provides dielectric constant much closer to unity, better efficiency and higher bandwidth (James, Hall and Wood, 2015).

It is known fact that low dielectric constant material patch antenna provides better bandwidth. Hence a microstrip monopole antenna can be considered as a microstrip antenna with lower value of the dielectric constants (approximately equal to one) along with moderately thick substrate, leading to improvement of the bandwidth. Also, various higher-order modes will get excited in the radiating metallic patch contributing to a large bandwidth and the antenna will undergo a smaller impedance variation. By optimising the shape and size, various modes can be excited to bring these within the $VSWR \leq 2$, leading to very large impedance bandwidth (Kumar and Ray, 2003).

1.6 Literature Survey

This section presents the literature survey on the UWB patch antennas. Interesting UWB designs and the corresponding results are highlighted.

UWB Patch Antennas

In 1997, Wong and Lin carried out the design and simulation of a small broadband rectangular microstrip antenna with 1Ω chip-resistor using a probe feed and an inset microstrip-line feed (Wong and Lin, 1997). A large reduction was achieved in size for a given frequency (710 MHz) and wide antenna bandwidth (9.3%) as compared to a normal

rectangular microstrip antenna. However, due to the insertion of a chip resistance, a reduction in gain of 2dB was also reported.

In 1998, Herscovici investigated an aperture-coupled stacked patch antenna for wide bandwidth (Herscovici, 1998). In this paper, a patch is suspended over a large ground plane, supported by a nonconductive pin and the antenna was fed by a three-dimensional transition connecting the patch to a perpendicular connector. Typical bandwidth of approximately 90% with front-to-back ratio better than 25dB across the band was reported.

In 2000, Wong and Hsu investigated a broadband patch antenna with a thick air or foam substrate having good radiation characteristics over a wide operating bandwidth (Wong and Hsu, 2000). They observed excitation of such broadband patch antennas through a probe feed. The bandwidth was typically limited to less than 10% due to longer probe generating large inductance in the thick substrate. To compensate these inductances, several slots were introduced to the radiating patch and investigations were carried out on a circular patch loaded with wide slits at the boundary of the radiating patch. Improved wide impedance bandwidth (26%) and good radiation characteristics for a U-slotted patch antenna were also reported

In 2001, Jang proposed a T-shaped aperture-coupled microstrip-fed, triangular patch antenna (Jang, 2001). The proposed antenna was physically smaller than the aperture-coupled rectangular patch antenna or microstrip slot antenna and achieved a 44.5% bandwidth for $VSWR \leq 2$.

In 2001, Anob, Ray and Kumar proposed the design of a wideband orthogonal square monopole antenna with semi-circular base operating from 1.4 to 7.5 GHz (137%) for VSWR less than 2 (Anob, Ray and Kumar, 2001). They have used two orthogonal square monopoles with a semi-circular base to achieve omni-directional radiation patterns over a wide bandwidth.

Wong and Tung, in 2003, presented a compact air-substrate patch antenna with an inverted U-shaped radiating patch (Wong and Tung, 2003). The patch was formed by adding two

downward rims at the two radiating edges of a planar rectangular or square patch. Due to the added rims, the surface current of the excited patch follows longer length, leading to lower resonant frequency and reduction in size ($>50\%$) and achieved a bandwidth of 9%.

Clasen and Langley presented a meshed patch antenna in 2004 in which both the patch and the ground plane were meshed (Clasen and Langley, 2004). Due to meshing, a reduction of 30% in resonant frequency was achieved.

In 2004, Mulgi, Vani and Hunagund presented a new design of a patch antenna using a parasitic patch along with main radiating patch and achieved an improvement of 22% in bandwidth with respect to the original design (Mulgi, Vani and Hunagund, 2004).

D'Assuncao, Cruz and Costa carried out theoretical analysis and experimental investigation on tapered microstrip patch antenna in 2006 (D'Assuncao, Cruz and Costa, 2006). They have designed and developed many prototype microstrip antennas. It was proved through measurement that tapered microstrip antennas without slots help in bandwidth improvement.

Ge, Esselle and Bird presented a compact E-shaped patch antenna in 2006 along with corrugated wings (Ge, Esselle and Bird, 2006). Approximately 25% reduction was reported in antenna size by introducing corrugations into the two side wings of the E-shaped patch. The antenna worked satisfactorily from 5 to 6 GHz.

In 2008, Kasabegoudar and Vinoy presented a wideband microstrip antenna with symmetric radiation patterns (Kasabegoudar and Vinoy, 2008). The antenna was designed with stacked air-dielectric substrate with only one metal layer above the ground plane. Approximately 50% impedance bandwidth was achieved with coplanar capacitive feeding. In 2009, Wu, Jin and Geng proposed two quasi-circular planar monopole antennas with rectangular and trapezoidal grounds (Wu, Jin and Geng 2009). They reported return-loss bandwidths of better than 10 dB from 1.3 to 18.4 GHz and 1.1 to 13.5 GHz, respectively. Simulated and experimental results proved that the antenna with trapezoidal ground has improved radiation compared to that with the rectangular ground.

In 2011, Koohestani, Moghadasi and Virdee designed a microstrip-fed planar monopole antenna operating satisfactorily in FCC-defined UWB frequency range (Koohestani, Moghadasi and Virdee, 2011). The radiating patch consisted of a dome-topped, bowl-shaped patch and a truncated ground plane. The ground plane was tapered in shape having a notch below the feedline. The antenna performance was found to be satisfactory within 10 dB return-loss, from 2.65 to 13 GHz frequencies (132% impedance bandwidth). The fabricated antenna was compact with $18 \times 20 \times 1.6 \text{ mm}^3$ size on FR4 substrate.

In 2014, Dikmen, Gonca and Sibel designed an ultra-wideband planar octagonal-shaped monopole antenna with reduced radar cross-section (Dikmen, Gonca and Sibel, 2014). It was modified using a geometrical shaping method to reduce the RCS in which metal areas having the minimum current distributions on the surface of printed antenna were removed. During testing, both the reference and modified octagonal-shaped antennas were reported operating from 2.5 to 18 GHz frequency band with 151% fractional bandwidth.

In 2015, Alsath and Kanagasabai proposed an UWB compact planar monopole antenna with modified ground plane suitable for modern automotive applications (Alsath and Kanagasabai, 2015). It was designed with hybrid geometry using a half-circular ring and a half-square ring. The ground plane of the fundamental radiator was curved and defected to improve the VSWR bandwidth from 3.1 to 10.9 GHz. An extended ground stub was used to further improve the bandwidth to cover the entire FCC approved frequency range. This antenna can be placed either inside the shark fin housing or printed along with the existing PCB electronics nullifying the need for dedicated location for in-car communications. Further, a simple two-port multiple input multiple output (MIMO) antenna was fabricated for diversity performance.

UWB Patch Antennas with Different Shapes and Slots

In 2004, Guo, Luk and Lee presented a broadband and dual-frequency shorted U-shaped microstrip antenna (Guo, Luk and Lee, 2004). The U-shaped patch has two different lengths to produce staggered resonant frequencies. The lower band frequency was controlled by the width of U-shaped slots, while the higher band frequency was controlled

by the length of a U-shaped slot. Wide impedance bandwidth (20%) was obtained for a given substrate material and thickness.

In 2005, Chair, Mak and Lee proposed half U and E slot antenna to miniaturise its size and achieve 20-30% antenna impedance bandwidth (Chair, Mak and Lee, 2005). This half-structure was tested by simulation and experimental studies and was found that in both the cases though the size of the antenna was reduced, performance was almost similar. It was reported that impedance bandwidths, radiation patterns, radiation efficiencies and gains of the half-structures are comparable to the corresponding full structures.

In 2005, Xiao, Wang and Shao proposed a novel design to improve the bandwidth and reduce the size of an ultra-low-profile patch antenna by using multiple slots (Xiao, Wang and Shao, 2005). Two right-angled slots with an additional U-shaped slot were used near non-radiating patch and two resonant modes, TM_{10} and TM_{01} , were excited at very close frequencies leading to bandwidth enhancement. The compact size was obtained by utilising the slot-loading technique. Since most of the patch current of the two modes was flowing in the same direction, similar radiation characteristics were observed at two resonance frequencies.

In 2006, Kim and Park proposed an UWB microstrip monopole antenna operating from 3 to 17 GHz with a notch band from 5.15 to 5.825 GHz. A parasitic element behind the main radiating patch was used to achieve wide bandwidth (Kim and Park, 2006). The size of this antenna was $20 \times 20 \text{ mm}^2$ and fabricated on an FR4 substrate. This paper has established the fact that a parasitic strip at the back side can be used for good impedance matching as well as the notched band.

In 2008, Wong and Sze carried out a simulation and experimental study of a rectangular microstrip antenna loaded with a pair of right-angled slots and a modified U-shaped slot (Wong and Sze, 2008). With right-angled slots and modified U-shaped slot, bandwidth enhancements as large as 2.4 times that of a corresponding un-slotted rectangular microstrip antenna with good radiating characteristics were achieved.

In 2008, Ahmed and Sebak proposed a printed monopole antenna with two steps and a circular slot for ultra-wideband applications (Ahmed and Sebak, 2008). The main radiating patch consisted of a half-circular disc and a rectangular patch fed by $50\ \Omega$ microstrip line. The antenna was manufactured on RT/duroid 5880 substrate of size 41×50^2 mm. Bandwidth from 3 to 11.4 GHz for return-loss better than 10dB was reported.

In 2010, Singh, Gupta and Sarkar proposed a single-layer single-feed rectangular patch antenna with different sized cross slots and were able to achieve hexa, penta, quad, and tri-frequency bands (Singh, Gupta and Sarkar, 2010). The antenna was realised using air/foam substrate and had achieved a bandwidth of 1.1 to 3.8 GHz.

In 2010, Zhang, Yin and Ma proposed a racket-shaped slot ultra-wideband microstrip antenna coupled with two parasitic strips for band-notched application (Zhang, Yin and Ma, 2010). By utilising two parasitic rectangular strips at the bottom of the substrate, a band notched characteristic was achieved. By adjusting the length and width of these two strips and the distance between them, a band-rejected filter characteristic at the WLAN frequency band of 5.15–5.825 GHz was achieved. Ultra-wide impedance BW from 3.1 to 10.6 GHz for $VSWR \leq 2$ except for the designed band notch at 5.15-5.825 GHz was reported.

In 2011, Liu, Cheung and Azim proposed a compact circular ring monopole microstrip antenna for ultra-wideband applications (Liu, Cheung and Azim, 2011). A simple circular-ring planar-monopole antenna with a compact size of $26 \times 28\text{ mm}^2$ was fed by an offset-microstrip line. A rectangular ground plane on the other side of the substrate with a small slot is used for impedance matching. Experimentally, impedance bandwidth of more than 132% from 3.7 to 18 GHz for the $VSWR \leq 2$ with a stable unidirectional radiation pattern and an average peak gain of 3.97 dBi was reported.

In 2011, Shagar and Wah designed a rectangular slot monopole antenna with a band-notched function suitable for 2.4 GHz wireless local area network and ultra-wideband applications (Shagar and Wah, 2011). Two pairs of slits were made into the ground plane to obtain a band-notch filter. By tuning the position, the length, and width of the slits, a

suitable frequency rejection band can be obtained. For proper impedance matching, a rectangular cut in the ground plane was made. The authors claimed ultra-wideband performance in the 2–12 GHz frequency range with a band-notch function from 5.1 to 5.9 GHz. The reported radiation patterns were nearly omni-directional. Group delays were reported within 1.5 ns except for the notch band.

In 2013, Mazhar, Tarar and Tahir have designed a compact microstrip UWB antenna with step impedance microstrip line (Mazhar, Tarar and Tahir, 2013). The antenna consisted of a rectangular patch with slits on the top face and a partial ground with slots at the rear end. It can operate between 3 and 10.26 GHz with approximately 7.26 GHz bandwidth. It has omni-directional radiation patterns on most of the operating band.

Co-planar Feed UWB Patch Antennas

In 2000, Tong and Hu proposed a CPW-fed circular microstrip antenna suitable for FCC defined ultra-wideband wireless communications system (Tong and Hu, 2000). Satisfactory impedance bandwidth from 2.3 to 15.6 GHz with return-loss better than 10 dB was reported. In comparison with the normal microstrip line-fed circular microstrip antenna, the CPW-fed antenna enabled 50% more bandwidth.

In 2008, Abed, Kimouche and Atrouz proposed the design of a novel printed monopole antenna fed by a coplanar waveguide for ultra-wideband applications (Abed, Kimouche and Atrouz, 2008). The main patch consisted of a modified elliptical patch while the CPW ground plane had a modified semicircular shape. Impedance bandwidth for voltage standing-wave ratio two is attained from 3 to 11.3 GHz with a fractional bandwidth of 116%.

In 2013, Gautam, Yadav and Kanaujia proposed a coplanar waveguide-fed compact ultra-wideband microstrip antenna (Gautam, Yadav and Kanaujia, 2013). Two inverted L-strips, extended from the ground over the conventional monopole patch antenna, were used to lower the height of the monopole antenna. The large space around the main radiating patch was effectively utilised. Bandwidth from 2.6 to 13.04 GHz for VSWR better than two (2) was achieved with antenna size of 25×25^2 mm on the FR4 substrate. Good impedance

matching, constant gain, stable radiation patterns, and constant group delay were achieved throughout the entire band.

In 2014, Liu, Wang and Qin proposed a compact Asymmetric Coplanar Strip (ACS)-fed UWB monopole antenna with additional Bluetooth band for various wireless applications (Liu, Wang and Qin, 2014). The antenna composed of a modified ACS-fed structure and a staircase-shaped patch covering the UWB band in the 3.1–10.6 GHz range, fabricated on a very compact FR4, $32.5 \times 10 \text{ mm}^2$ substrate. A snake-shaped slot was etched in the staircase shape to realise the Bluetooth band from 2.4 to 2.484 GHz. The radiation patterns of the designed antenna attained nearly omni-directional with consistent group delays and stable gains in the operating frequency bands.

In 2016, Li, Zhu and Cao proposed a design of UWB compact co-planar microstrip monopole antenna with enhanced bandwidth and triple band rejections (Li, Zhu and Cao, 2016). The base of the proposed antenna was a semicircular patch fed by a modified tapered CPW. A trident-shaped feed line was used to achieve wider impedance bandwidth. To avoid interference of 3.5 GHz WiMAX and 5.2/5.8 GHz WLAN bands, two trapezoid stubs and a C-shaped stub were printed on the back surface of the substrate and connected through three vias to the main patch. The proposed antenna was fabricated with a compact size of $20 \times 24 \text{ mm}^2$. Approximately 149% bandwidth covering 3.02 to 20.8 GHz with triple band rejections, i.e. 3.5 GHz WiMAX and 5.2/5.8 GHz WLAN, was achieved.

From the exhaustive literature survey, it can be concluded that efforts are being made to design ultra-wideband antennas covering a few GHz to 20 GHz and more in a few cases. The technique involved to achieve the UWB behaviour is mainly dependent on the shape of the radiating patch, size and the relative position of the partial ground with reference to the main radiating patch. The antenna radiation patterns reported were mostly broad.

1.7 Problem Statement

The prime objective of this work is to develop a practical solution to overcome the limitations of narrowband microstrip antenna, so that a single antenna can be used to detect any signal being transmitted by any transmitter from a few to 40 GHz, especially for the

spectrum monitoring purpose. Bandwidth enhancement and size reduction in microstrip patch antenna can be realised by inserting different shape and size slots to main radiating patch and ground plane. Tunable frequency ratios may be obtained by varying the length of the slots. For more clarity, the problem undertaken is stated below:

To design ultra-wideband printed antennas able to operate satisfactorily from 3 to 40 GHz or more with omni-directional radiation patterns and moderate gain.

1.8 Organization of the Thesis

The research work carried out during the Ph.D. course has been presented in a total of five chapters. Chapter-wise summary is as follows:

Chapter 1: This chapter comprises the motivation, objectives and brief description of the thesis content. Exhaustive literature survey was carried out on designing printed monopole antennas with emphasis on achieving higher bandwidth.

Chapter 2: This chapter deals with the simulation and design of a few printed antennas able to operate satisfactorily from 3 to 20 GHz to cover the entire FCC authorized frequency band. The simulated and measured return-loss and parametric analysis of the antennas under consideration are discussed.

Chapter 3: This chapter presents the design and development of printed monopole antennas able to operate satisfactorily from 3 to 30 GHz. In this chapter, design methodology, simulation and parametric analysis are discussed. A few selected antennas are fabricated and a comparison is made between simulated and experimental results.

Chapter 4: This chapter elaborates the design of an ultra-wideband printed antenna suitable for spectrum monitoring from 3 to 40 GHz. A few antennas are fabricated and their measured performance is discussed.

Chapter 5: The conclusions drawn from the investigations and the scope for future work are discussed in this chapter.

1.9 Summary

Spectrum monitoring and interference resolution is a vital component of spectrum management. To resolve the interference problem, every country has its own mechanism to report the unwanted signal in a particular format which includes probable frequency and direction of interfering transmitter. Lack of access to sophisticated automated frequency monitoring systems can be overcome by a simple system incorporating an ultra-wideband compact patch antenna.

Through literature survey, it is also clear that a large quantum of research work is under progress to design compact multiband antenna to operate optimally at selected bands of frequencies. However, very little work has been reported to design an UWB antenna operating in full band from a few GHz to 40 GHz and beyond.

In the next chapter, a few novel prototype designs are presented that are capable of operating satisfactorily from 3.1 to 20 GHz, while the other chapters cover several other antennae designs capable of operating up to 40 GHz and beyond.

UWB PATCH ANTENNAS-CLASS I

In this chapter, we discuss a few UWB patch antennas operating in the range 3–20 GHz. All such antennas are given the name Class-I UWB patch antennas. We discuss their design details, sketches, results, etc.

Over last two decades, many techniques have been developed to increase the bandwidth of the microstrip patch antennas. A few are as below:

- Antenna designed with substrate of lower permittivity, thicker and multiple stacked substrates (Kumar and Ray, 2003)
- Quarter wave transformer as feed line (Lim, 2008)
- Tapered feed line (Srifi, 2009)
- Excitation of patch through aperture coupling
- Applications of parasitic element near the main patch (Vera, Georgiadis and Collado, 2010)
- Use of coplanar ground (Mokhtaari and Bornemann, 2010)
- L and other shape ground planes (Zhiyong, Qian and Huilong, 2010)
- Different shapes and dimensions of slots in a microstrip patch (Rafi and Shafai 2004, Sadat; Fardis and Geran 2006), etc.

In the subsequent sections, we discuss a few novel designs of microstrip antennas which are compact in size and have comparatively higher bandwidth.

2.1 Rectangular Printed Monopole Antenna-1

In 2005, Jung, Choi and Choi presented a small microstrip-fed monopole antenna of size $16 \times 18 \times 1.6 \text{ mm}^3$ designed with FR-4 substrate (Jung, Choi and Choi, 2005). The main radiating patch was rectangular in shape ($11 \times 7 \text{ mm}^2$) with two notches at its two lower corners and a truncated ground plane with the notch structure. With partial ground plane and notches, the authors have achieved ultra-wide bandwidth over 3.1–11.0 GHz.

2.1.1 Design of the Proposed UWB Patch Antenna-1

The antenna layout proposed by Jung, Choi and Choi was modified and shown in Fig. 2.1. Rogers TMM3 with dielectric constant 3.27 was used as the substrate with thickness 1.6 mm. The optimised design parameters of the antenna are listed in Table 2.1.

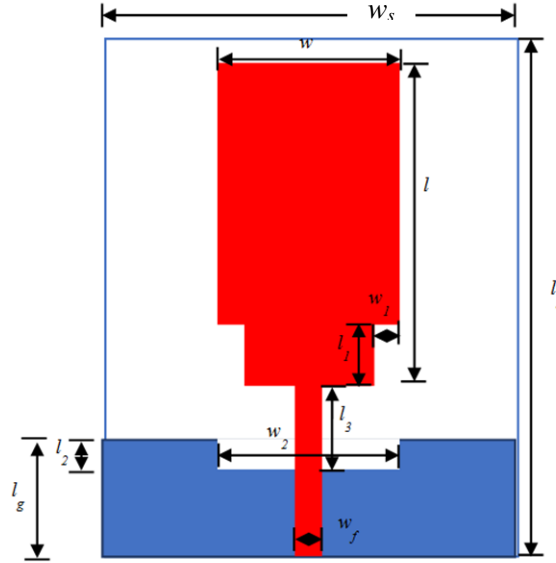


Fig. 2. 1 Design of the proposed UWB antenna-1 under consideration.

Table 2.1 Design Parameters of UWB Antenna-1

Design Parameter	Value (mm)	Design Parameter	Value (mm)
w_s	16	w_2	6.8
l_s	18	l_2	0.8
w	7	l_3	3.5
l	9	w_f	2.1
w_l	1	l_g	4.5
l_l	4	a	2.5

2.1.2 Return-Loss Performance of the UWB Antenna-1

The antenna was simulated using the commercially available antenna design Software-High Frequency Structure Simulator (HFSS V13). The simulated return-loss performance is shown in Fig. 2.2 and is also compared with that of an antenna proposed by Jung, Choi and Choi. The modified design offers 59% more impedance bandwidth as compared to the original design.

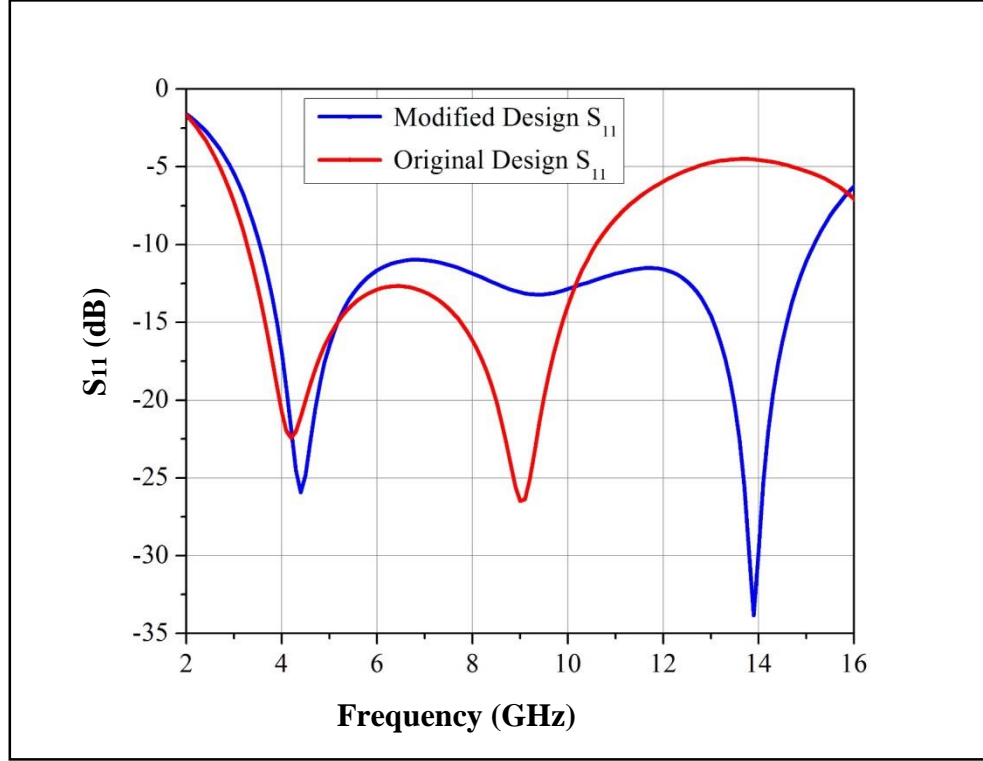


Fig. 2. 2 Return-loss performance of the proposed UWB antenna-1.

2.1.3 Parametric Study of the Proposed UWB Antenna-1

To study the effect of various design parameters on antenna performance, a parametric study was conducted and its outcomes are discussed here.

Change in Substrate Materials

Keeping all the design parameters unaltered, the effect of change in substrate material was studied. Three different substrate materials, namely, FR-4 ($\epsilon_r = 4.4$), Roger TMM3 ($\epsilon_r = 3.27$) and Roger RT/duroid 5880 ($\epsilon_r = 2.2$) with thickness 1.6 mm were considered. The simulated results plotted in Fig. 2.3; show that the lower cutoff frequency is

independent of the substrate material variations, while the upper cutoff frequency is highly dependent on them. On further optimisation, it was found that the substrate material Rogers TMM3 (tm) provides the maximum bandwidth for the given dimensions.

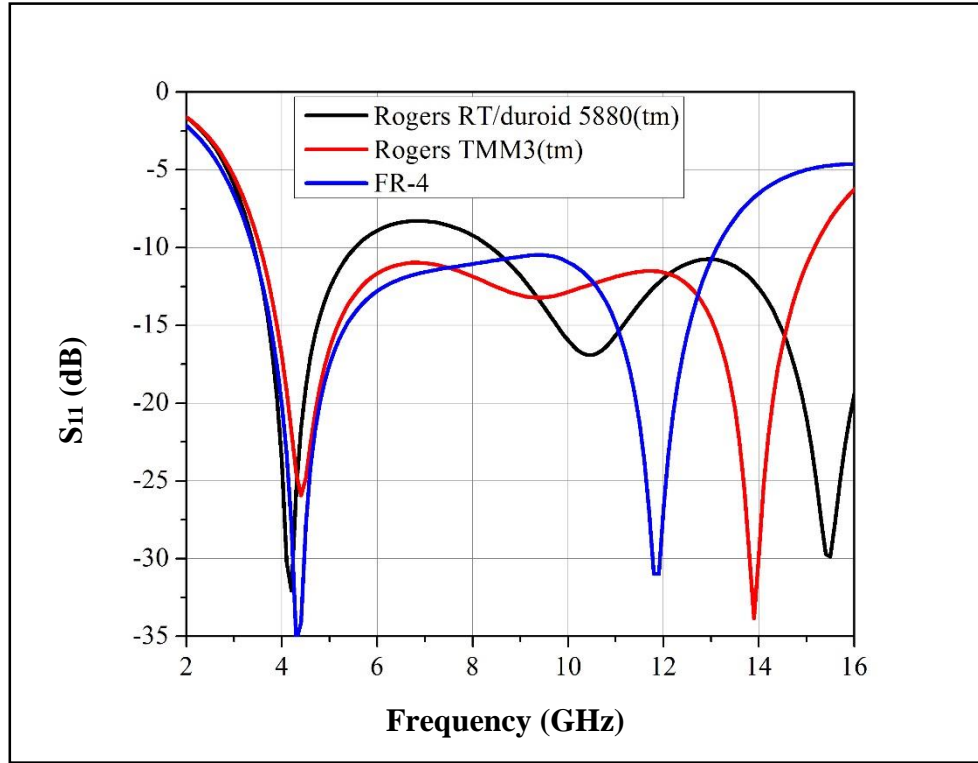


Fig.2.3 Effect of change in substrate material on the return-loss performance of the proposed UWB antenna-1.

Change in the Dimensions of the Radiating Patch

The effect of change in the dimensions l_1 and w_1 on the antenna return-loss is shown in Figs 2.4 and Fig. 2.5, respectively. It is apparent from Fig. 2.5 that as the patch width w_1 changes from 0.5 to 1.5 mm, the lower cutoff frequency remains unchanged but the upper one changes. The variations in length l_1 do not affect the cutoff frequencies appreciably. However, the return-loss performance of the antenna is better for the lower value of l_1 .

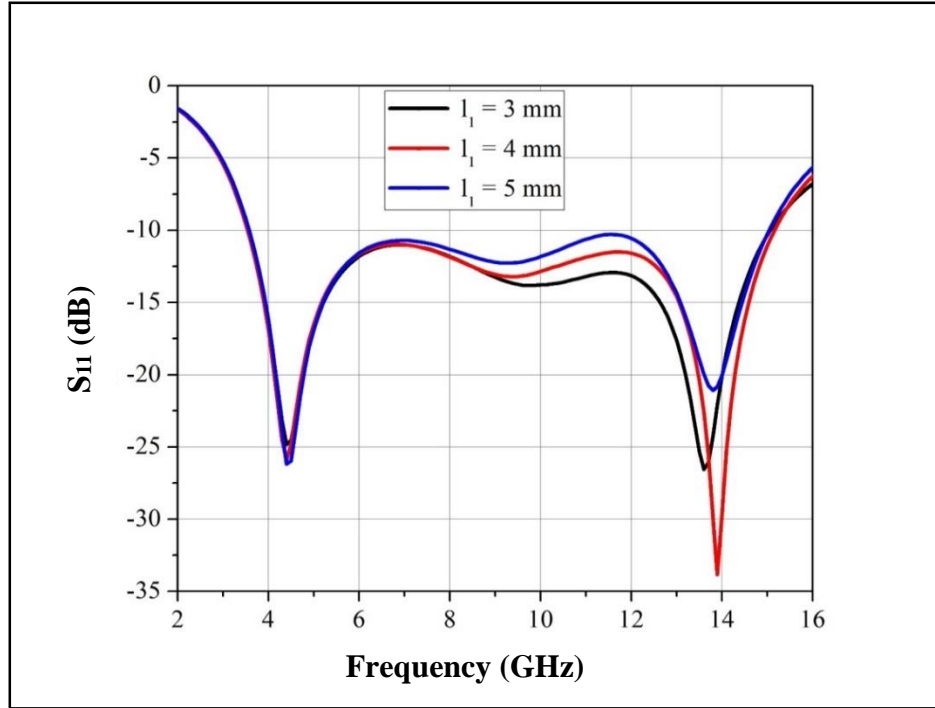


Fig. 2.4 Effect of change in patch dimension (l_1) on the return-loss performance of the proposed UWB antenna-1.

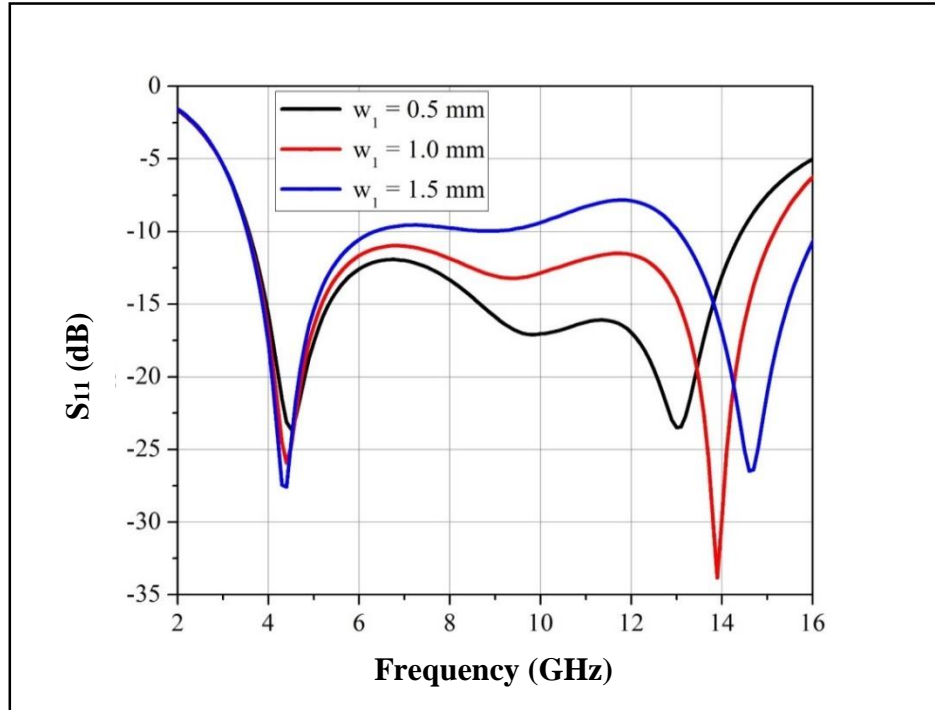


Fig. 2.5 Effect of change in patch dimension (w_1) on the return-loss performance of the proposed UWB antenna-1.

Change in Dimensions of the Partial Ground Plane (l_g)

The proposed antenna has partial ground plane with length l_g and a notch with dimensions $l_2 \times w_2$. These dimensions were also varied to see their effect on the return-loss performance. The simulated performance with different values of l_g is plotted in Fig. 2.6. The results show that the change in l_g affects the return-loss and hence utmost care needs to be taken while fixing its value.

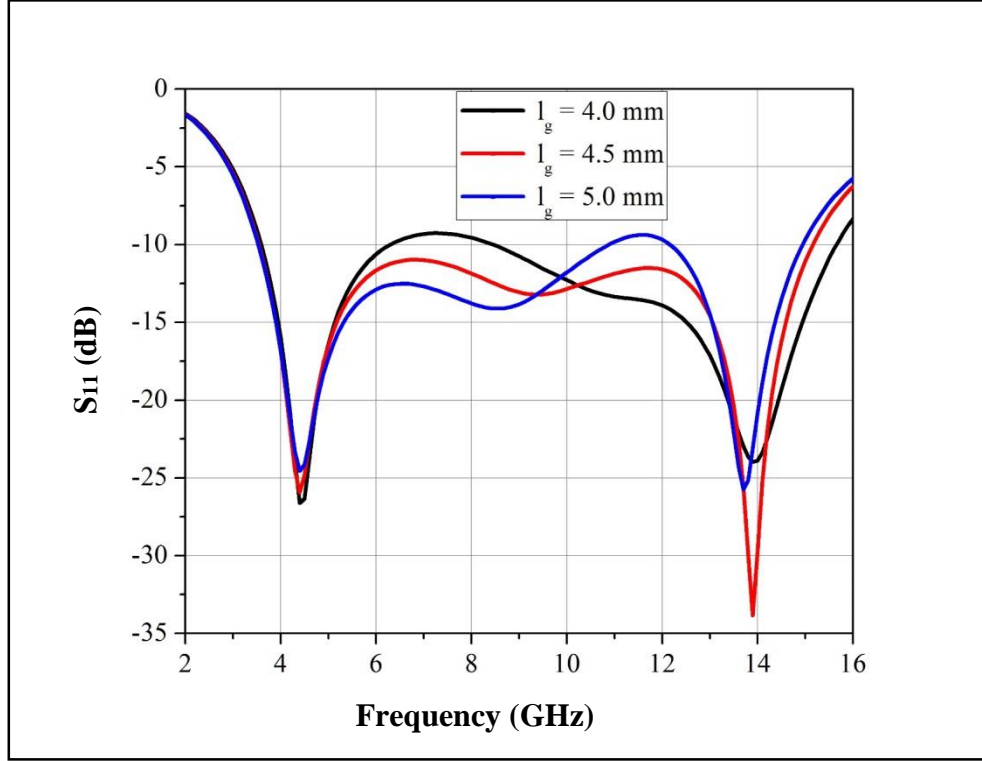


Fig. 2. 6 Effect of change in length (l_g) of the ground plane on the return-loss performance of the proposed UWB antenna-1.

The effect of change in the notch dimensions (l_2 and w_2) of the ground plane on the return-loss performance is shown in Figs 2.7 and 2.8, respectively. It is almost independent of the dimensions, l_2 and w_2 . However, the notch width of 0.8 mm and length of 6.8 mm yield optimal impedance bandwidth.

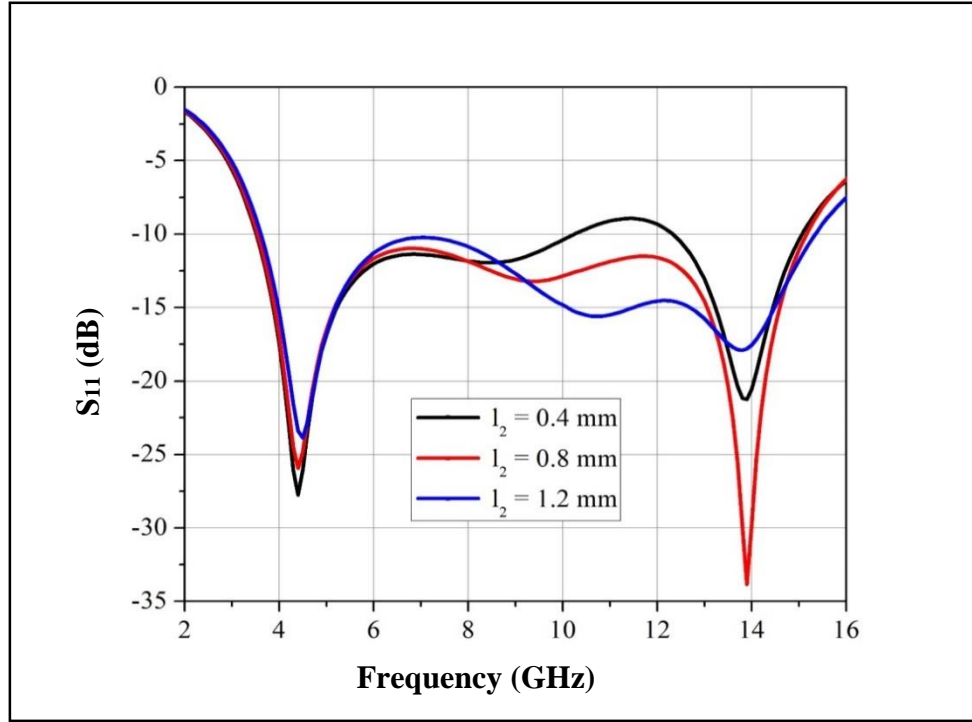


Fig. 2.7 Effect of change in the notch dimension (l_2) of the ground plane on the return-loss performance of the proposed UWB antenna-1.

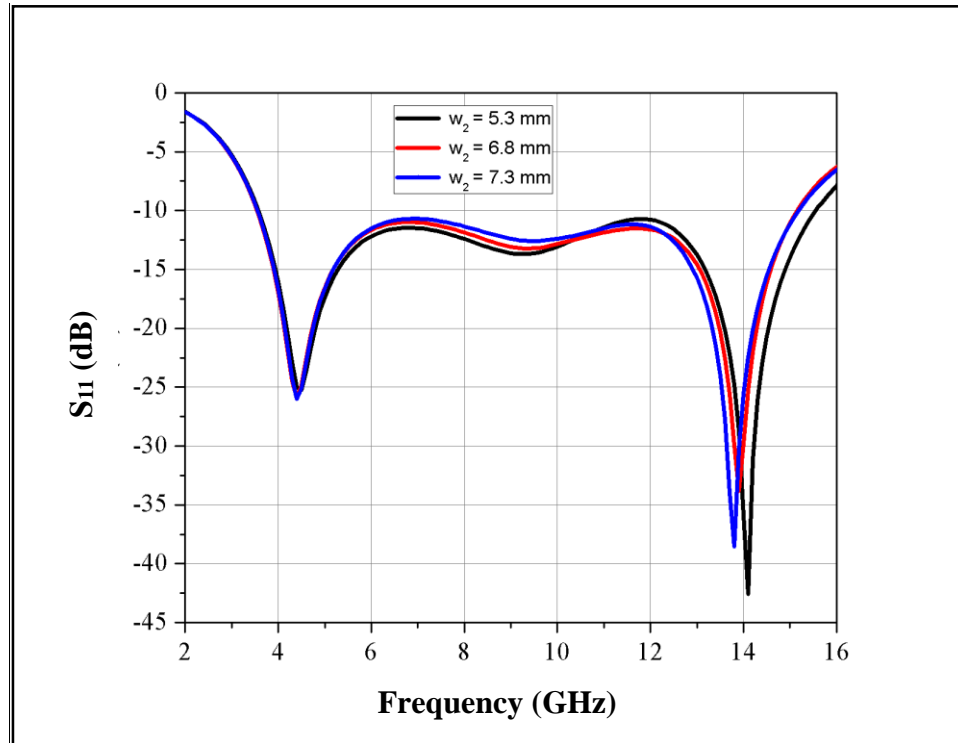


Fig. 2.8 Effect of change in the notch dimensions (w_2) of the ground plane on the return-loss performance of the proposed UWB antenna-1.

2.1.4 Radiation Patterns of the Proposed UWB Antenna-1

The simulated radiation patterns of the proposed antenna at 5, 10 and 15 GHz are shown as Fig. 2.9. The radiation pattern in horizontal plane at 5 GHz is in a donut shape of a dipole, while at 10 GHz it is distorted. At 15 GHz, a back lobe also appears. The peak gain of the proposed antenna for different frequencies is shown as Fig. 2.10.

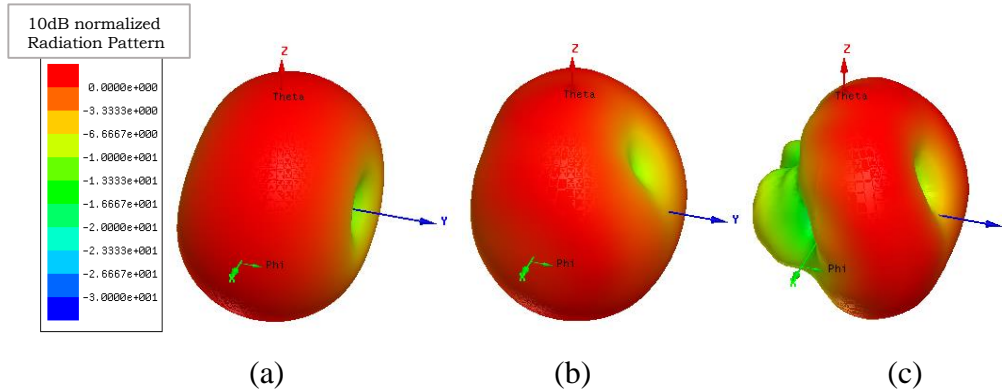


Fig. 2.9 Radiation patterns of the proposed UWB antenna-1: (a) 5, (b) 10, and (c) 15 GHz.

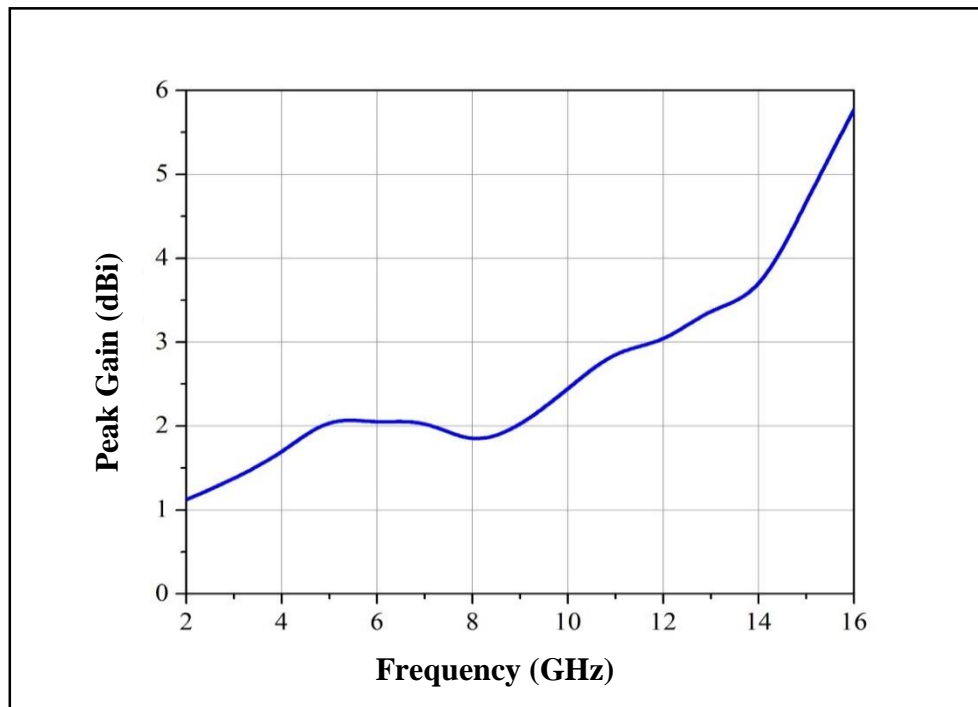


Fig. 2.10 Peak Gain of the proposed UWB antenna-1.

Thus, a compact microstrip-fed monopole antenna as proposed by Jung, Choi and Choi has been modified and optimised to improve the impedance bandwidth. The designed antenna

satisfies the 10 dB return-loss requirement from 3.5 to 15.2 GHz and provides good monopole-like radiation patterns.

2.2 Hexagonal and Circular-Shaped Printed Monopole Antenna-2

In this design, a microstrip monopole antenna of size $50 \times 35 \times 1.6 \text{ mm}^3$ was designed and fabricated on RT/duroid 5880. The antenna was tested and the measured return-loss bandwidth (10 dB reference) from 3.1 to 14.1 GHz was achieved.

2.2.1 Design of the Proposed UWB Patch Antenna-2

The proposed antenna is a patch monopole antenna with a stepped microstrip feed line matched to 50Ω impedance. The RT/duroid 5880 substrate has thickness $h = 1.6 \text{ mm}$, copper cladding of 0.035 mm and relative permittivity, $\epsilon_r = 2.2$, $\tan \delta = 0.0004$, $l_s = 50 \text{ mm}$ and $w_s = 35 \text{ mm}$. The characteristic impedance Z_0 was calculated using the empirical formulas suggested by Pozar (2012) and Liao (1989). For 50Ω impedance, the calculated feed line width is 5 mm . For a given radiating patch area, circular and hexagonal shapes are widely used to achieve the UWB behavior. In this design, a circular radiating patch was initially used as a main radiating patch. Further, a hexagonal radiating patch was used to overlap the circular patch. Through optimization, the dimensions of circular and hexagonal patch were decided to achieve the maximum return-loss BW.

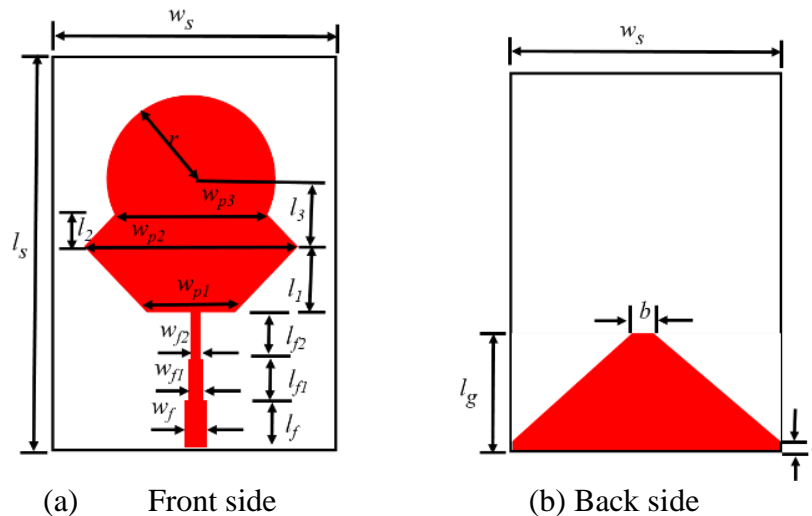


Fig. 2.11 Layout of the proposed UWB antenna-2 under consideration.

A tapered partial ground has been used to achieve better return-loss after optimisation. Figure 2.11 illustrates the geometry of the proposed antenna. A photograph of the fabricated antenna is shown in Fig. 2.12. The design parameters are given in Table 2.2.

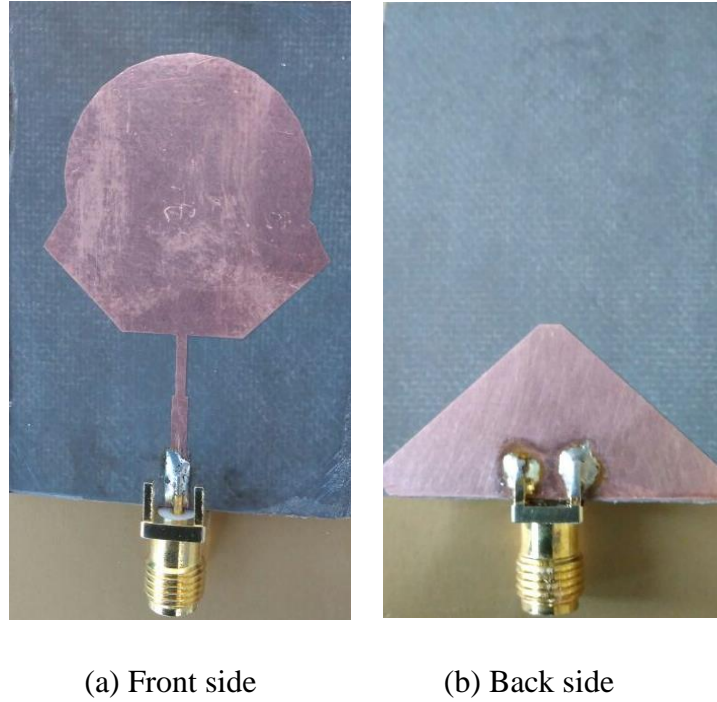


Fig. 2.12 Photograph of the proposed UWB antenna-2 under consideration.

Table 2.2 Design Parameters of UWB Antenna-2

Design Parameter	Value (mm)	Design Parameter	Value (mm)
l_s	50.0	l_1	8.0
w_s	35	w_{p2}	28
w_f	2.4	l_2	4.1
l_f	6	w_{p3}	20
w_{f1}	1.6	l_3	78
l_{f1}	5.5	r	12
w_{f2}	1	l_g	16.2
l_{f2}	6.2	a	1
w_{p1}	12	b	2

2.2.2 Return-Loss Performance of UWB Antenna-2

The proposed antenna was simulated using the commercially available software, HFSS and a 10 dB return-loss bandwidth, from 2.1 to 16.5 GHz, was achieved. The same antenna was fabricated and the measured 10 dB return-loss bandwidth was found for the frequency range of 3.1–14.1 GHz. The simulated and measured return-loss graphs are plotted in Fig. 2.13. The difference between the simulated and measured return-loss may be due to the antenna fabrication tolerances, undercuts at sharp corners of substrate material, effect of SMA connector and/or limitations of the simulation software.

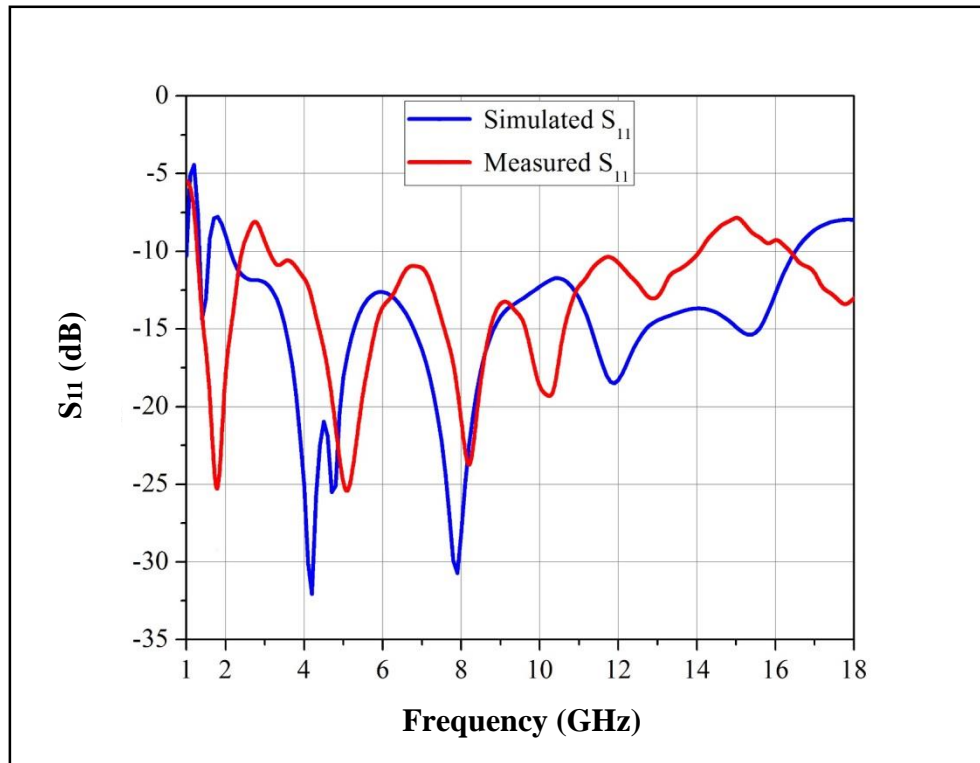


Fig. 2.13 Measured and simulated return-loss performance of the proposed UWB antenna-2.

2.2.3 Parametric Study of the Proposed UWB Antenna-2

The proposed antenna was optimised to maximise the 10 dB return-loss bandwidth. The most important parameters affecting the return-loss performance are the substrate material, the feed line width and the size of the ground plane. The outcomes of the parametric study are presented here.

Change in Substrate Materials

The substrate material used for designing a microstrip antenna plays very critical role as the size of the patch antenna is inversely proportional to $\sqrt{\epsilon_r}$. Also, the loss tangent decides the return-losses at different frequencies. As the loss tangent increases, the losses of microstrip antenna increase. In turn, this affects the return loss at different frequencies. Variations in return-loss for different substrate material are shown as Fig. 2.14. The study shows that RT/duroid-5880 provides the maximum return-loss bandwidth.

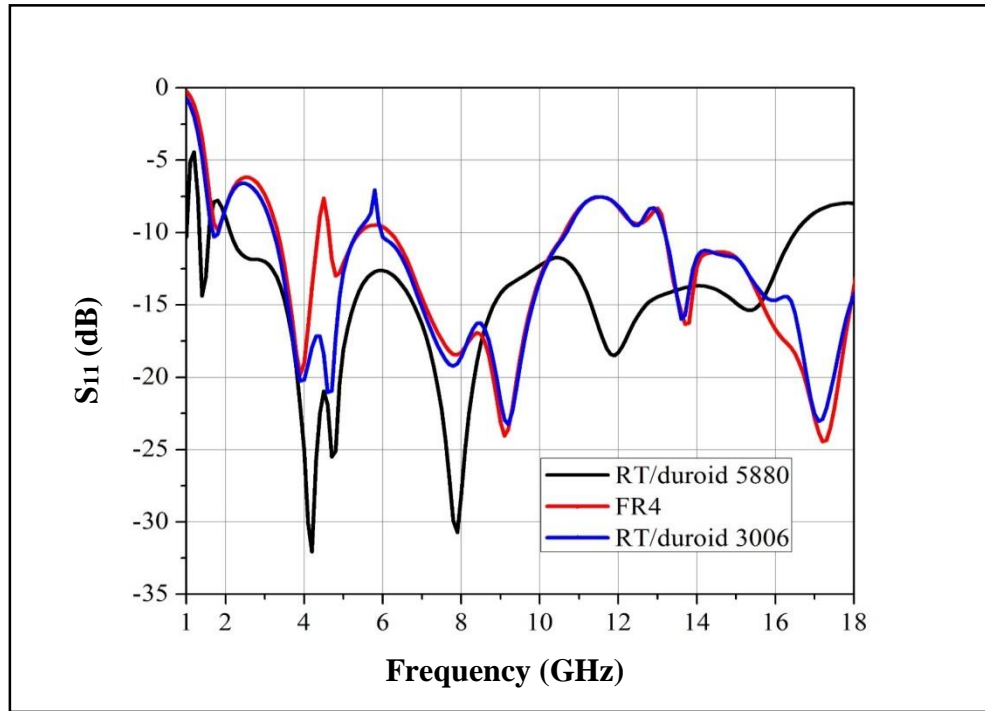


Fig. 2.14 Effect of change in substrate material on the return-loss performance of the proposed UWB antenna-2.

Change in Dimensions of the Feed Width (w_f)

The width of the feed line determines the input impedance Z_0 of the antenna. It is evident from Fig. 2.15 that as we increase the feed line width, the return-loss improves in mid band, but at the cost of impedance bandwidth (lowers on the frequency side). The higher cutoff frequency does not depend much on w_f , but the lower frequency depends highly on it.

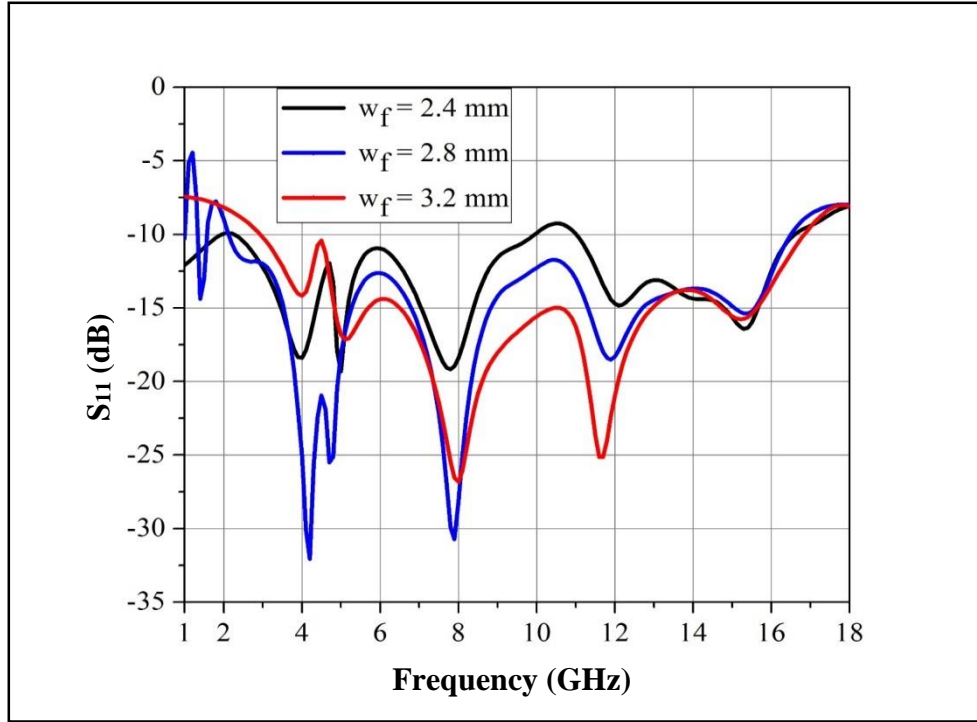


Fig. 2.15 Effect of change in feed width dimension (w_f) on the return-loss performance of the proposed UWB antenna-2.

Change in the Dimensions of the Partial Ground Plane (l_g)

The size of the partial ground plane plays a very critical role in impedance matching. The separation between the radiating patch along with the feed line and the ground plane forms a capacitor, which is required for impedance matching. However, the inductance formed by feed line becomes dominating to the total capacitance formed by the radiating patch along with feed line and ground plane at higher frequencies. Hence, at higher frequencies antenna behaves inductively. It was observed that a tapered partial ground plane of size l_g provides better impedance bandwidth as compared to a plane rectangular partial ground of size $w_s \times l_g$. The antenna was optimised and found to offer maximum impedance bandwidth for $a = 1$ mm, $b = 2$ mm and $l_g = 16.2$ mm, as shown in Fig. 2.16.

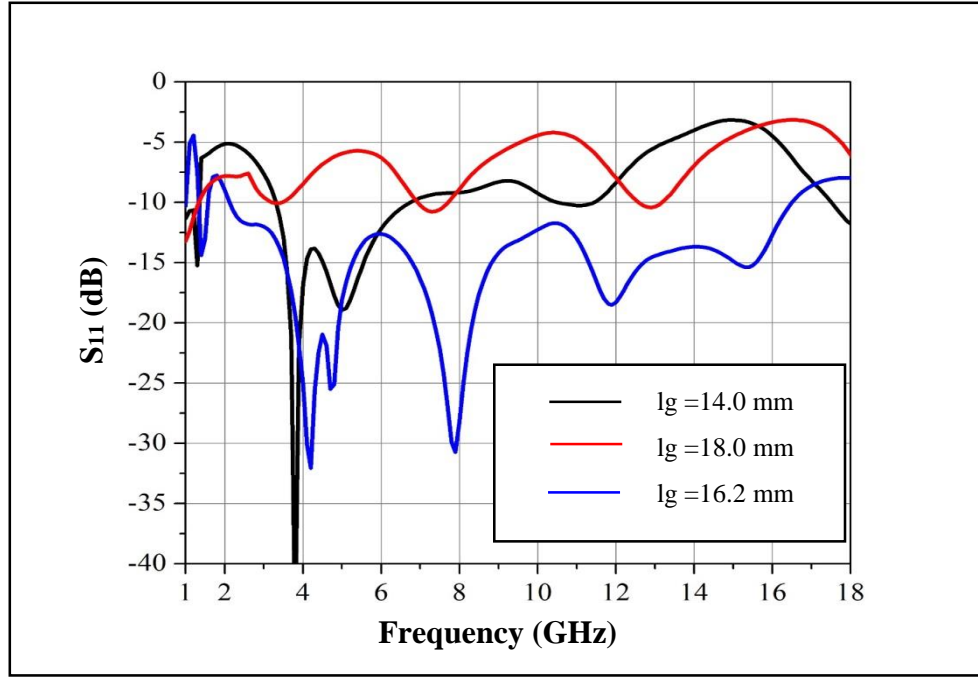


Fig. 2.16 Effect of change in length (l_g) of the ground plane on the return-loss performance of the proposed UWB antenna-2.

2.2.4 Radiation Patterns of the Proposed UWB Antenna-2

The radiation patterns of the proposed antenna for 4, 8 and 12 GHz, shown in Fig. 2.17, show that they are like that of a dipole antenna. However, at higher frequencies a few side lobes start appearing. The peak gain is between 2 and 4 dBi throughout the band. A plot of variations in maximum gain for different frequencies is shown in Fig. 2.18.

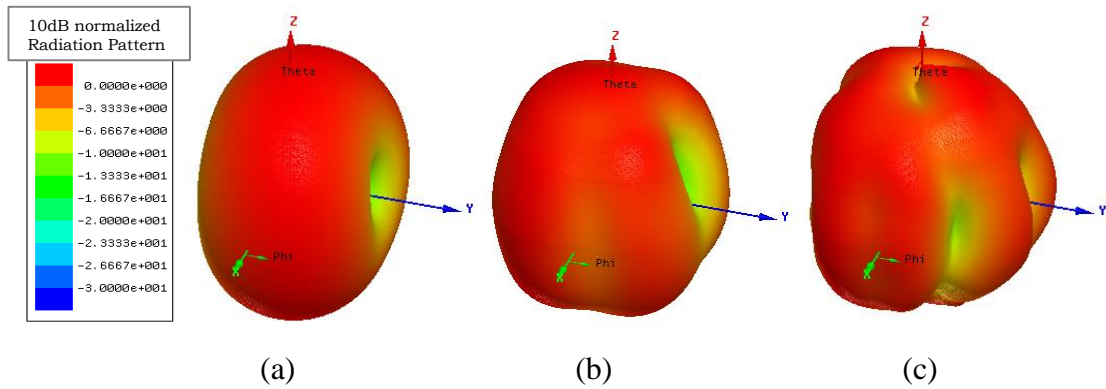


Fig. 2.17 Radiation patterns of the proposed UWB antenna-2 (a) 4, (b) 8, and (c) 12 GHz.

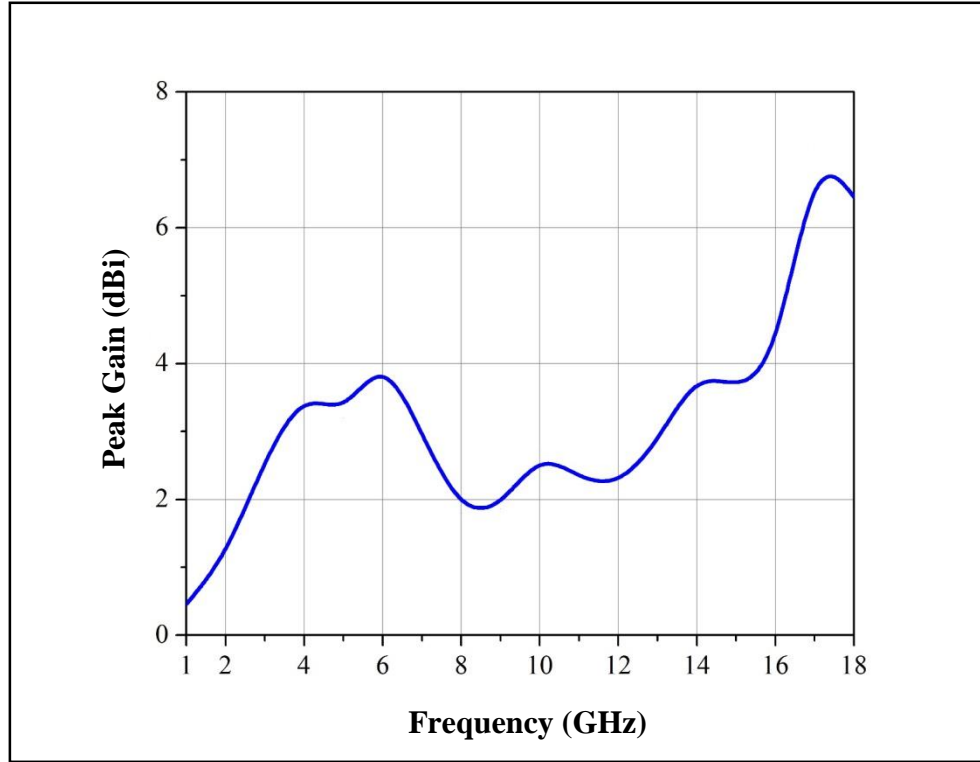


Fig. 2.18 Variations in peak gain for the proposed UWB antenna-2.

A compact-size monopole patch antenna with a tapered partial ground was designed, simulated and tested. The antenna was optimised to achieve minimum return-loss over the entire FCC-authorized frequency band (3.1 to 14.1 GHz). This antenna can be used for frequency monitoring, geological and metrological signaling, radar navigation, hand-held UWB applications, etc.

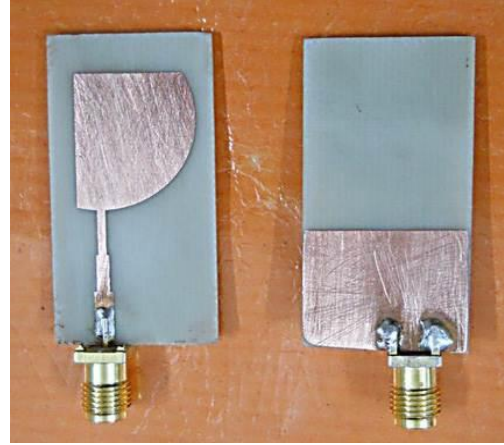
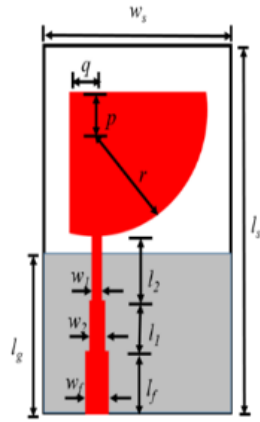
2.3 Quarter Circular Printed Monopole Antenna-3

In this section, a quarter circular microstrip antenna design with stepped microstrip feed line is discussed. A prototype antenna was fabricated on FR-4 substrate of size $35 \times 20 \times 1.6 \text{ mm}^3$. The antenna offers better than 10 dB return-loss over a frequency band of 3.1–16.3 GHz.

2.3.1 Design of the Proposed UWB Patch Antenna-3

The proposed microstrip antenna consists of a quarter circular radiating patch with small circular sector as shown in Fig. 2.19. Three microstrip lines of different widths are used to

feed the patch. A partial ground plane has been utilised to force the radiating patch to act as monopole. The design parameters are given in Table 2.3.



(a) Layout

(b) Photograph of the fabricated antenna

Fig. 2.19 Design of the proposed UWB antenna-3 under consideration.

Table 2.3 Design Parameters of UWB Antenna-3

Design Parameter	Value (mm)	Design Parameter	Value (mm)
l_s	35	w_1	1.6
w_s	20	l_2	6.2
r	12	w_2	1
l_f	6	l_g	15.2
w_f	2.4	p	6
l_l	5.5	q	3

2.3.2 Return-Loss Performance of the UWB Antenna-3

Figure 2.20 shows the simulated and measured return-loss performance of the antenna-3. Three simulated resonant frequencies located at about 4.6, 9.8 and 13.6 GHz were observed to be matching with the measured resonant frequencies. The simulated impedance bandwidth is from 1.9 to 14.3 GHz, while that from fabricated antenna is from 3.1 to 16.3 GHz. This variation might have been due to manufacturing tolerances and limitations of the software.

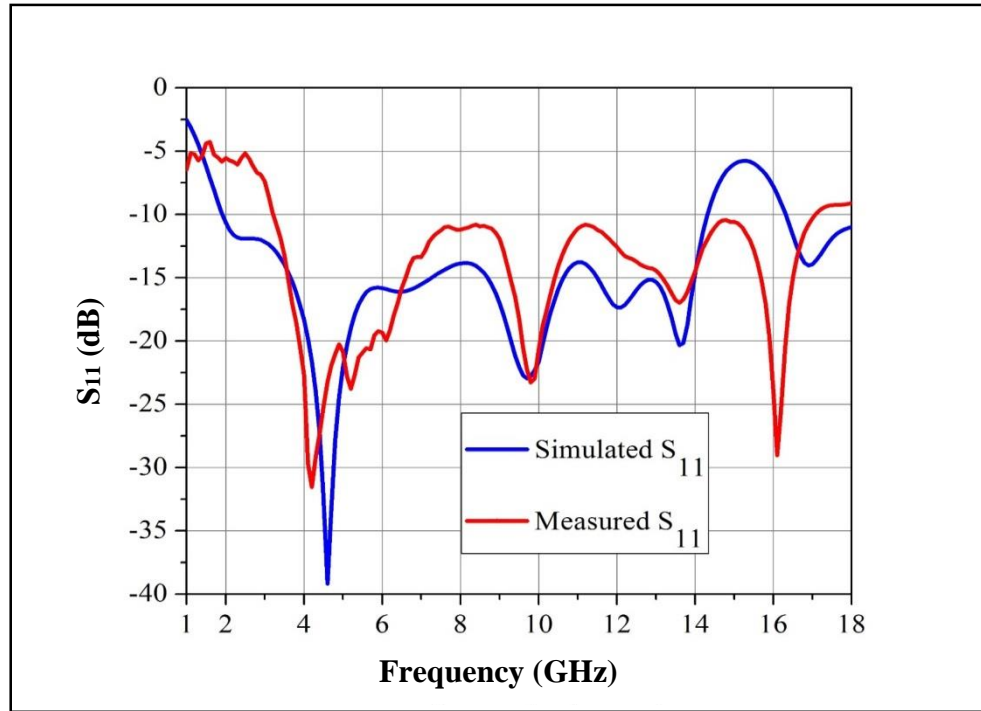


Fig. 2.20 Measured and simulated return-loss performance of the proposed UWB antenna-3.

2.3.3 Parametric Study of the Proposed UWB Antenna -3

A parametric study was conducted to investigate the effect of substrate material, ground size, patch size and main feed line width on the return-loss performance of the proposed UWB antenna. The details are discussed below:

Change in Substrate Materials

Figure 2.21 demonstrates how variations in substrate material affect the return-loss. The other antenna design parameters remained unaltered. It was observed that the first resonant frequency at 4.6 GHz was mostly dominated by the antenna shape/size and was less dependent on the substrate material. It was observed that FR-4 substrate provides the minimum return-loss and maximum impedance bandwidth in comparison to other two substrate materials under consideration.

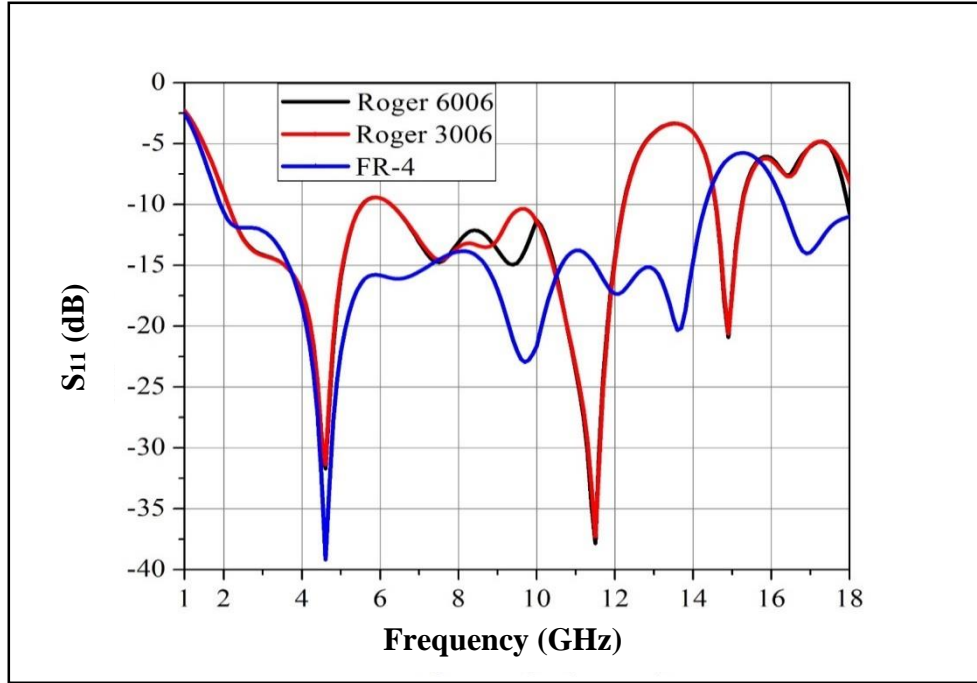


Fig. 2.21 Effect of change in substrate material on the return-loss performance of the proposed UWB antenna-3.

Change in Dimensions of the Partial Ground Plane (l_g)

The effect of change in ground size was simulated and the results are shown in Fig. 2.22. In general, the ground plane also works as an impedance matching network and also tunes the resonant frequencies of the antenna. The dimension $l_g = 15.2$ mm was found to be the optimal.

Change in Dimensions of Feed Width (w_f)

In this design, a microstrip feed has been used to feed the main radiating patch. A stepped feedline has been directly connected to the edge of the microstrip patch. The feed line width w_f was calculated as 3 mm (Pozar, 2012; Liao, 1989). However, after optimisation, a feed width of 2.4 mm was found to provide the best impedance matching as shown in Fig. 2.23. As the feed width increases to 3.4 mm, the overall impedance bandwidth improves marginally. For the feed width of 1.4 mm, the return-loss was observed to degrade.

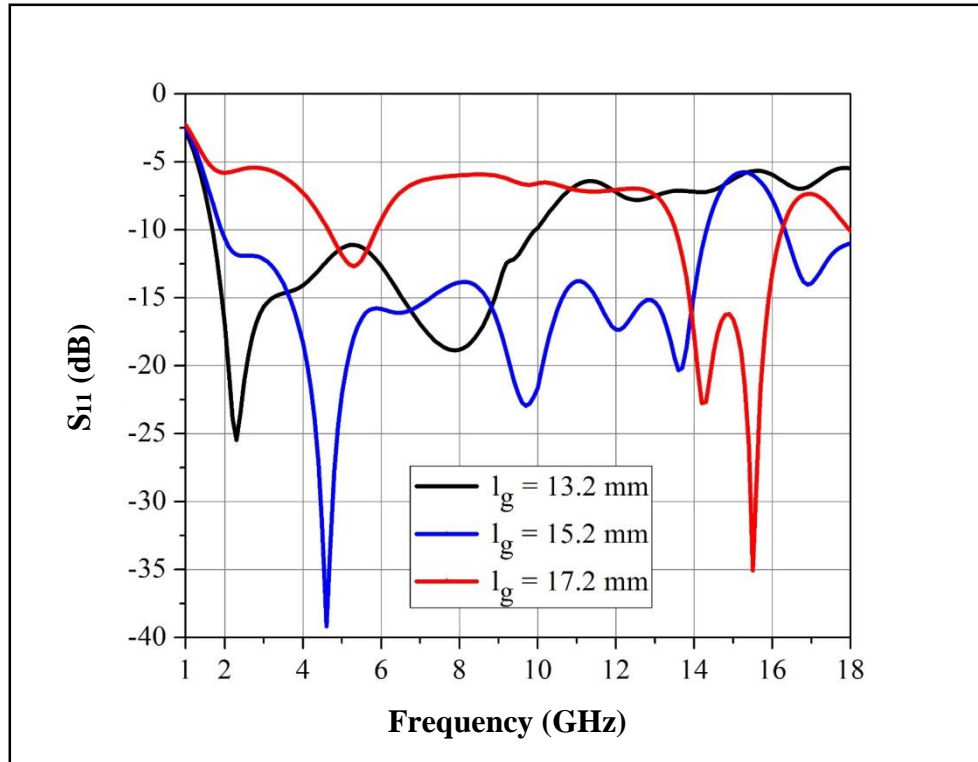


Fig. 2.22 Effect of change in length (l_g) of the ground plane on the return-loss performance of the proposed UWB antenna-3.

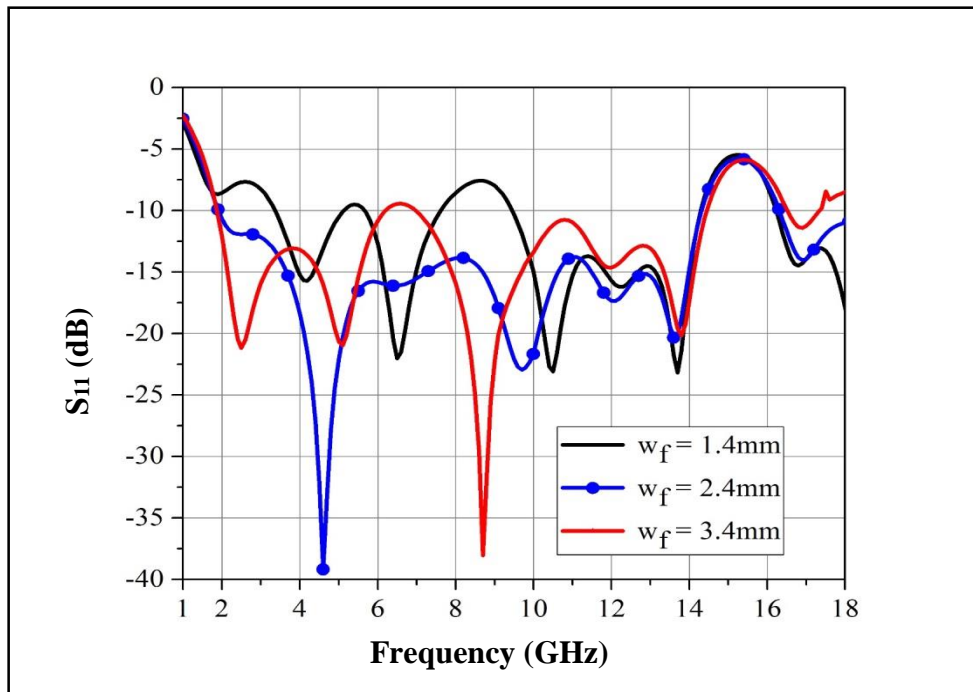


Fig. 2.23 Effect of change in feed width dimension (w_f) on the return-loss performance of the proposed UWB antenna-3.

2.3.4 Radiation Patterns of the Proposed UWB Antenna-3

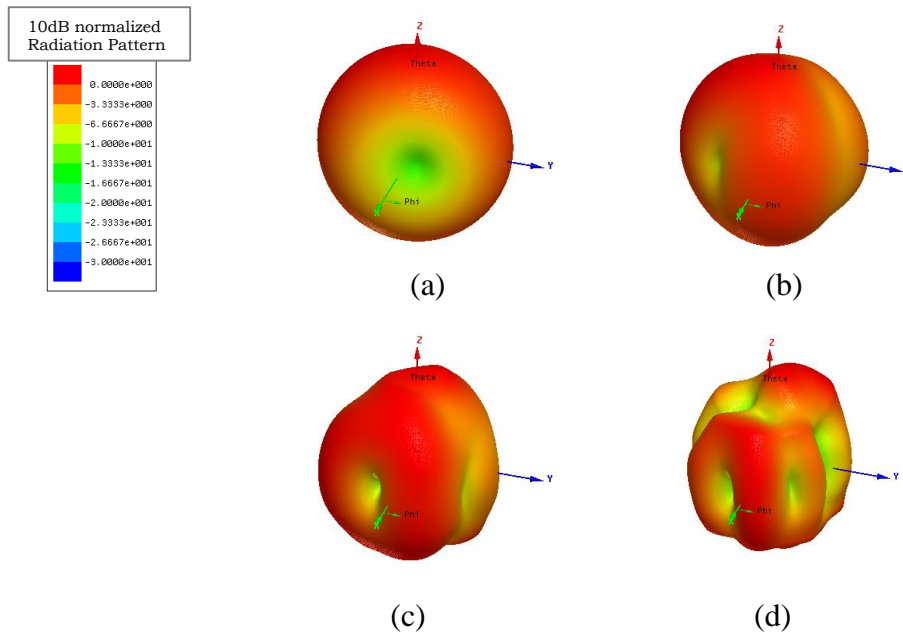


Fig. 2.24 Radiation patterns of the proposed UWB antenna-3 (a) 3.5, (b) 7, (c) 10.5, and (d) 14 GHz.

The three-dimensional radiation patterns of antenna under consideration at 3.5, 7, 10.5 and 14 GHz are shown in Fig. 2.24. They are mostly omni-directional. At lower frequencies till 10.5 GHz, the performance is mostly like omni-directional which becomes more directional at higher frequencies. Since a microstrip monopole antenna is an ultra-wideband one, the average gain is found to be low and vary between 0 to 5 dBi at different frequencies.

The peak gain of the antenna varies from 2 to 6 dBi in the entire band. It is low due to its omni-directional radiation pattern. A plot of the peak gain versus frequency is shown in Fig. 2.25.

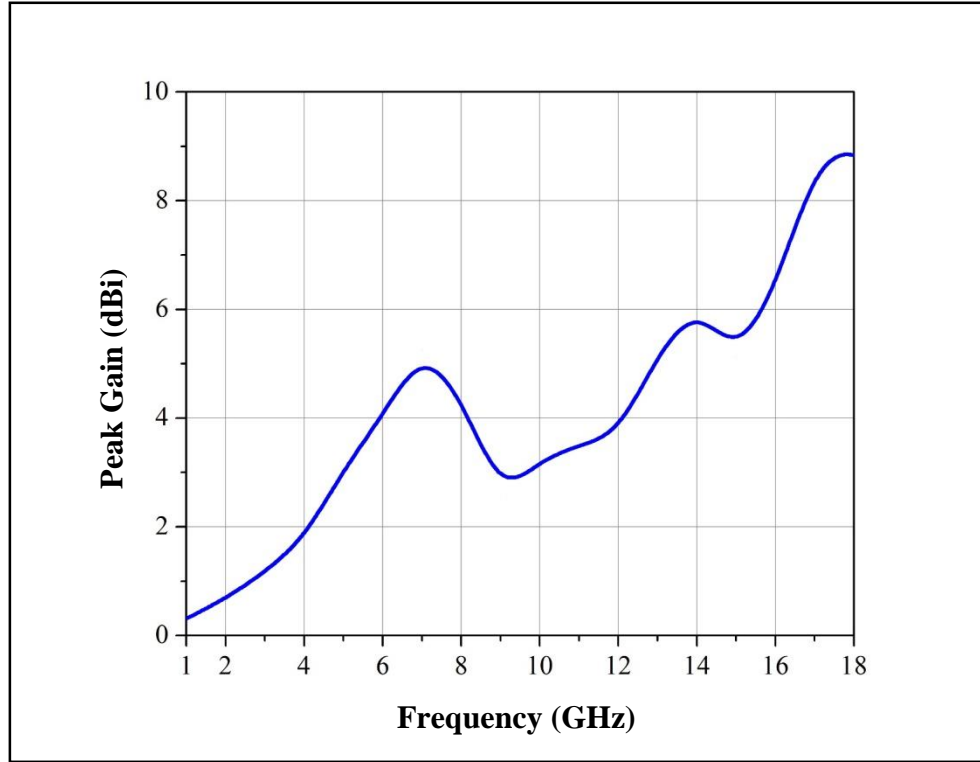


Fig. 2. 25 Peak gain of the proposed UWB antenna-3.

The proposed prototype antenna exhibits good UWB characteristics with its simulated impedance bandwidth from 1.9 to 14.3 GHz and a fractional bandwidth of 153%. The measured 10 dB impedance bandwidth is approximately 136%, covering 3.1–16.3 GHz frequency. The proposed antenna exhibits good UWB characteristics and is suitable for wireless communication systems.

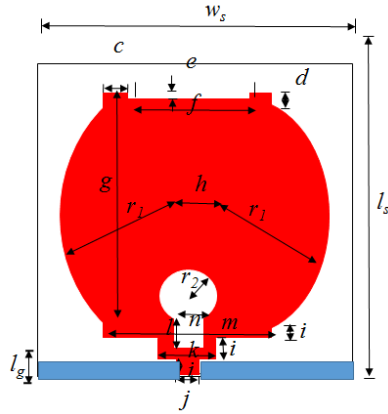
2.4 Goblet-Shaped Printed Monopole Antenna-4

In this section, a compact novel goblet-shaped microstrip monopole with a stepped microstrip feed line is presented. Circular and rectangular slots in the radiating patch have been made to achieve the UWB performance.

2.4.1 Design of the Proposed UWB Patch Antenna-4

The proposed antenna design is shown in Fig. 2.26. The top layer comprises of a feed line and a radiating patch, while the bottom layer comprises of the partial ground. The substrate is made of RT/duroid-5870 (tm) with dielectric constant of 2.33 and dimension of $24 \times 24 \times 0.787$ mm³. The radiating patch comprises of a goblet-shaped patch with two

circular segments attached to a rectangular patch. Three microstrip lines with different widths are utilised to feed the radiating patch. The antenna geometrical parameters are listed in Table 2.4.



(a) Layout



(b) Photograph of the fabricated antenna

Fig. 2.26 Design of the proposed UWB antenna-4 under consideration.

Table 2.4 Design Parameters of UWB Antenna-4

Design Parameter	Value (mm)	Design Parameter	Value (mm)
l_s	24	j	1.5
w_s	24	k	4
c	2.5	l	1.4
d	1.5	m	12
e	0.85	n	2
f	7	r_1	9
g	15	r_2	1.9
h	2	l_g	2
i	1.5		

2.4.2 Return-Loss Performance of UWB Antenna-4

Satisfactory simulated results encouraged us to fabricate a prototype antenna. The simulated and measured return-loss performance is shown in Fig. 2.27. The antenna exhibits multiband and UWB characteristics. The simulated impedance bandwidth is approximately 151%, covering the frequency band from 2.6 to 18.5 GHz in contrast with the measured bandwidth of 139% from 3.1 to 17.1 GHz. This variation may be due to manufacturing tolerances, effect of SMA connectors and/or limitations of the simulating software.

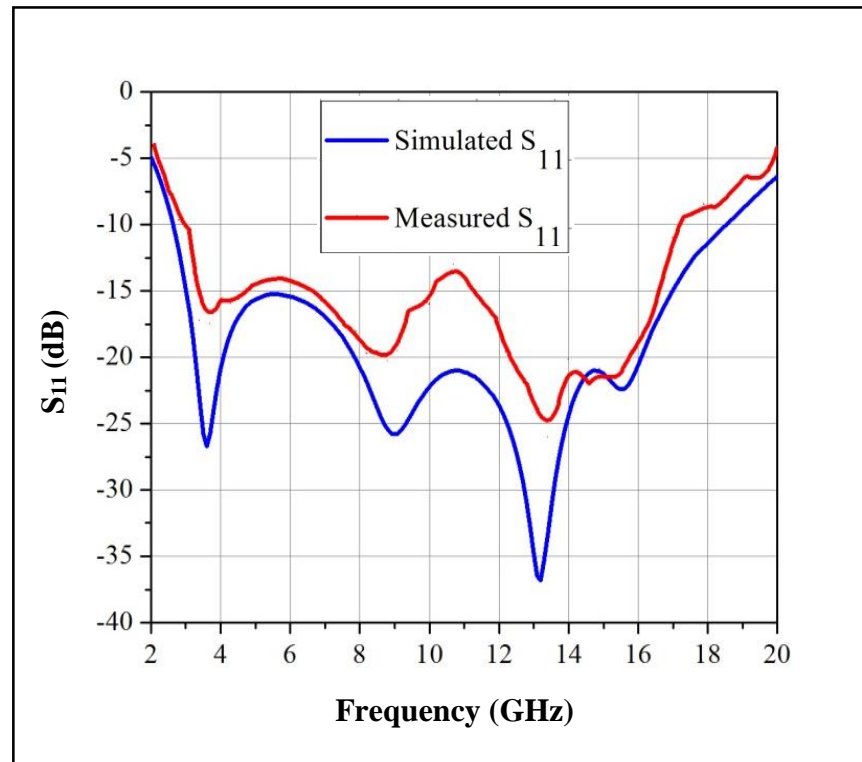


Fig.2.27 Measured and simulated return-loss performance of the proposed UWB antenna-4.

2.4.3 Parametric Study of the Proposed UWB Antenna-4

A thorough parametric study was carried out to finalise the antenna design, and the effect of different design parameters on the return-loss performance of the antenna is discussed in detail.

Change in Substrate Materials

Figure 2.28 shows how variation in the substrate material affects the antenna return-loss. In this simulation, substrate materials like Roger RT/duroid 5870 ($\epsilon_r = 2.33$), FR-4 ($\epsilon_r = 4.4$) and Roger RO 6003($\epsilon_r = 6.15$), with thickness of 0.787 mm have been considered. It is observed from Fig. 2.28 that Roger RT/duroid 6003 substrate provides the minimum impedance bandwidth. This may be due to its high permittivity. The substrate Roger RT/duroid 5870 was found to be the best in terms of return-loss performance.

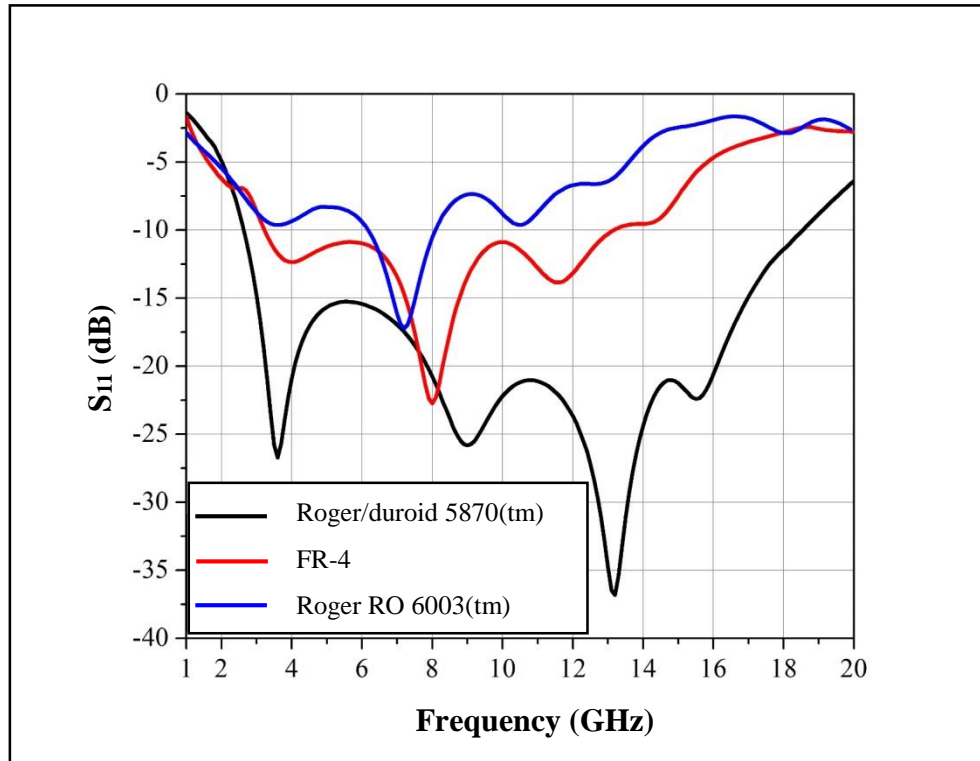


Fig. 2.28 Effect of change in substrate material on the return-loss performance of the proposed UWB antenna-4.

Change in Dimensions of the Partial Ground Plane (l_g)

The width of the ground plane plays the most important role in the design of a monopole microstrip antenna. The effect of variation in ground plane size was studied through simulation and the results are shown in Fig. 2.29. In general, ground plane additionally works as an impedance matching network. The optimum value of ground height $l_g = 2$ mm found to provide minimum return-loss and maximum impedance bandwidth. The lower

value of l_g reduces the return-loss bandwidth, while $l_g = 3$ mm degrades the antenna performance.

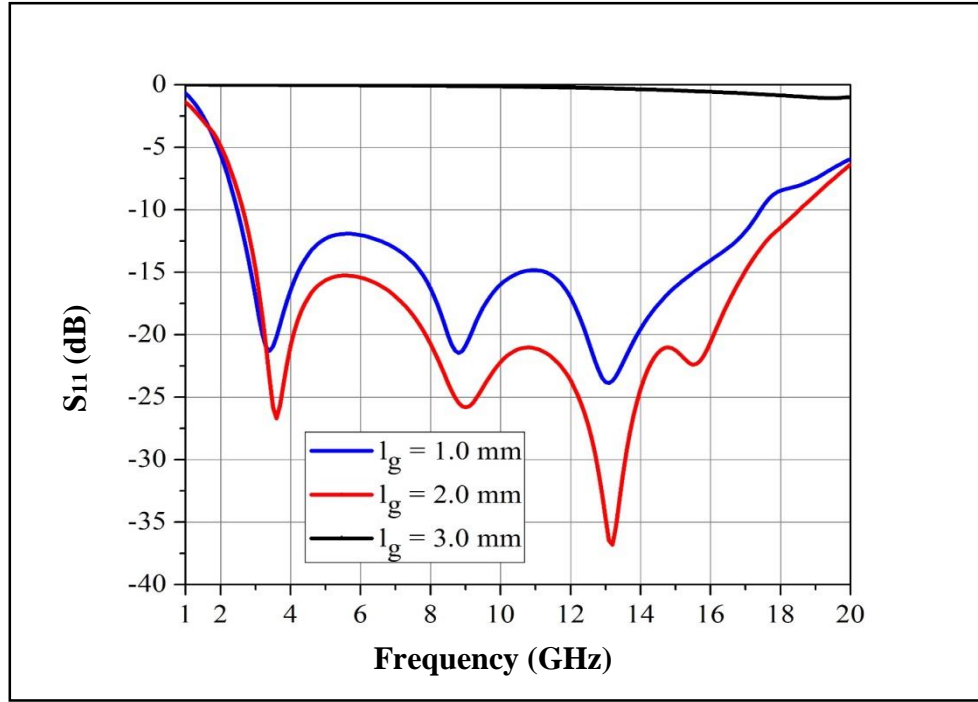


Fig. 2.29 Effect of change in length (l_g) of the ground plane on the return-loss performance of the proposed UWB antenna-4.

Change in Dimensions of Semicircular Patch Radius (r_1)

As shown in Fig. 2.30, the return-loss bandwidth is not much affected by the variations in the semicircular patch radius (r_1). For the antenna under consideration, the value of r_1 was finalised as 9 mm.

Change in the Dimensions of Slot Radius (r_2)

For better impedance matching, a circular slot along with a rectangular slot has been created near the stepped feed line. The slot introduces capacitance which in turn nullifies the inductance formed due to the feed line, resulting in improved impedance matching. The shape and size of this slot plays very important role in the optimisation of antenna performance. The return-loss performance for different slot sizes is shown in Fig. 2.31. It can be seen that $r_2 = 1.9$ mm is the most optimal value.

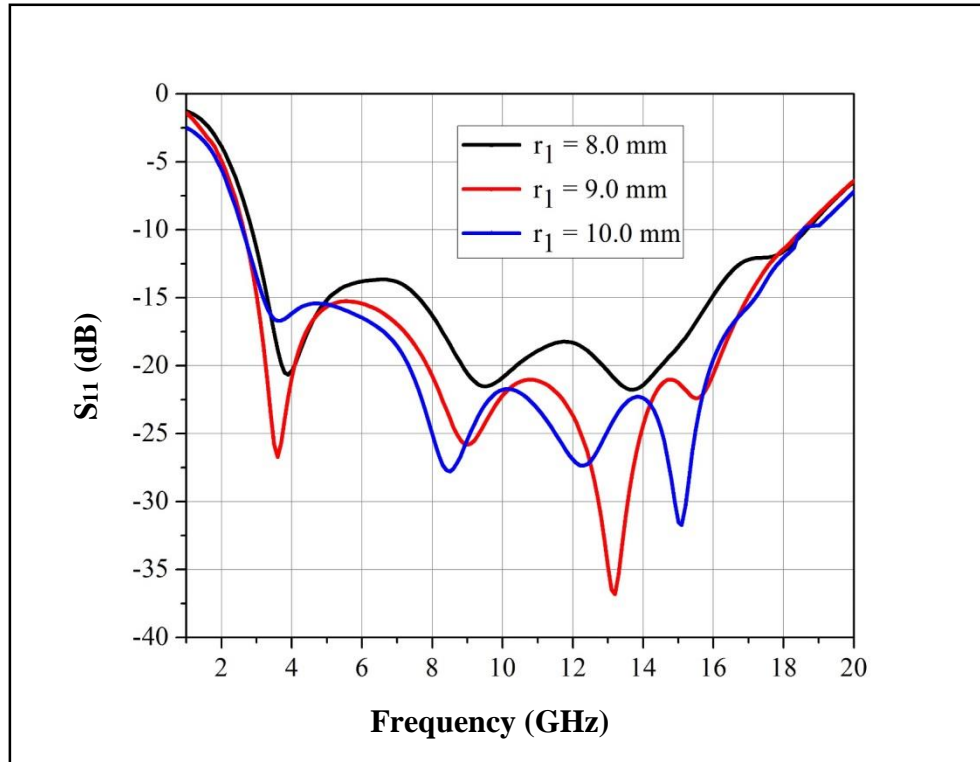


Fig. 2.30 Effect of change in patch dimension (r_1) on the return-loss performance of the proposed UWB antenna-4.

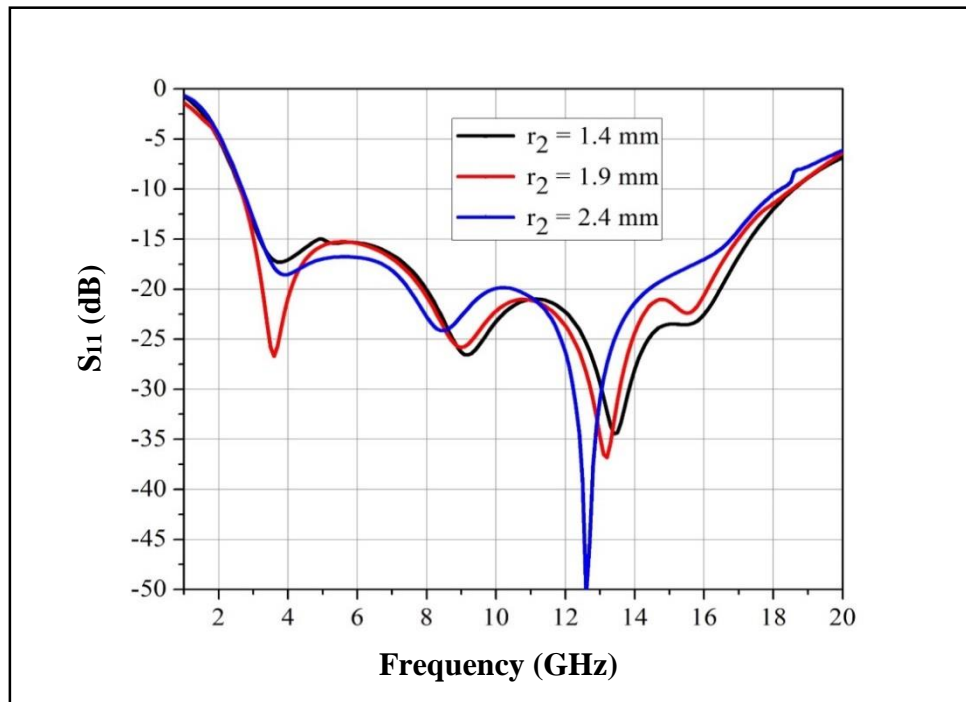


Fig. 2.31 Effect of change in slot dimension (r_2) on the return-loss performance of the proposed UWB antenna-4.

2.4.4 Radiation Patterns of the Proposed UWB Antenna-4

The simulated radiation patterns of the proposed antenna at 5, 10 and 15 GHz are shown in Fig. 2.32. At lower frequencies, they are omni-directional. However, for 15 GHz and above, the antenna becomes more directional. Also at 10 GHz a back lobe is observed. In this design, a circular slot along with a rectangular slot has been used for better impedance matching. The dimension of these slots may not be effective at lower frequencies due to its small size in comparison to wavelength but might have impact at higher frequency leading to leakage of RF and formation of side lobes. Since a microstrip monopole antenna is designed as an ultra-wideband antenna, the average gain is low and found to vary between 1 to 5 dBi throughout the band. A graph of the peak gain versus frequency is shown in Fig. 2.33.

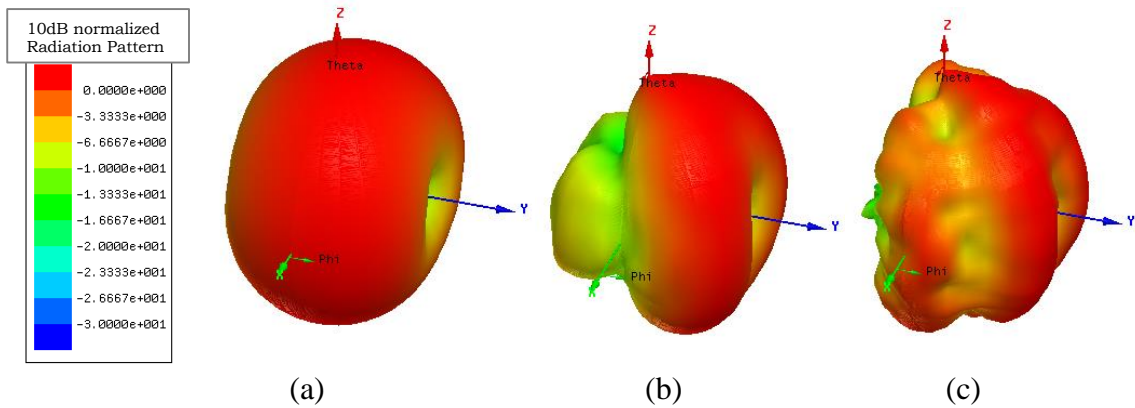


Fig. 2.32 Radiation patterns of the proposed UWB antenna-4 (a) 5 (b) 10 and (c) 15 GHz.

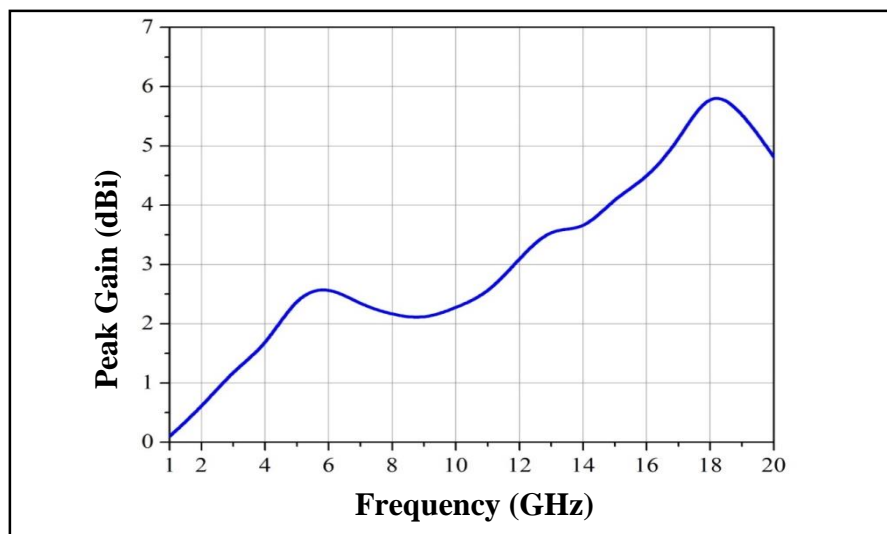


Fig. 2.33 Peak gain of the proposed UWB antenna-4.

A new design of compact printed monopole antenna has been proposed for use in portable devices. Stepped feed line for impedance matching technique has been used to enhance the antenna performance. Return-loss, better than 10 dB has been achieved in 3.1–17.1 GHz frequency band. The average gain of the antenna under consideration is about 1 to 5 dBi. A maximum simulated efficiency of 94% was achieved from the proposed design.

2.5 Summary

In this chapter, the design, development and results of four microstrip-fed printed monopole antennas operating in the range of 3.1–20 GHz have been discussed. The measured return-loss results are in close agreement with the simulated ones for all the prototypes. Minor variations may be due to fabrication tolerance, effects of SMA connectors, limitations of the simulation software, etc.

The important features of the prototype antennas are summarised in Table 2.5. It can be seen that a quarter circular and a goblet-shaped patch antenna are compact in size and provide ultra-wide impedance bandwidth. The radiation patterns of all the proposed antennas are like those of a dipole antenna at low frequencies, which become directional towards higher frequencies. It was also observed that the size of the partial ground plane and its distance from the main radiating patch are the most critical design parameters and decide the impedance bandwidth of the antenna.

Table 2.5 Summary of Proto Type Patch Antennas: Class I

Design	Substrate	Size (mm ²)	Area (mm ²)	BW (GHz)
Modified rectangular printed monopole antenna	TM-3	16×18	288	3.5–15.2
Half hexagonal circular-shaped patch antenna	RT/duroid-5880 (TM)	50×35	1750	3.1–14.1
Quarter circular patch antenna	FR-4	35×20	700	3.1–16.3
Goblet-shaped patch antenna	RT/duroid-5870 (TM)	24×24	576	3.1–17.1

The design details and associated results of a few Class-II UWB patch antennas operating in the range 3.1–30 GHz are discussed in the next chapter.

UWB PATCH ANTENNAS-CLASS II

In the previous chapter, we have examined various designs of microstrip monopole antennas operating with bandwidths up to 20 GHz. Very few antennas have been reported in the open literature operating in the frequency range 3-30 GHz. In this chapter, we have concentrated on the design of two UWB antennas that can be used up to that range. For comprehension, these two antennas have been discussed here under Class-II category. Such antennas find application in spectrum monitoring, wireless communication, vehicular radars, through-wall imaging systems, etc.

2.1 Truncated Circular Printed Monopole Antenna-5

In this design, a truncated circular patch antenna has been designed and simulated. The antenna achieves the impedance bandwidth (10 dB return-loss) from 2 to 22.2 GHz. Its design details and results are described below:

2.1.1 Design of the Proposed UWB Patch Antenna-5

The design layout of the proposed antenna is shown in Fig. 3.1. The antenna was designed on RT/duroid 5880 substrate with size $40 \times 35 \times 1.6$ mm³. A circular monopole microstrip antenna was selected as the starting point, as it offers the maximum impedance bandwidth in comparison with other monopole configurations. The width of the main feed line (w_f) was calculated for 50 Ω characteristic impedance using the empirical formulas given in (Pozar, 2012; Liao 1989). The lower frequency of operation for the patch antenna under consideration can be approximately determined as suggested by Kumar and Ray (2003) at 2.7 GHz. For proper impedance matching, a microstrip feed line with different stepped widths has been used. Since the impedance of the microstrip antenna is observed to be maximum at its edges (around 300 Ω), the same needs to be matched to 50 Ω at SMA connector. To achieve this, three segments of different width and length have been used. The width of the stepped feed line is maximum at SMA connector to match 50 Ω and minimum at circular radiating patch to match the impedance around 300 Ω . As starting

point, the lengths of all the three segments were selected as 4.5 mm. This is about quarter wavelength at center operating frequency and the same was further optimized to achieve maximum UWB behavior. Initially Different slots have been introduced on the main radiating patch to increase the perimeter of the antenna and its physical length. This helps in reducing the lower operating frequency. The different geometrical parameters of the antenna and corresponding dimensions are listed in Table 3.1.

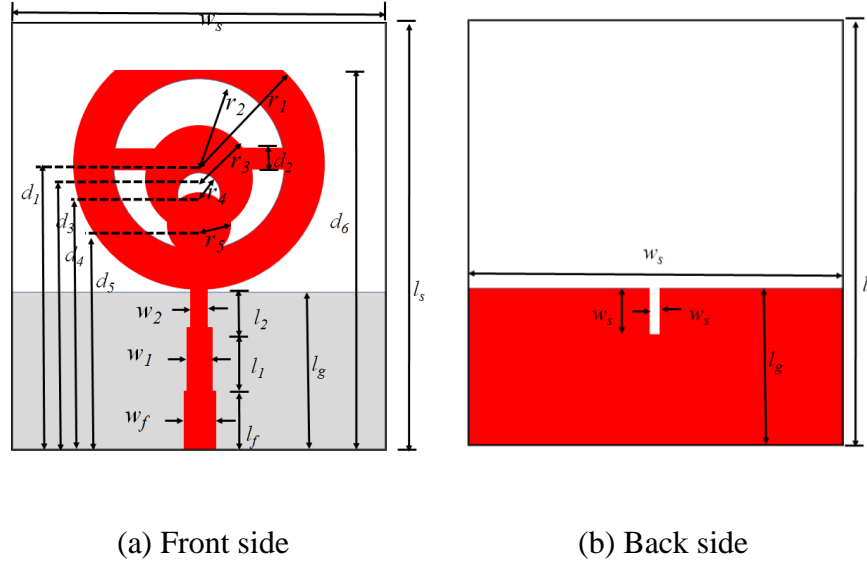


Fig. 3. 1 Layout of the proposed UWB antenna-5 under consideration.

Table 3.1 Design Parameters of UWB antenna-5

Design Parameter	Value (mm)	Design Parameter	Value (mm)	Design Parameter	Value (mm)
l_s	40	l_3	4	d_1	27.1
w_s	35	w_3	1	d_2	27
l_f	5.5	r_1	11.8	d_3	25.3
w_f	3	r_2	8	d_4	24
l_1	6	l_g	14.8	d_5	21
w_1	2.4	r_3	5	d_6	35.9
l_2	4	r_4	2		
w_2	1.6	r_5	3		

2.1.2 Return-Loss Performance of the UWB Antenna-5

The return-loss performance of the proposed antenna under consideration was simulated using the commercially available simulation software, HFSS. All the design parameters were optimised to achieve the maximum return-loss bandwidth. As shown in Fig. 3.2, the simulated return-loss bandwidth covers 2–22.2 GHz frequency band for better than 10 dB return-loss.

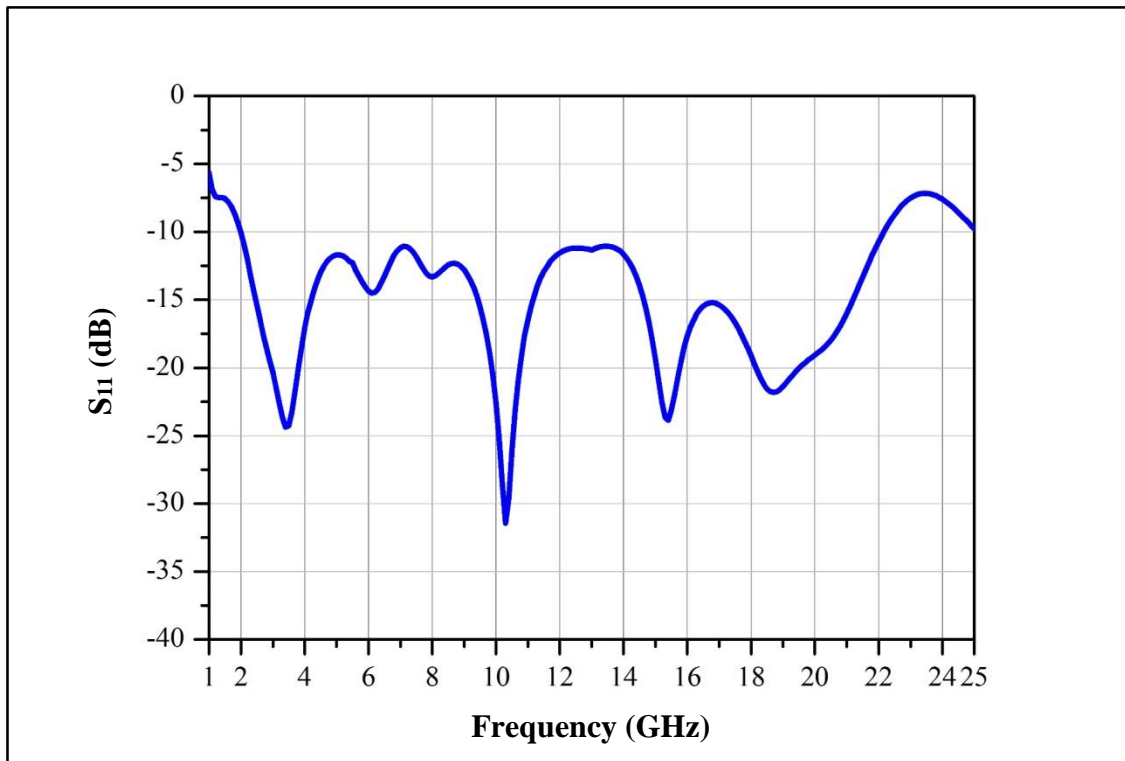


Fig. 3. 2 Return-loss performance of the proposed UWB antenna-5.

2.1.3 Parametric Study of the Proposed UWB Antenna-5

The antenna design parameters were selected based on the parametric analysis of the design under consideration. Different geometrical parameters like substrate material, ground size, patch size and main feed line width were varied to see their effect on the return-loss performance of the antenna. The details are presented here.

Change in Substrate Materials

The effect of change in the substrate material on the antenna impedance bandwidth is shown in Fig. 3.3. For this study, substrate materials like Roger RT/duroid5880 (relative permittivity 2.2, loss tangent 0.0009), Roger RO 3003 (relative permittivity 3, loss tangent 0.0013) and FR-4 (relative permittivity 4.4, loss tangent 0.02), all with thickness 1.6 mm have been considered. It can be seen that the selection of the substrate material affects both the lower and upper cutoff frequencies. Further, Roger RT/duroid 5880 substrate provides the optimum performance covering frequencies from 2 to 22.2 GHz (167%).

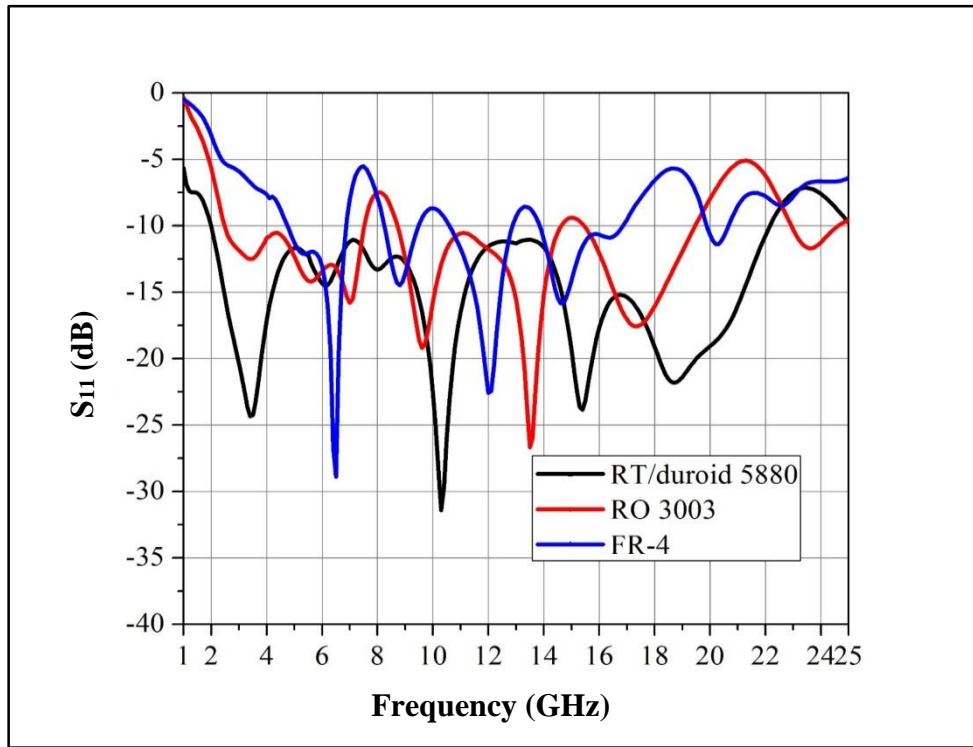


Fig. 3.3 Effect of change in the substrate material on return-loss performance on the proposed UWB antenna-5.

Change in the Dimensions of the Radiating Patch

The antenna performance is highly decided by the shape and size of the main radiating patch. The lower cutoff frequency of the antenna is governed by the radius of radiating

patch. Figure 3.4 depicts the return-loss performance of the antenna under different values of patch radius. It can be seen that $r_l = 11.8$ mm offers the best performance.

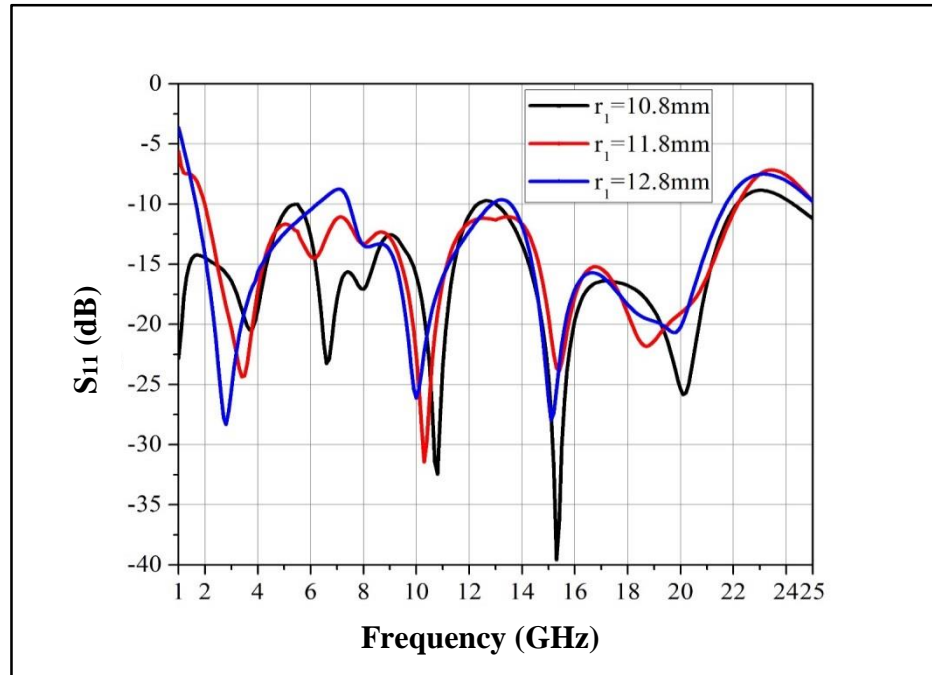


Fig. 3.4 Effect of change in the patch dimension (r_l) on the return-loss performance of the proposed UWB antenna-5.

Main Feed Width

The width of the feed line determines the impedance (Z_0). As the feed line width increases, Z_0 will start decreasing. It is evident from Fig. 3.5 that for $w_f = 2.5$ mm, the return-loss is better than 10 dB throughout the band, except at 7.4 GHz frequency. The best performance can be achieved at $w_f = 3$ mm. If its value is increased to 3.5 mm, the loss is drastic.

Partial Ground Plane Dimensions

The small feed gap between the finite partial ground plane and the main radiating patch decided by l_g is a very critical parameter which affects the antenna impedance matching between the microstrip feed line and the radiating disc. The effect of change in ground plane dimensions is simulated and is shown in Fig. 3.6. The ground size $l_g = 14.8$ mm provides the optimum performance. At $l_g = 13.8$ mm, the lower cutoff frequency is not affected much; however, the return-loss is degraded after 4.1 GHz. The value of $l_g = 15.8$ mm, shifts the lower cutoff frequency to 1.3 GHz and the higher cutoff frequency to 6.3 GHz. Thus, in this case, the overall bandwidth reduces.

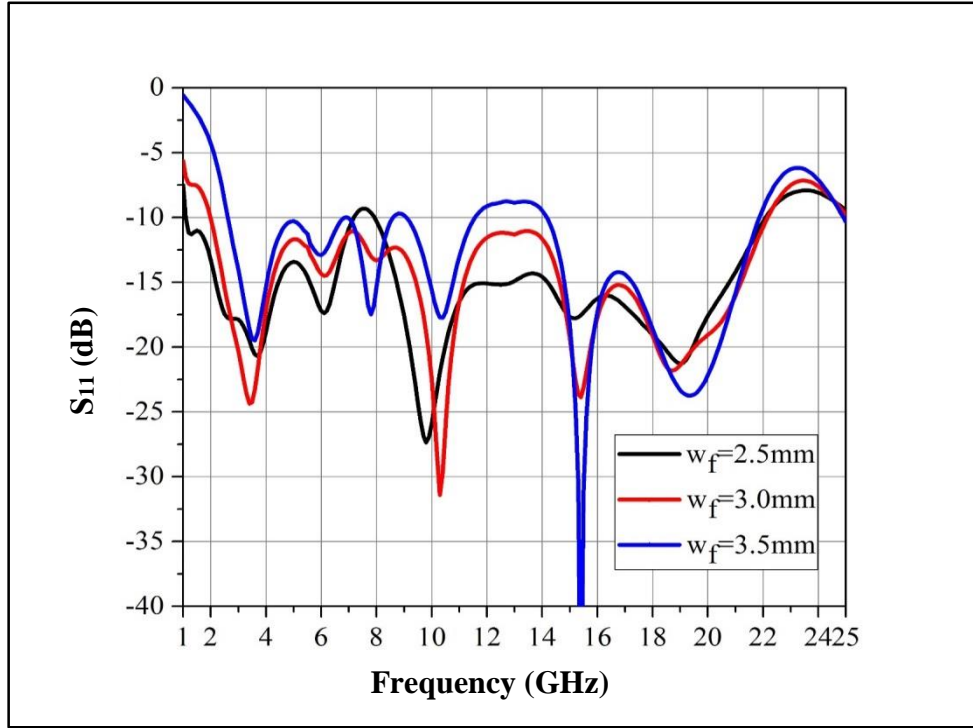


Fig. 3.5 Effect of change in the main feed width (w_f) on the return-loss performance of the proposed UWB antenna-5.

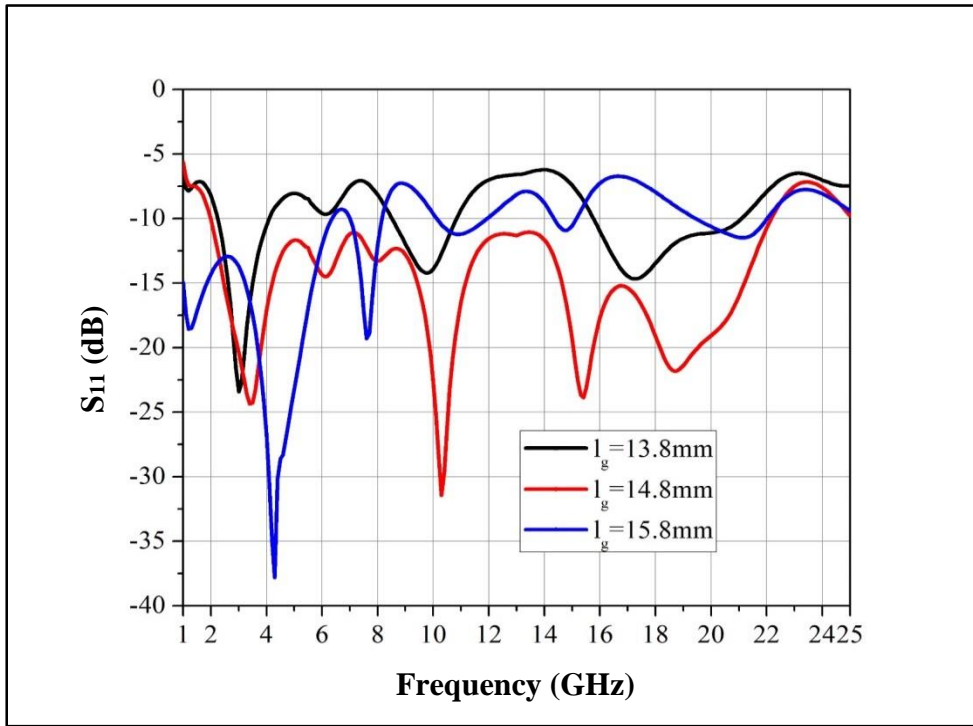


Fig. 3.6 Effect of change in length (l_g) of the ground plane on the return-loss performance of the proposed UWB antenna-5.

2.1.4 Radiation Patterns of the Proposed UWB Antenna-5

The radiation patterns of antenna under consideration at 5, 10, 15 and 20 GHz are shown in Fig. 3.7. It is observed that the pattern at lower frequencies (up to 10 GHz) in horizontal plane is of donut shape of a dipole antenna. For frequency of 15 GHz and above, the patterns become directional. The plot of peak gain versus frequency is shown in Fig 3.8. The maximum gain of the antenna is in the range of 2–6 dBi up to 18 GHz. The peak gain shoots up above 18 GHz.

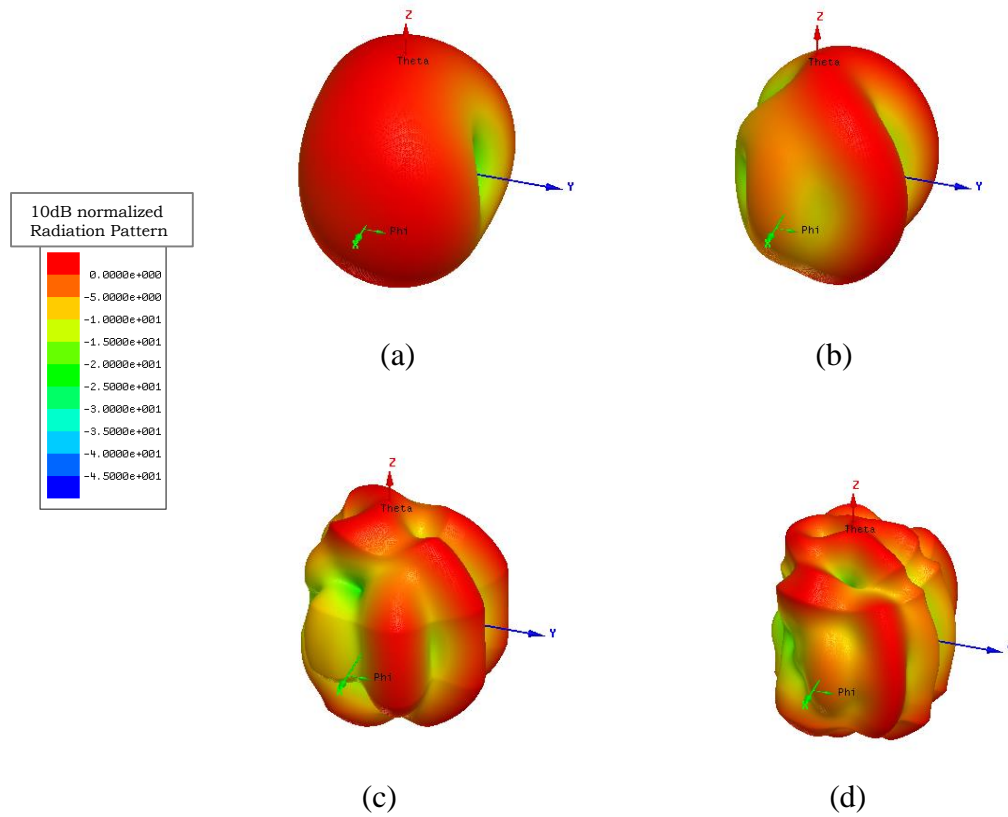


Fig. 3.7 Radiation patterns of the proposed UWB antenna-5: (a) 5, (b) 10, (c) 15 and (d) 20 GHz.

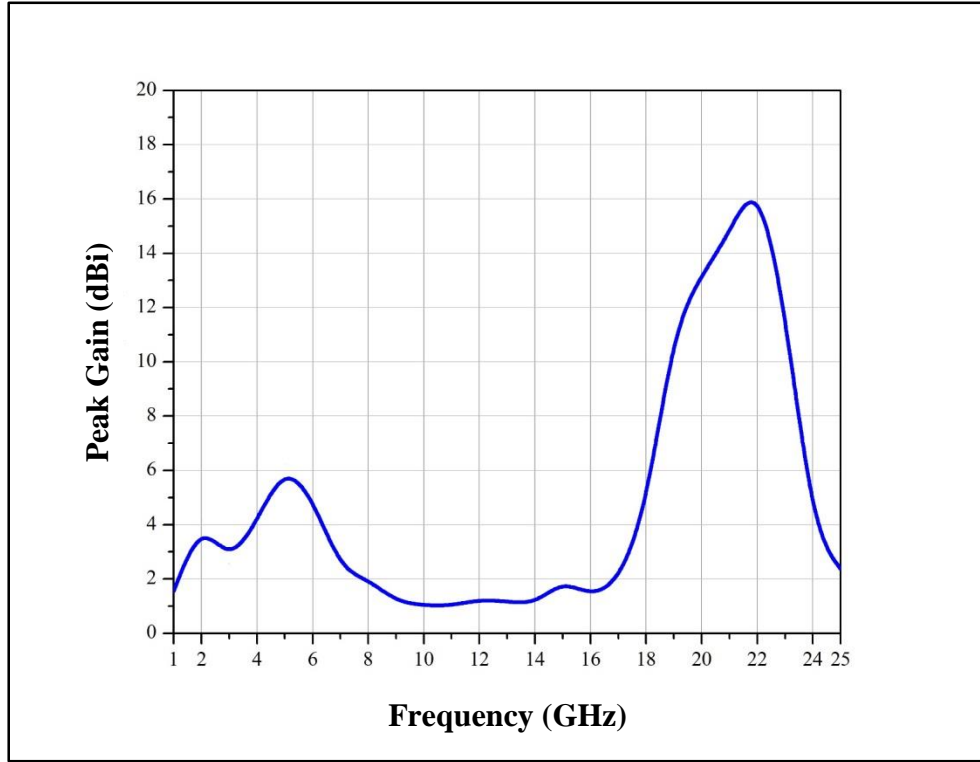


Fig. 3.8 Peak gain of the proposed UWB antenna-5.

In this antenna design, a compact circular monopole antenna has been designed and simulated. Its overall size is $35 \times 40 \times 0.787 \text{ mm}^3$. A stepped microstrip feed matching network with a partial ground plane has been used to enhance the antenna's bandwidth. A simulated return-loss better than 10 dB was achieved for frequency band covering 2–22.2 GHz.

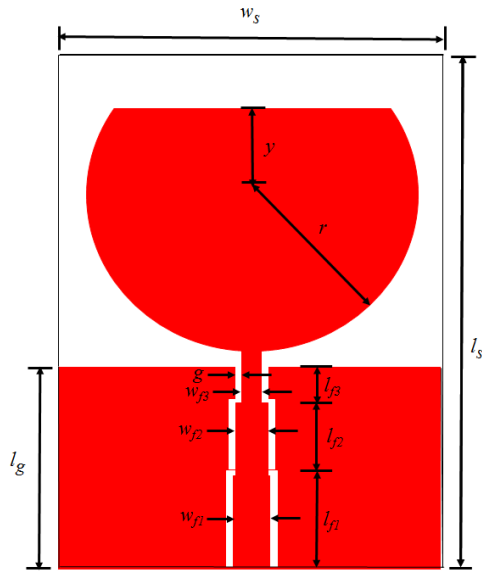
2.2 CPW-Fed Truncated Circular-Shaped Printed Monopole Antenna-6

There are various feeding techniques, such as microstrip line feed, coaxial probed feed, aperture-coupled and electromagnetically coupled, coplanar waveguide (CPW), etc. to excite a microstrip antenna (Kumar and Ray, 2003). However, the most widely used techniques are the microstrip line and co-planar waveguide (CPW) feed. A CPW consists of a center metallic strip deposited on the surface of a dielectric substrate slab with two narrow slits ground electrodes running adjacent and parallel to the strip on the same surface.

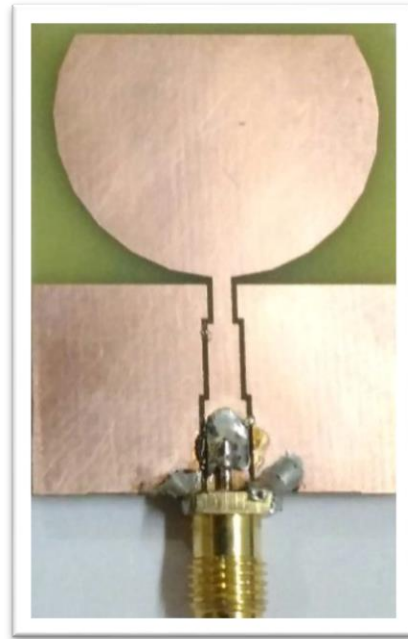
A microstrip antenna fed by a co-planar waveguide (CPW) feed has many advantages over the conventional microstrip line feed antenna. Apart from small size, light weight, ease of fabrication, it offers wide impedance bandwidth, low dispersion and lower radiation loss as compared to the conventional microstrip line feed antennas. In this section, a CPW-fed truncated circular-shaped printed monopole antenna is discussed.

2.2.1 Design of the Proposed UWB Patch Antenna-6

This is the design of a microstrip monopole antenna with a stepped microstrip feed line. It has FR-4 substrate with thickness $h = 0.787$ mm, copper cladding of 0.035 mm thickness and relative permittivity $\epsilon_r = 4.4$, and loss tangent $\tan \delta = 0.02$. The dimensions of the feed line are decided using the empirical formula suggested by Simons (Simons, 2004). The main radiating patch consists of a truncated circular patch of radius 13 mm, truncated horizontally at height of 6.7 mm from the center of the patch. The antenna geometry is shown in Fig. 3.9. The optimised antenna design parameters are listed in Table 3.2.



(a) Layout



(b) Photograph of fabricated antenna

Fig. 3.9 Layout of the proposed UWB antenna-6 under consideration.

Table 3.2 Design Parameters of UWB Antenna-6

Design Parameter	Value (mm)	Design Parameter	Value (mm)
l_s	40	w_{f3}	1.6
w_s	30	l_{f3}	4
w_{f1}	3	l_g	16.1
l_{f1}	7	r	13
w_{f2}	2.4	y	6.7
l_{f2}	6	g	0.52

2.2.2 Return-Loss Performance of UWB Antenna-6

The antenna was simulated using the Electromagnetic Simulator, HFSS. The variations in return-loss (for $S_{11} \leq 10$ dB) for different frequencies are plotted in Fig. 3.10. For the prototype antenna, the return-loss was measured using the Vector Network Analyser. From the figure, it can be seen that the measured response follows the simulated performance closely. The simulated impedance bandwidth is observed from 2.8 to 28.2 GHz, whereas the measured bandwidth is from 2.6 to 26.5GHz.

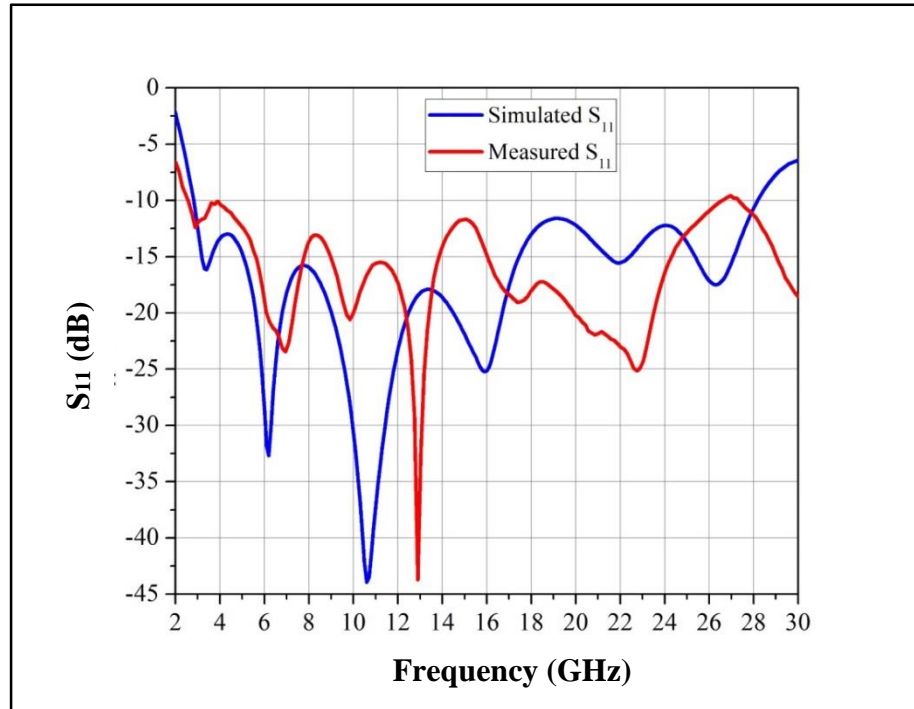


Fig. 3.10 Simulated and measured return-loss performance of the proposed UWB antenna-6.

2.2.3 Parametric Study of the Proposed UWB Antenna-6

In order to study the effect of change in various parameters on the antenna return-loss, a comprehensive parametric study was carried out. The results are discussed with suitable graphs.

Change in the Substrate Material

The effect of change in substrate material on the return-loss performance is plotted in Fig. 3.11. It is important to note that while carrying out this parametric study all other antenna design parameters were kept the same. In this simulation study, substrate materials like Roger RT/duroid 5880 (tm), FR-4 and RT/duroid 3006 (tm) have been considered. It can be seen that the lower and higher cutoff frequencies are dependent on the type of substrate material. For the design under consideration, we have used the FR-4 substrate.

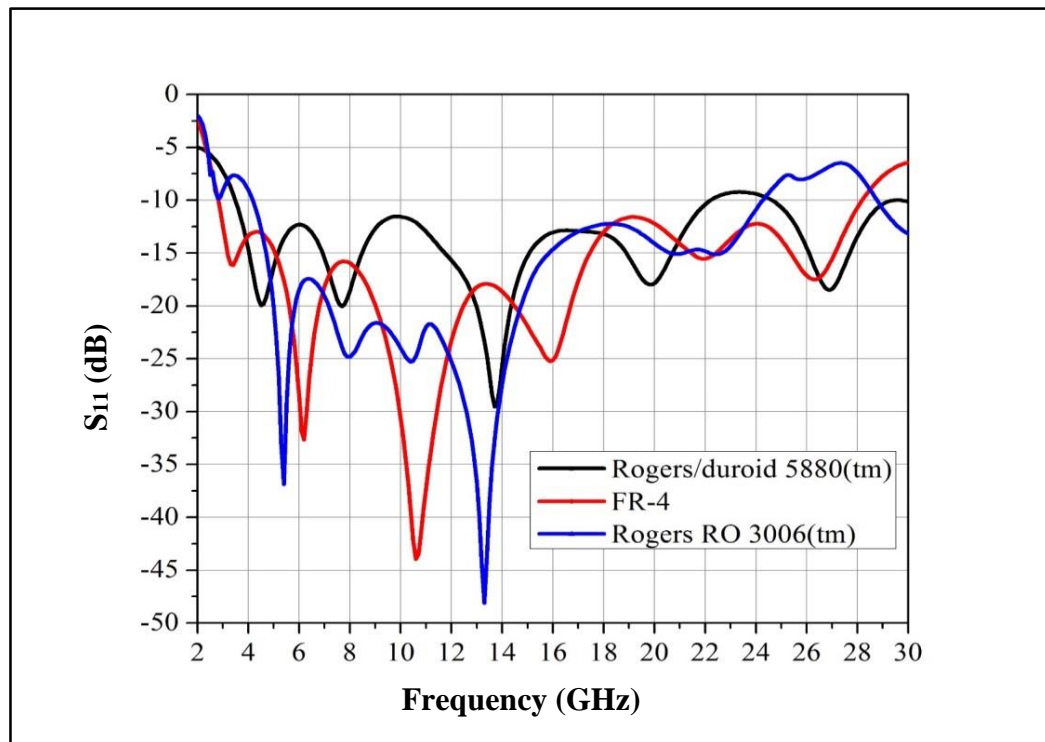


Fig. 3.11 Effect of change in the substrate material on the return-loss performance of the proposed UWB antenna-6.

Change in Dimensions of the Gap Size (g)

The gap size (g), seen in Fig. 3.9, is also an important parameter and affects the performance of an antenna. The simulated results of return-loss for different values of g are plotted in Fig. 3.12. From the simulation results it can be seen that the smaller value of g helps in extending the impedance bandwidth towards the lower end of frequency. However, it affects the upper cutoff frequency also. After several trials, we decided to keep the value of g at 0.52 mm.

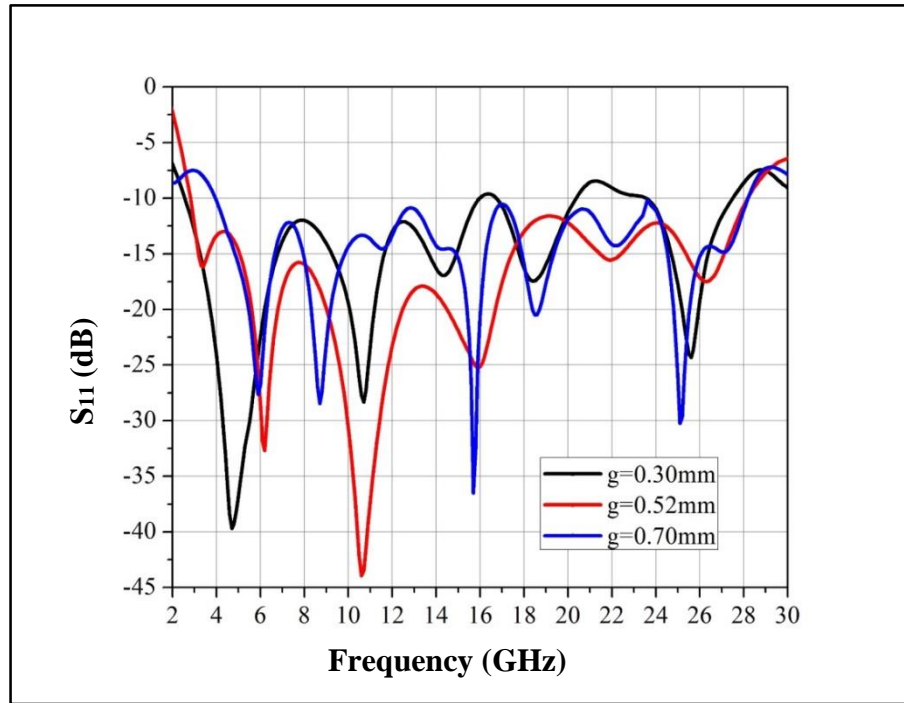


Fig. 3.12 Effect of change in feed gap (g) on the return-loss performance of the proposed UWB antenna-6.

Change in the Dimensions of the Partial Ground Plane (l_g)

Generally, for this type of antenna configuration, the dimensions of the ground plane should be decided with utmost care, as it affects its performance. As part of the parametric study, we have changed the value of l_g and studied its dependence on the antenna return-loss. The simulated results are presented in Fig. 3.13. From the plot, it can be seen that the antenna return-loss is highly dependent on the value of l_g . Finally, we decided to keep l_g at 16.1 mm.

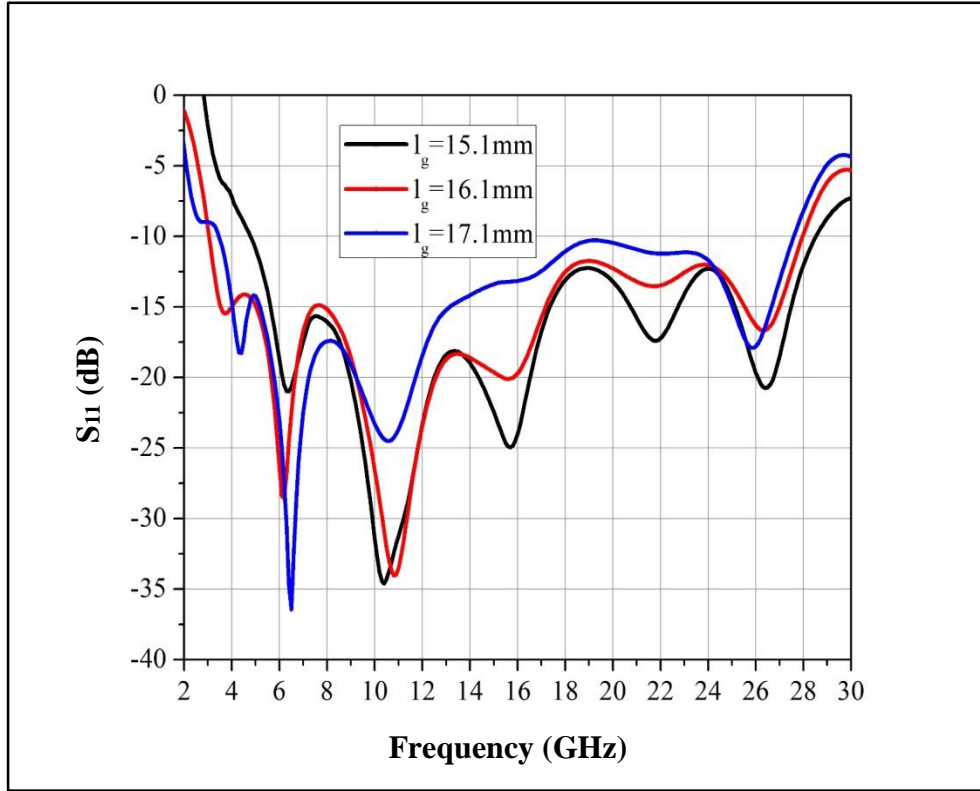


Fig. 3.13 Effect of change in the length (l_g) of the ground plane on the return-loss performance of the proposed UWB antenna-6.

2.2.4 Radiation Patterns of the Proposed UWB Antenna-6

The radiation patterns of the proposed antenna at 5, 10, 15, 20 and 25 GHz are shown in Fig. 3.14. It is observed that the pattern at lower frequencies (up to 10 GHz) in horizontal plane is in donut shape of a dipole, while at 15 GHz and higher the shape gets distorted and multiple side lobes appear. The simulated antenna gain for different frequencies is shown in Fig. 3.15. The antenna gain is found to vary between 1 and 4.4 dBi.

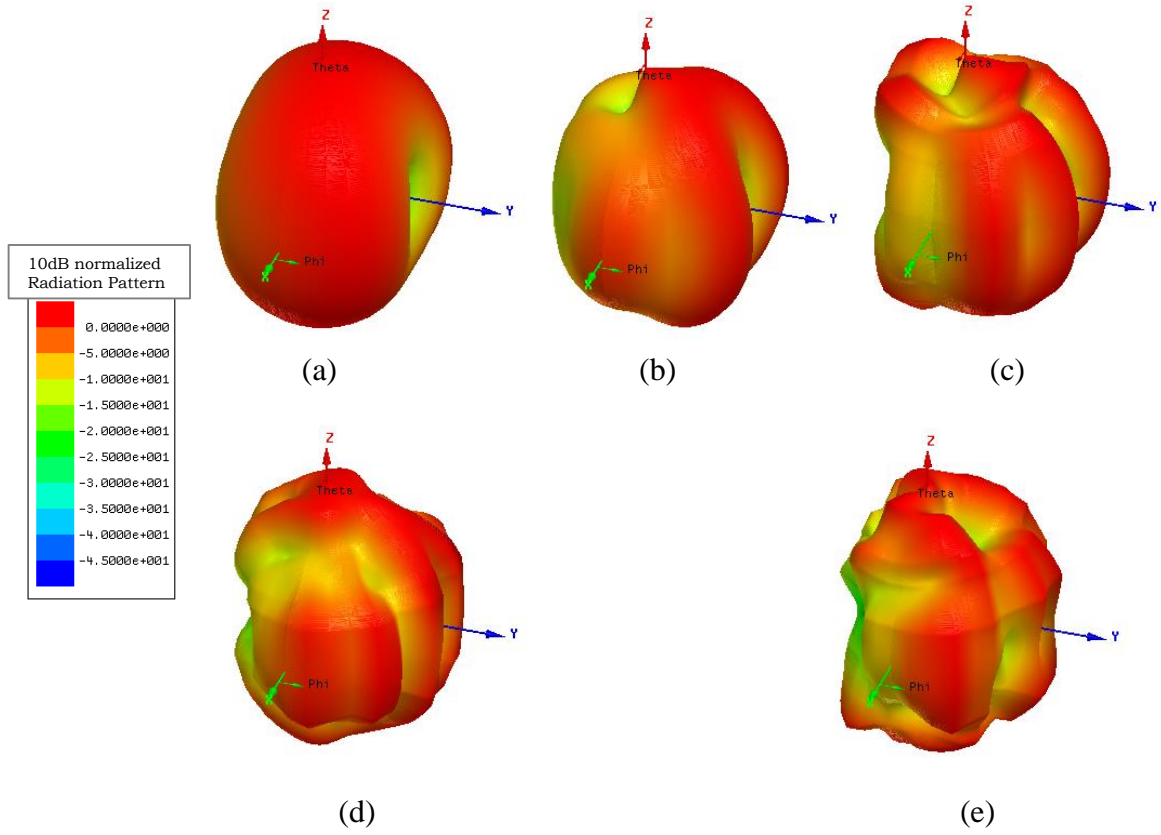


Fig. 3.14 Radiation patterns of the proposed UWB antenna-6: (a) 5, (b) 10, (c) 15, (d) 20, and (e) 25 GHz.

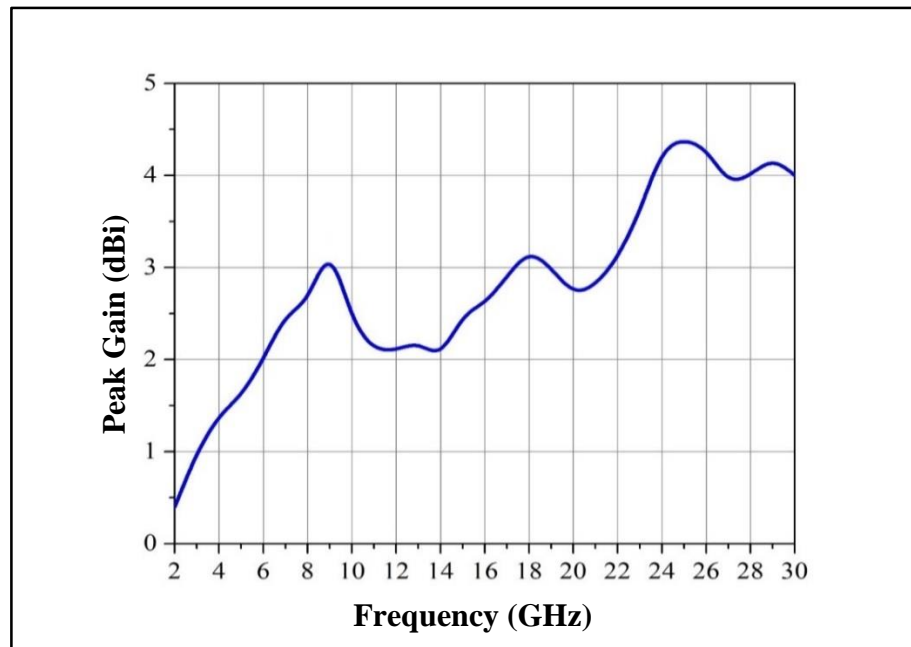


Fig. 3.15 Peak gain of the proposed UWB antenna-6.

In this section, the design of a compact CPW-fed microstrip monopole antenna is discussed. The antenna operates from 2.6 to 26.5 GHz. The measured return-loss characteristic almost matches with the simulated results.

2.3 Summary

In this chapter, the design and corresponding results of two microstrip-fed printed monopole antennas have been presented. The impedance bandwidth of antenna-5 is 166.9% and of antenna-6 is 164.3%. The radiation patterns of both the antennas are like a dipole antenna at low frequencies, which become directional towards higher frequencies. From parametric studies it is observed that the size of the partial ground and its distance from the main radiating patch and gap size are the most critical parameters for microstrip-fed patch antenna. The summary of the both proposed design is summarised in Table 3.3.

Table 3.3 Summary of Proto Type Patch Antennas: Class II

Design	Substrate	Size (mm ²)	Area (mm ²)	BW (GHz)
Truncated circular patch antenna	RT/duroid -5880	40×35	1400	2.0–22.2
CPW fed truncated circular patch antenna	FR-4	40×30	1200	2.6–26.5

Mokhtaari and Bornemann have proposed a patch antenna of size $40.75 \times 46 \text{ mm}^2$, operating from 3 to 25 GHz (Mokhtaari and Bornemann, 2011) with a notch at desired frequency by using the Electromagnetic Band Gap (EBG) pattern at feed line. The UWB antenna was designed by selecting six points on a circular patch and optimizing the resulting polygon for maximum voltage standing wave ratio (VSWR) bandwidth on RT3003 substrate of 1mm thickness. The proposed CPW-fed patch antenna, discussed in this chapter, operates from 2.6 to 26.5 GHz with a comparatively compact size ($40 \times 30 \text{ mm}^2$).

In the next chapter, we discuss a few prototype UWB antennas operating in the 3.1–40 GHz frequency range.

CHAPTER-4

UWB PATCH ANTENNAS-CLASS III

In the previous chapters, several designs of patch antennas with bandwidth from 3 to 30 GHz are discussed. Till date, mostly the commercially available equipment are designed for Ku band (up to 18 GHz) while a few military applications utilize K band (up to 26.5 GHz). However, congestion in the lower gigahertz (GHz) frequency band has made the scientists, the researchers and the industries to look for alternative antenna designs in the millimeter-wave frequency range. Many military and aerospace industries are looking to millimeter-wave technology to increase connectivity and sensing for the next generation of tactical networks, security and electronic warfare (DeLisle, 2014). The millimeter waves provide high directive beam, leading to good angular resolution with small antennas. The millimeter wave systems are generally small in size and light in weight compared to their microwave counterparts. Such systems require suitable antenna(s) for EM wave transmission and reception (Millimeter Waves Enhance Military Projects, 2017).

This chapter describes the designs of four microstrip patch antennas able to cover from 3 to 40 GHz frequency. For bifurcation purpose, these four antennas are put under Class-III antenna category.

2.1 Tri-Circular Printed Monopole Antenna-7

In this design, a tri-circular microstrip patch antenna fed with a microstrip feed line; operating from 2.3-37.6 GHz is presented. The main radiating patch comprises of a circular patch, overlapped by two off-centered circular patches. The design details and the results are presented in different sub-sections.

2.1.1 Design of the Proposed UWB Patch Antenna-7

A tri-circular patch antenna consists of a circular radiating patch along with two overlapping circular patches fed with a microstrip feedline was designed and simulated. The partial ground plane has been used to provide UWB characteristics. Three microstrip lines with different width have been used to feed the radiating patch. The initial value of r_1

and r_2 was considered 13 mm based on antenna design-6. After optimization for maximum UWB return-loss behavior, r_1 and r_2 were found to be 13 and 11 mm, respectively.

Figure 4.1 is the schematic diagram of the antenna developed on the FR-4 substrate. The dimensions of the antenna are $40 \times 50 \times 1.6 \text{ mm}^3$. The different geometrical parameters of the antenna and corresponding dimensions are listed in Table 4.1.

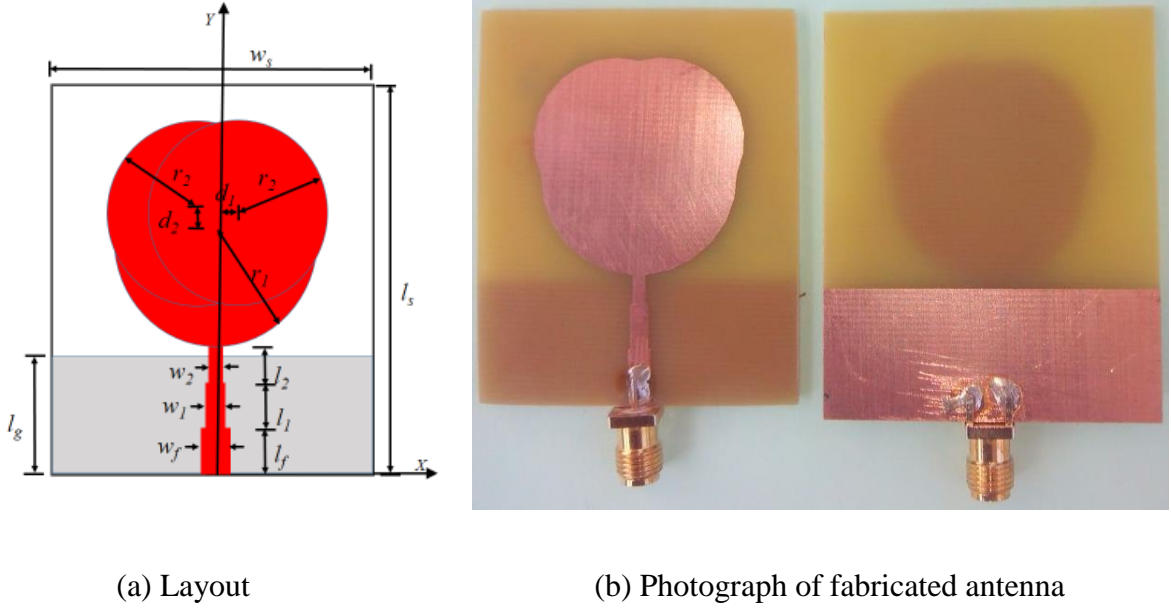


Fig. 4.1 Design of the proposed UWB antenna-7 under consideration.

Table 4.1 Design Parameters of UWB Antenna-7

Design parameter	Value (mm)	Design parameter	Value (mm)
l_s	50	l_2	4
w_s	40	w_2	1.6
r_1	13	l_g	15
l_f	6	r_2	11
w_f	3	d_1	3
l_l	6	d_2	5
w_l	2.4		

4.1.2. Return-Loss Performance of UWB Antenna-7

The proposed antenna was designed and simulated using the HFSS simulation software and optimised to achieve maximum BW. The simulated and experimental return-loss of the optimised designs are plotted in Fig. 4.2. The return-loss bandwidth (for 10 dB reference) was achieved over a frequency band of 2.3–37.6 GHz (177%). Both simulated and experimental return-loss were mostly found to match over the entire band. Some small variations may be due to the manufacturing tolerances, effect of the SMA connector and the limitations of the simulator.

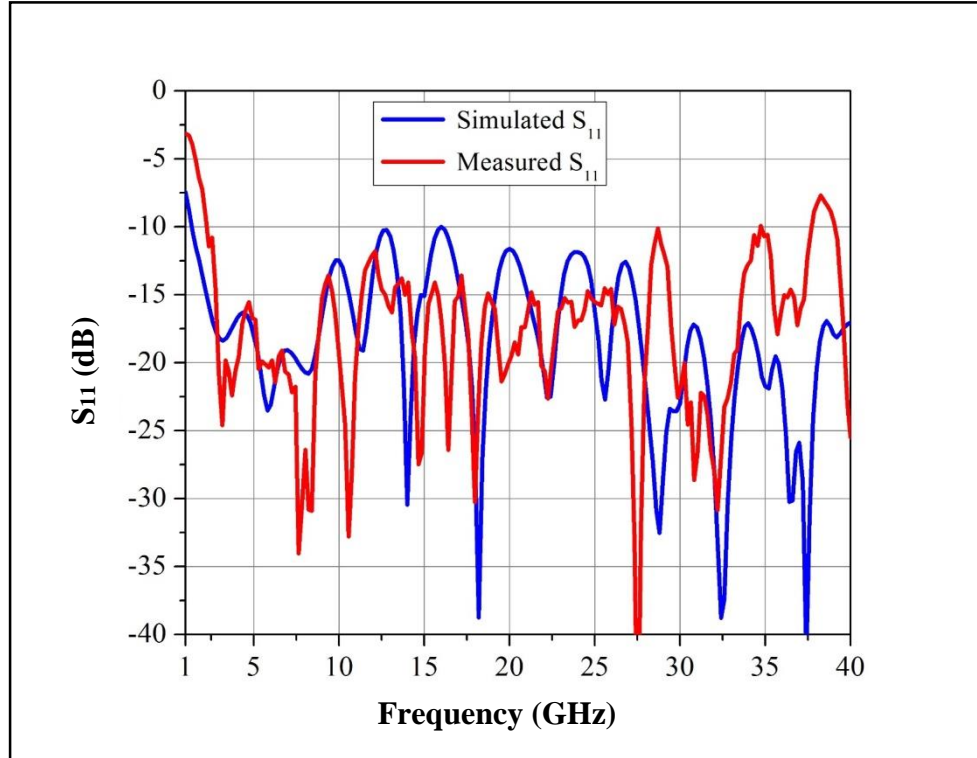


Fig. 4.2 Return-Loss Performance of the Proposed UWB Antenna-7.

2.1.3 Parametric Study of the Proposed UWB Antenna-7

The antenna geometrical parameters were finalised based on the parametric analysis of the design under consideration. The different parameters like the substrate material, ground size, radius of the main and off centered patch were varied to see their effects on the return-loss performance of the antenna. The details are given in the subsequent paragraphs.

Change in Substrate Materials

For this parametric study, different substrates like, Roger RT/duroid 5880 ($\epsilon_r = 2.2$), FR-4 ($\epsilon_r = 4.4$) and Roger RT/duroid 6006 ($\epsilon_r = 6.15$), with thickness of 1.6 mm were used to see their effect on the return-loss performance of the antenna. The results are shown in Fig. 4.3. It can be seen that the performance of Roger RT/duroid 5880 and FR-4 is similar. For the prototype design, we decided to use FR-4 substrate material.

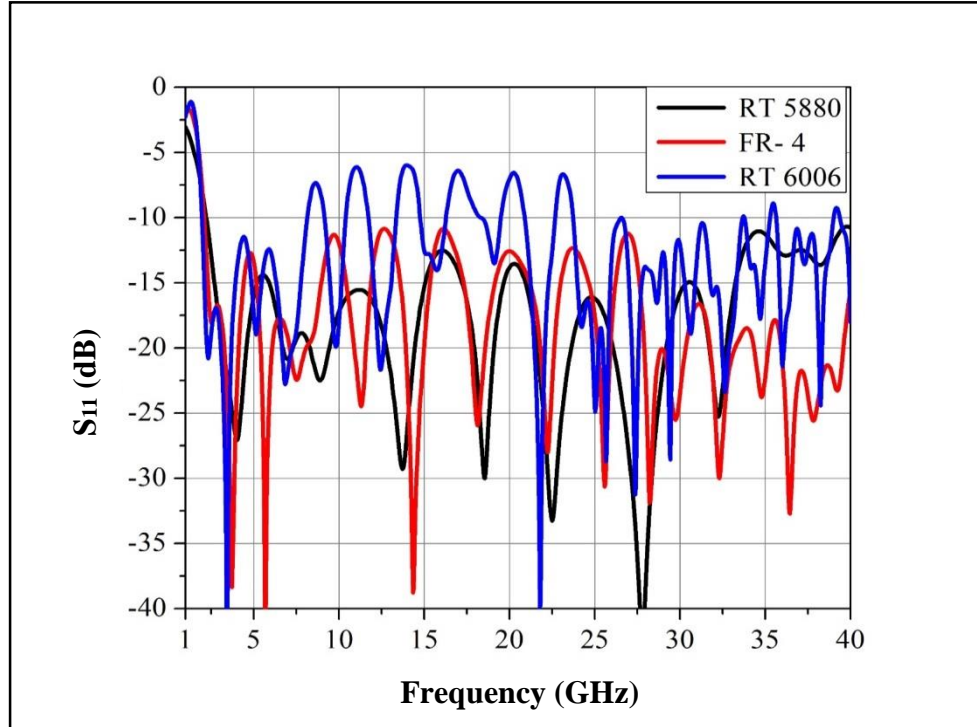


Fig. 4.3 Effect of change in substrate material on the return-loss performance of the proposed UWB antenna-7.

Change in the Dimensions of the Radiating Patch

The shape and size of any patch antenna controls the cutoff frequencies and ultimately the total bandwidth. The effects of change in r_1 and r_2 on the antenna return-loss are plotted in Figs 4.4 and 4.5, respectively. The change in any one radius (r_1 or r_2) will marginally increase the area of the monopole as most of the tri-circular patch area is overlapping to each other. Hence, there is no significant change in the return-loss characteristic. For this design, we selected $r_1=13$ mm and $r_2=11$ mm.

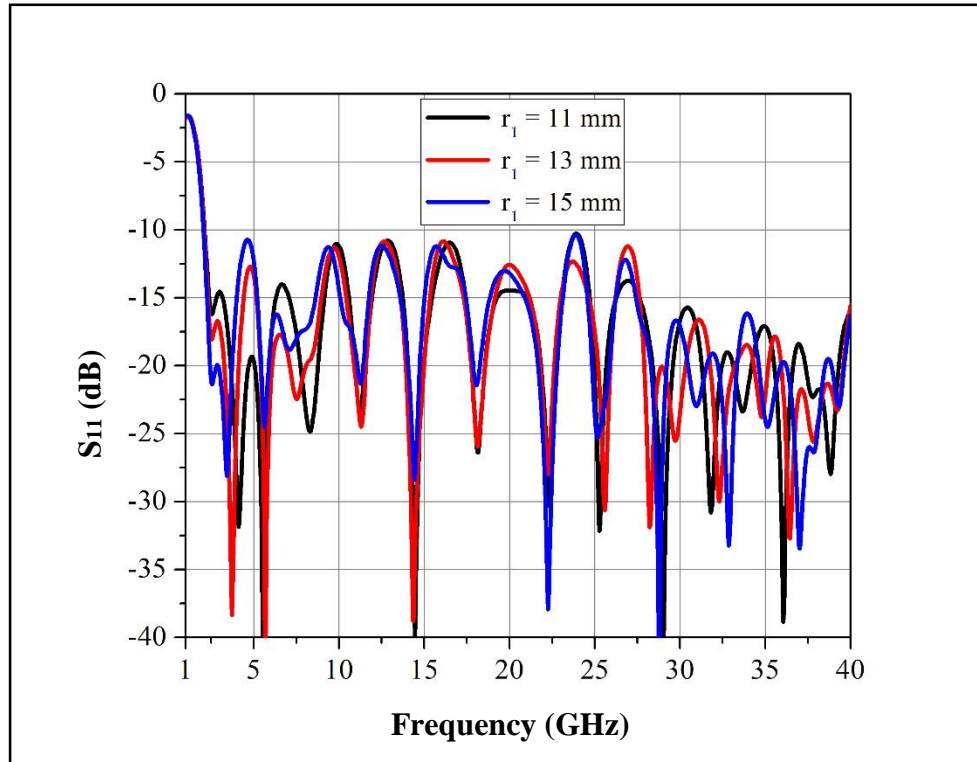


Fig. 4.4 Effect of change in patch dimension (r_1) on the return-loss performance of the proposed UWB antenna-7.

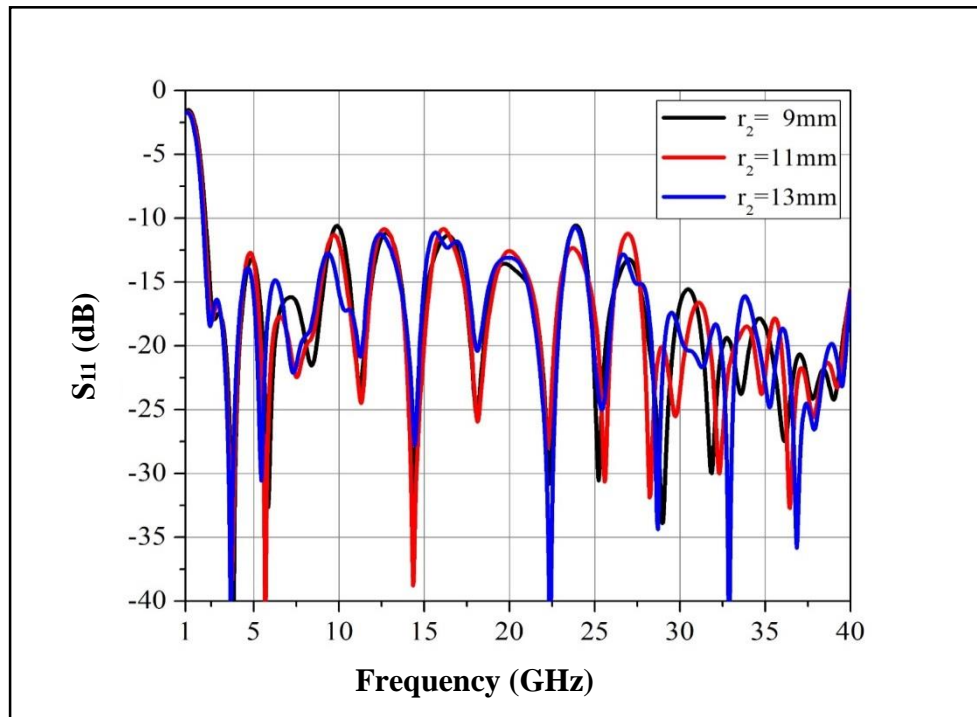


Fig. 4.5 Effect of change in patch dimension (r_2) on the return-loss performance of the proposed UWB antenna-7.

Change in the Dimensions of the Partial Ground Plane (l_g)

The partial ground plane of the patch antenna plays significant role in deciding the BW and the gain of a monopole patch antenna under consideration. The length of the ground plane (l_g) controls the coupling between the ground plane and the patch. It also acts as an additional impedance matching network. The effect of change in the ground plane length on the return-loss is shown in Fig. 4.6. Based on this study, the length of the ground plane $l_g = 15$ mm was found to provide the optimum result.

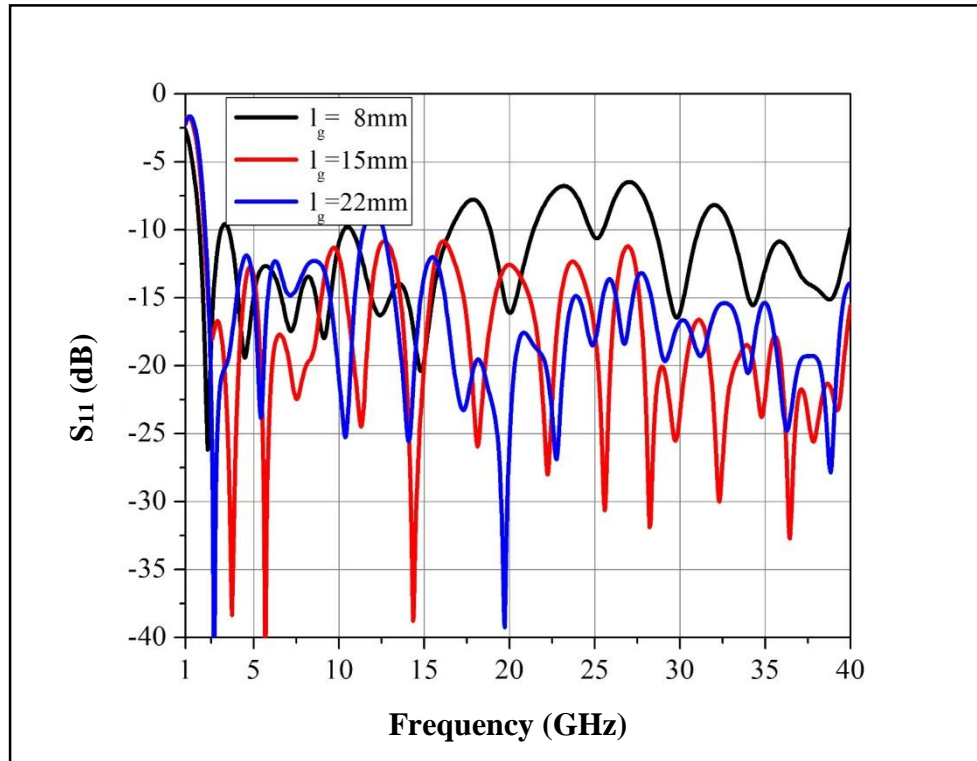


Fig. 4.6 Effect of change in length (l_g) of the ground plane on the return-loss performance of the proposed UWB antenna-7.

2.1.4 Radiation Patterns of the Proposed UWB Antenna-7

The simulated normalised radiation patterns of the proposed antenna at different frequencies are shown in Fig. 4.7. At lower frequencies, the E-plane patterns (X-Y plane) are bidirectional similar to a dipole antenna. However, as the frequencies increases, the radiation patterns become directional and more number of side lobe starts appearing. The maximum gain was observed between 2 and 6 dBi over the frequency band 2.3–30 GHz.

After 30 GHz frequency, the antenna becomes more directional and the peak gain goes up to 8.7 dBi. A plot of peak gain versus frequency is shown in Fig. 4.8.

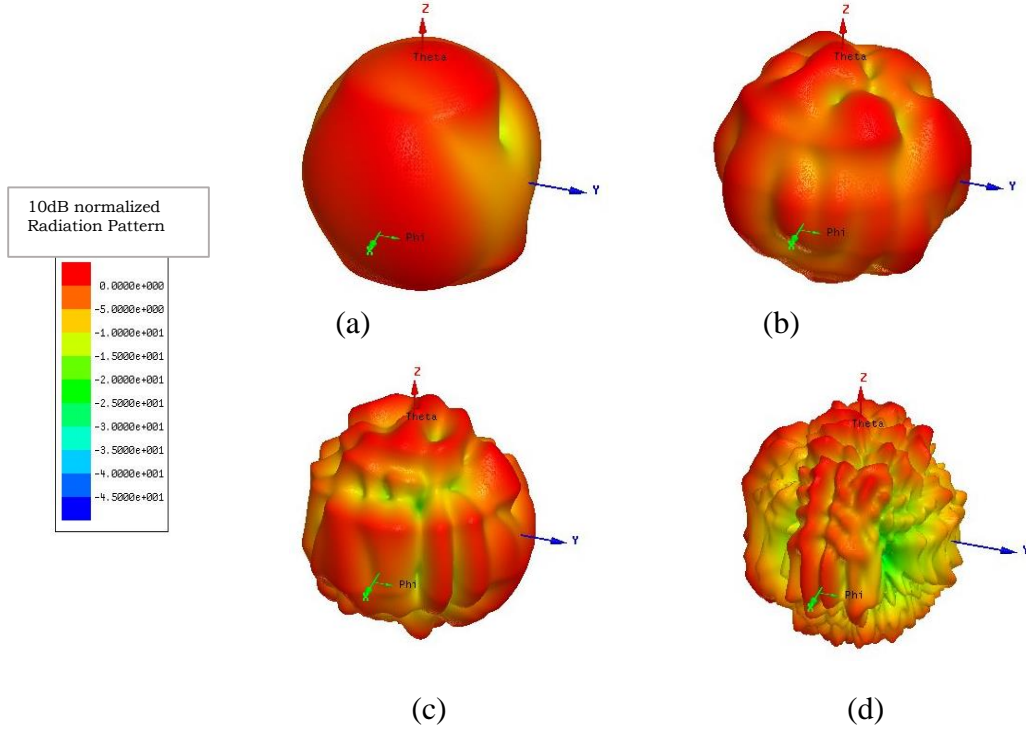


Fig. 4.7 Radiation patterns of the proposed UWB antenna-7: (a) 5 (b) 15 (c) 25 and (d) 45 GHz.

In this sub-section, the design of a tri-circular shape microstrip monopole antenna with partial ground plane was discussed. A microstrip feedline with different step dimensions is used for impedance matching and to improve the antenna performance. The return-loss better than 10 dB was achieved over 2.3 to 37.6 GHz frequency band. The peak gain of the antenna is 2-6 dBi up to 30 GHz and 6-8 dBi thereafter.

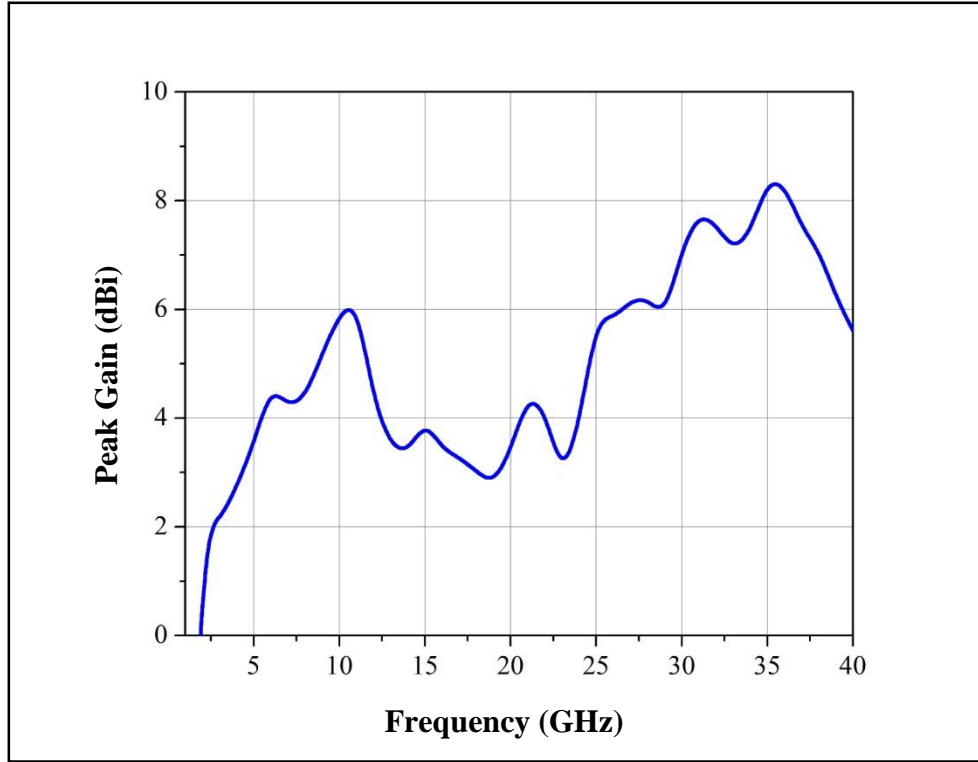


Fig. 4.8 Peak gain of the proposed UWB antenna-7.

2.2 Circular Printed Monopole Antenna-8

In this sub-section, design of a circular monopole patch antenna is discussed. As reported in the open literature, the bandwidth offered by a circular monopole microstrip antenna is larger as compared to monopole antenna of any other shape. This is because; various modes of a circular resonator are closely spaced. The bandwidth associated with these modes is large as the change in the input impedance from one mode to another mode is very small (Kumar and Ray, 2003)

2.2.1 Design of the Proposed UWB Patch Antenna-8A

The layout of the antenna is shown in Fig. 4.9. It comprises of a microstrip line-fed circular patch designed for 50Ω input impedance. The substrate is made of RT/duroid 5880, with thickness $h = 0.787$ mm, copper cladding of 0.035 mm and relative permittivity $\epsilon_r = 2.2$, $\tan\delta = 0.0004$, $l_s = 40$ mm and $w_s = 30$ mm. The characteristic impedance can be calculated using empirical formulas (Pozar, 2012; Liao, 1989). For 50Ω impedance, the calculated width of the microstrip feedline is 2.4 mm. However, simulated optimised width is fixed at $w_f = 1.6$ mm and length $l_f = 9.4$ mm. The conducting ground plane has a length of $l_g = 9.0$

mm and width $w_g = w_s = 30$ mm, the same as the substrate width. The different geometrical parameters of the antenna and corresponding dimensions are listed in Table 4.2.

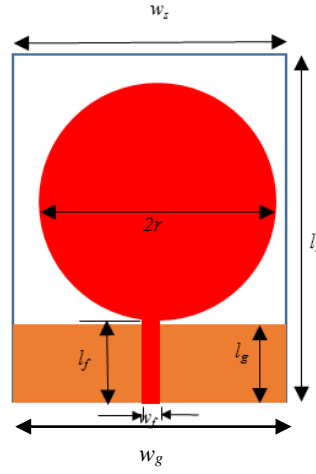


Fig. 4.9 Layout of the proposed UWB antenna-8A under consideration.

Table 4.2 Design Parameters of UWB Antenna-8A

Design parameter	Value (mm)	Design parameter	Value (mm)
l_s	40	w_f	1.6
$w_s = w_g$	30	r	12
l_f	9.4	l_g	9

Return-Loss Performance of UWB Antenna-8A

The lower cutoff frequency of the patch antenna can be determined by equating the circular monopole area to an equivalent cylindrical monopole antenna with the same height. For 12 mm circular patch, calculated lower frequency is 2.66 GHz which is matching with the simulated result. The simulated return-loss plot is shown in Fig. 4.10. The impedance bandwidth for $VSWR \leq 2$ is achieved from 2.2-23.2 GHz.

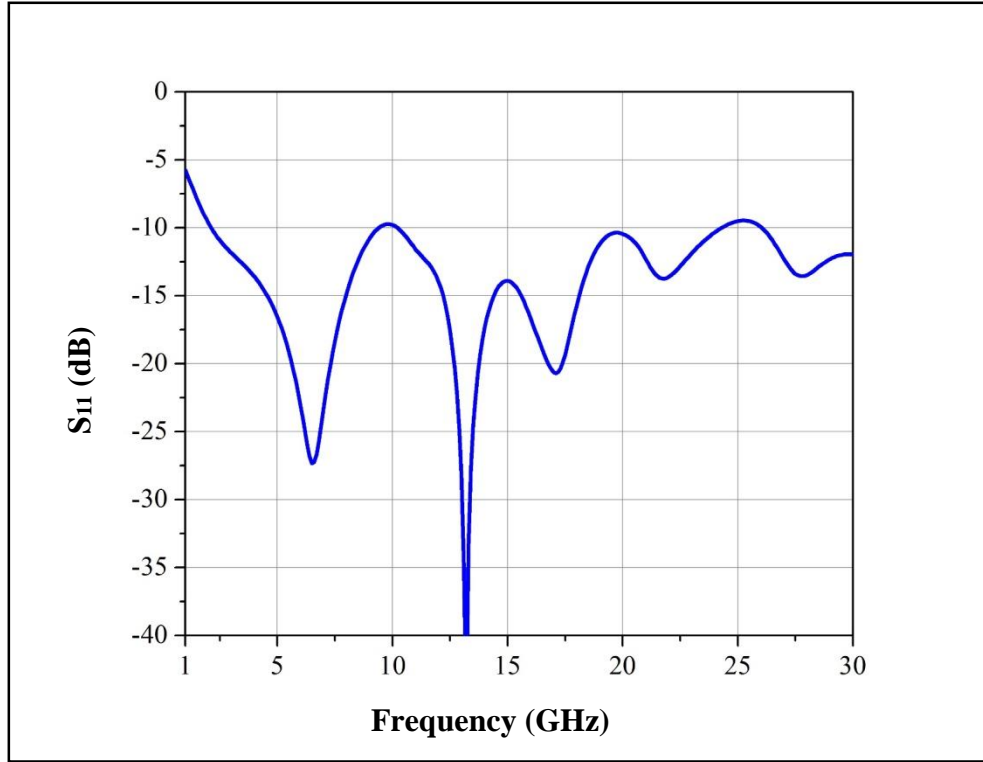


Fig. 4.10 Simulated return-loss performance of the proposed UWB antenna-8A.

2.2.2 Layout of a Stepped Circular Monopole with a Notch in the Ground Plane (Antenna-8B)

In order to improve the bandwidth, a few changes were made in the existing antenna. Two additional steps of dimensions $l_1=0.6$ mm, $w_1=2$ mm, $l_2=0.6$ mm and $w_2=5.5$ mm, were added in the main feed line. All remaining parameters were kept same. The length l_g was kept 8.3 mm. A notch of size $l_3=1$ mm and $w_3=3.6$ mm has been created in the ground plane. The final layout of the antenna is shown in Fig. 4.11. The design was simulated for the return-loss characteristic.

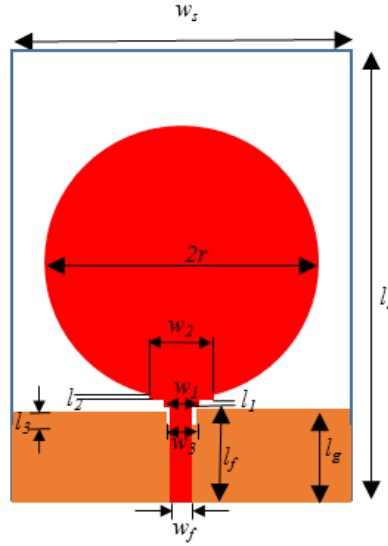


Fig. 4.11 Layout of the proposed UWB antenna-8B under consideration with stepped feedline and notch in the ground plane.

Return-Loss Performance of UWB Antenna-8B

The simulated return-loss performance is shown in Fig. 4.12. As shown, the bandwidth has improved as compared to a previous design. In this case, the impedance bandwidth for $VSWR \leq 2$ is achieved from 2.2-30.5 GHz.

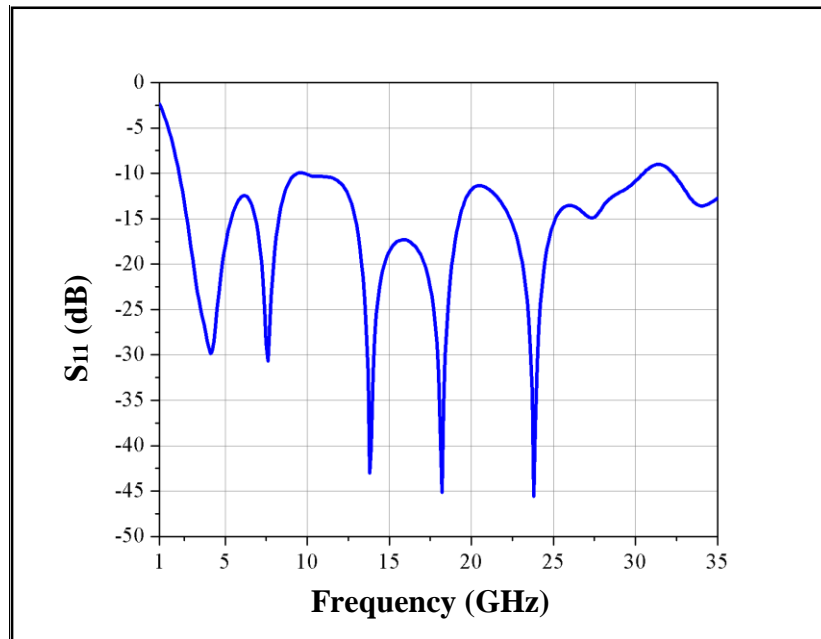


Fig. 4.12 Simulated return-loss performance of the proposed UWB antenna-8B.

2.2.3 Stepped Circular Monopole with a Notch in Ground Plane and Slot in Radiating Patch (Antenna-8C)

To further improve the UWB performance of the antenna, an additional slot is made in radiating the patch. The layout of the new design is shown in Fig. 4.13.

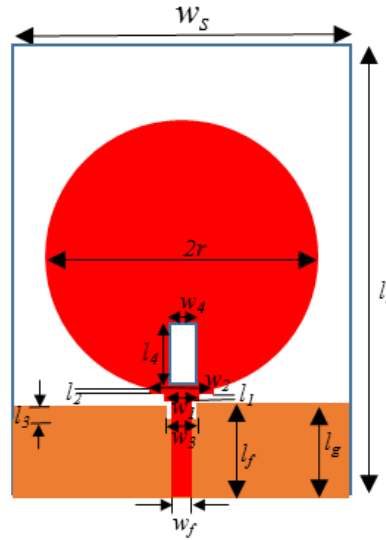


Fig. 4.13 Layout of the proposed UWB antenna-8C under consideration with stepped feedline, notch in the ground plane and slot in the radiating patch.

Return-Loss Performance of UWB Antenna-8C

The design was simulated and a proto type antenna was fabricated. The antenna was tested at the measurement facility of the Institute for Plasma Research, Gandhinagar (India). The simulated and the measured results are plotted in Fig.4.14. The measured results found mostly matching with the simulated results except some small variations. The simulated return-loss bandwidth for $VSWR \leq 2$ is from 2.2-38 GHz whereas the measured bandwidth is from 2.1-38.6 GHz.

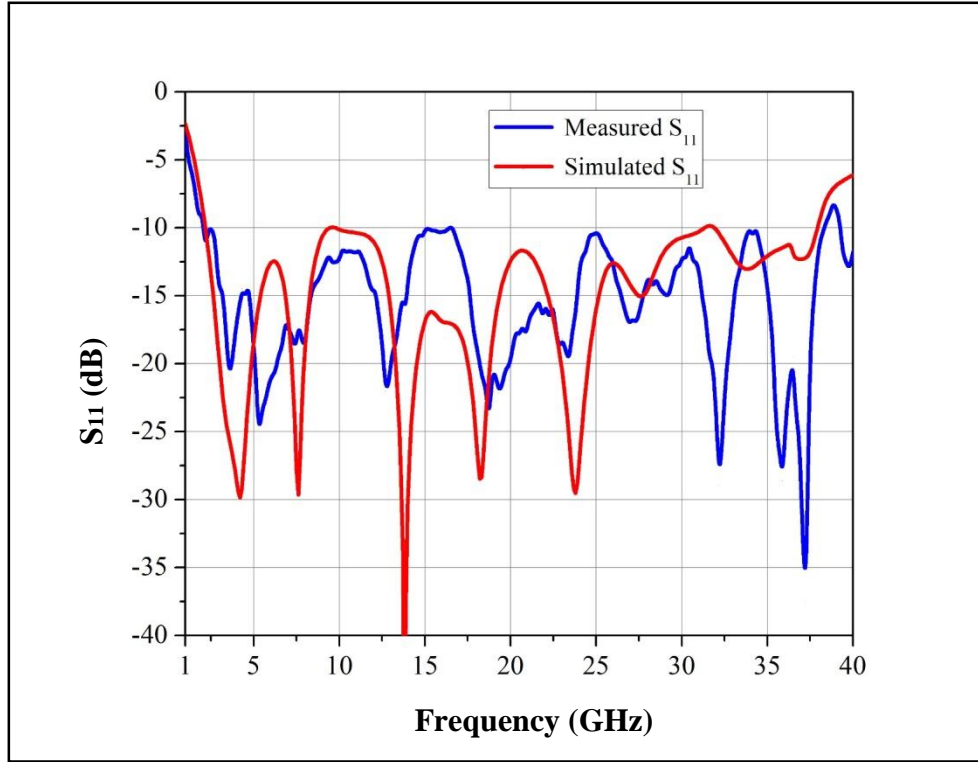


Fig. 4.14 Measured and simulated return-loss performance of the proposed UWB antenna-8C.

Parametric Study of the Proposed UWB Antenna-8C

In order to study the effect of change in various parameters on the antenna return-loss, a comprehensive parametric study was carried out. The results are discussed with suitable graphs.

Change in Feed Width (w_f)

The effect of feedline width variation is shown in Fig. 4.15. It is evident that, the lower cutoff frequency is not much dependent on w_f but the higher frequencies vary significantly with change in w_f .

Change in the Dimensions of the Partial Ground Plane (l_g)

The effects of change in ground plane height (l_g) on the antenna return-loss performance are shown in Fig. 4.16. As evident, for $l_g = 8.3$ mm, the best impedance matching is achieved and the antenna provides the maximum impedance bandwidth.

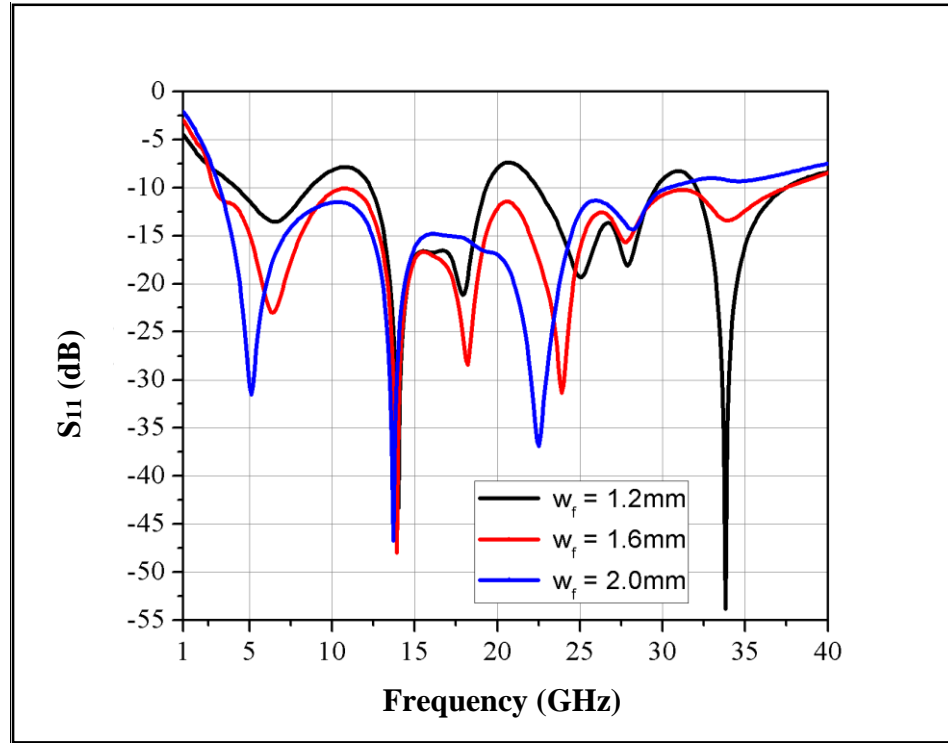


Fig. 4.15 Effect of change in feed width dimension (w_f) on the return-loss performance of the proposed UWB antenna-8C.

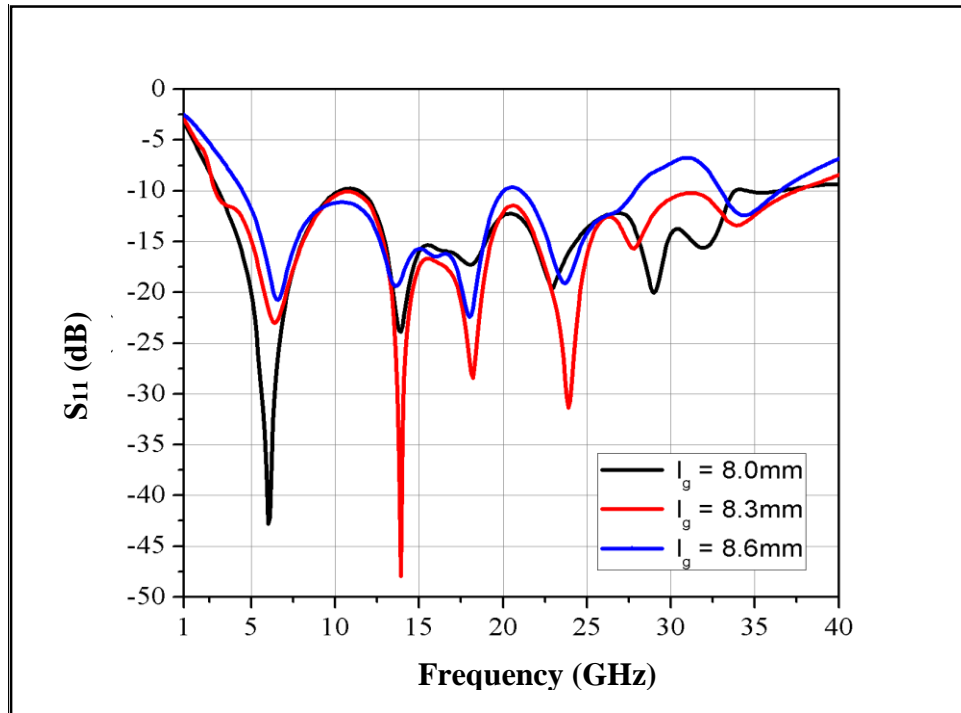


Fig. 4.16 Effect of ground height (l_g) on the antenna performance of the proposed UWB antenna-8C.

Radiation Patterns of the Proposed UWB Antenna-8C

The three-dimensional radiation patterns of the proposed antenna at 5, 10, 15, 20, 25, 30 and 35 GHz are shown in Fig. 4.17. At low frequencies, the radiation patterns are mainly omnidirectional. However, at high frequencies, more number of maxima and minima appeared due to large physical size of antenna at higher frequencies with reduced wavelength and antenna becomes relatively directional.

The peak gain of the proposed antenna is plotted in Figure 4.18 and found to vary between 1 and 5 dBi till 24 GHz and from 5 to 15 dBi beyond 24 GHz. The high gain is not expected as the antenna is designed as a monopole for UWB applications.

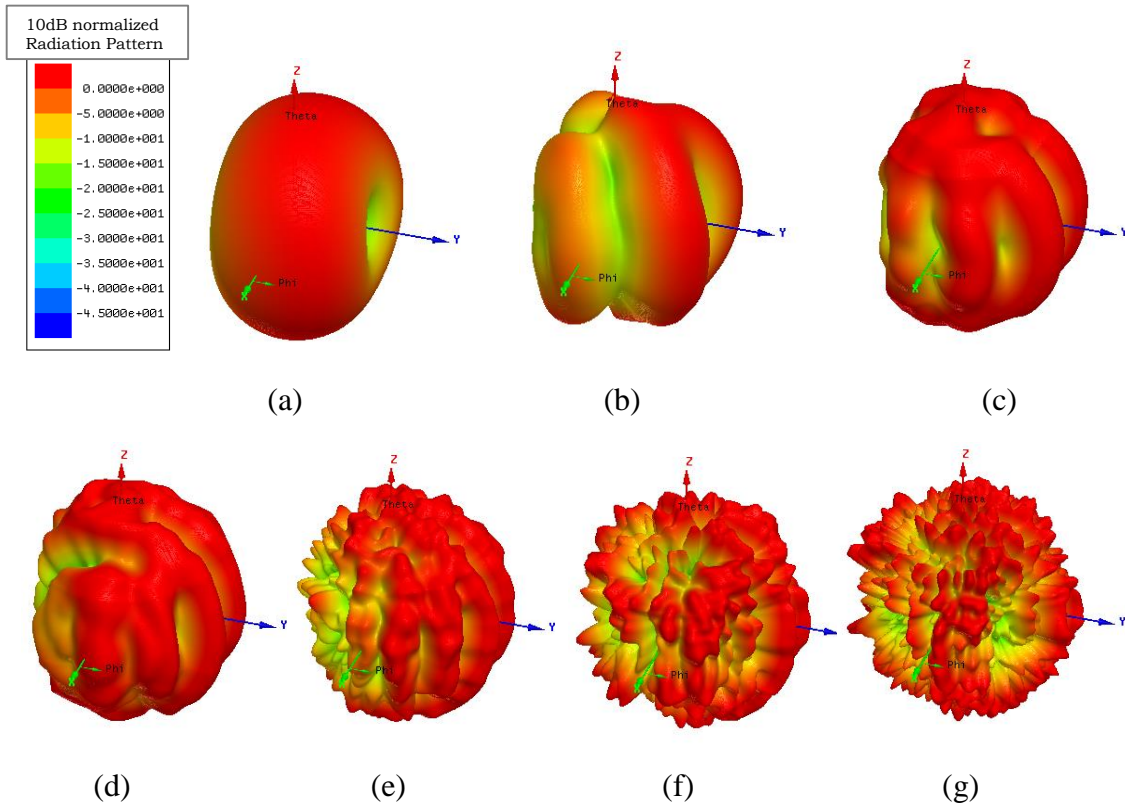


Fig. 4.17 Radiation patterns of the proposed UWB antenna-8C: (a) 5, (b) 10, (c) 15, (d) 20, (e) 25, (f) 30, and (g) 35 GHz.

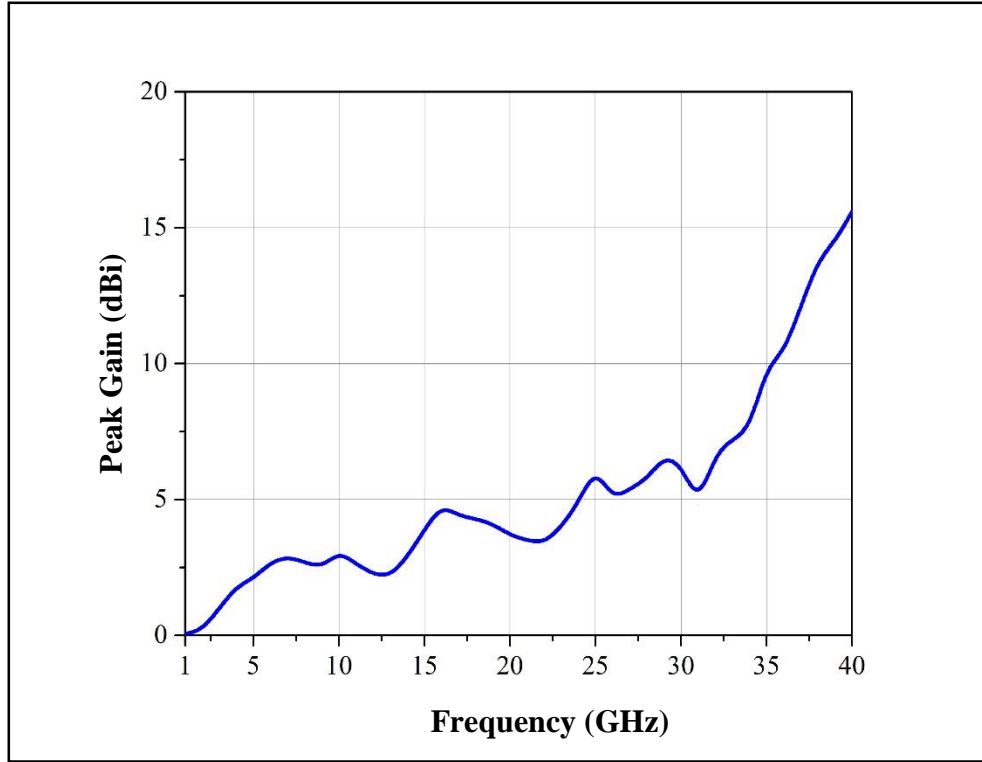


Fig. 4.18 Peak gain of the proposed UWB antenna-8C

In this design, a stepped circular microstrip monopole antenna is discussed as a viable option for ultra-wide band applications. After thorough optimisation, a prototype antenna was fabricated and found the ultra-wide band behaviour from 2.1 to 38.6 GHz (179% BW) for $VSWR \leq 2$.

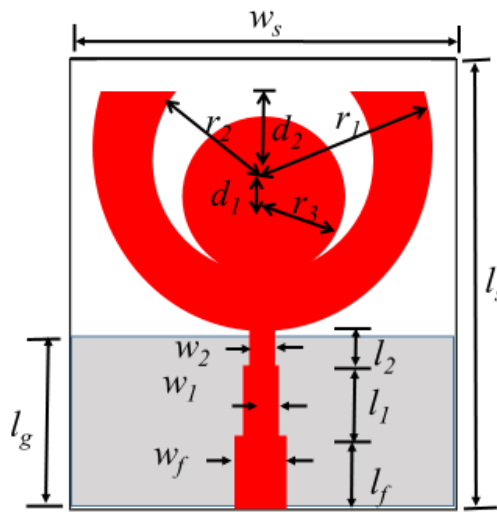
2.3 Truncated Annular Printed Monopole Antenna-9

In this section, a design of a truncated annular microstrip monopole antenna with partial ground is discussed. The antenna comprises of a circular patch with truncated annular patch. It is fed by a stepped microstrip line designed on FR-4 substrate. The antenna covers the ultra-wide band from 3-42.8 GHz for return-loss better than -10 dB. The proposed antenna is very compact in size occupying $35 \times 32 \times 1.6 \text{ mm}^3$. The HFSS simulation software was used to estimate the return-loss, radiation patterns and gain of the antenna. The simulated results of the return-loss are verified with the measured results.

2.3.1 Design of the Proposed UWB Patch Antenna-9

The antenna is designed on an FR-4 substrate of size $40 \times 40 \times 1.6 \text{ mm}^3$. The main radiating patch consists of a circular patch overlapping with a truncated annular patch. It is fed by three stepped microstrip feed line of different size. The feed structure provides a wide-band impedance matching transformer and guides the wave propagating from main radiating patch to the free space without causing destructive reflections. In order to achieve wideband characteristics, partial ground has been used.

The final schematic diagram and the photograph of the proposed antenna are shown in Fig. 4.19. The different geometrical parameters of the antenna and corresponding dimensions are listed in Table 4.3.



(a) Layout



(b) Photograph of the fabricated antenna

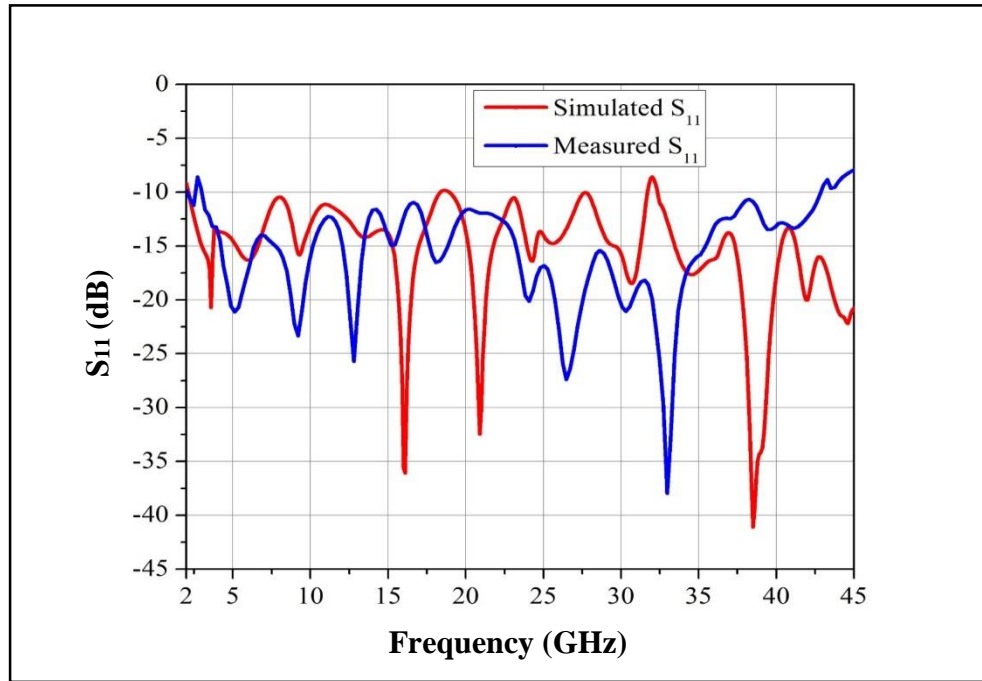
Fig. 4.19 Design of the proposed UWB antenna-9 under consideration.

Table 4.3 Design Parameters of UWB Antenna-9

Design parameter	Value (mm)	Design parameter	Value (mm)
l_s	35	w_2	1.6
w_s	32	l_g	14
l_f	5.5	d_1	2
w_f	3	d_2	6
l_1	6	r_1	12
w_1	2.4	r_2	10
l_2	4	r_3	8

2.3.2 Return-Loss Performance of UWB Antenna-9

The proposed antenna design was simulated using the HFSS software and optimised to provide the maximum bandwidth for return-loss better than -10dB. The antenna was fabricated and same is tested at the Institute of Plasma Research (IPR), Gandhinagar, India using R&S ZVA50 Vector Network Analyser.

**Fig. 4.20 Return-loss performance of the proposed UWB antenna-9.**

The measured and the simulated return-loss are compared and are shown in Fig. 4.20. The simulated and measured peaks are slightly shifted, probably due to fabrication tolerances, undercuts of substrate at corners during the copper etching process, software limitation in terms of modelling and simulating over a wide bandwidth and the effect of SMA connector. The return-loss bandwidth was found satisfactory over 3 to 42.8 GHz frequency band (174% BW).

2.3.3 Parametric Study of the Proposed UWB Antenna-9

To understand the antenna behaviour in relation to different design parameters, parametric analysis was carried out. The parametric study is important as it provides approximation measures before the antenna is fabricated. The effects of different design parameters are discussed here.

Change in the Dimensions of the Radiating Patch r_1 , r_2 and r_3

The radiating element in this antenna is circular in shape which is being controlled by r_1 , r_2 and r_3 . The lower cutoff frequency is primarily decided by the largest segment of patch, which is r_1 . The values of r_2 and r_3 decide the maximum bandwidth of an antenna. After optimisation, it is observed that $r_1 = 12$ mm, $r_2 = 10$ mm and $r_3 = 8$ mm provide the maximum bandwidth for 10dB return-loss. The same is shown in Figs. 4.21–4.23.

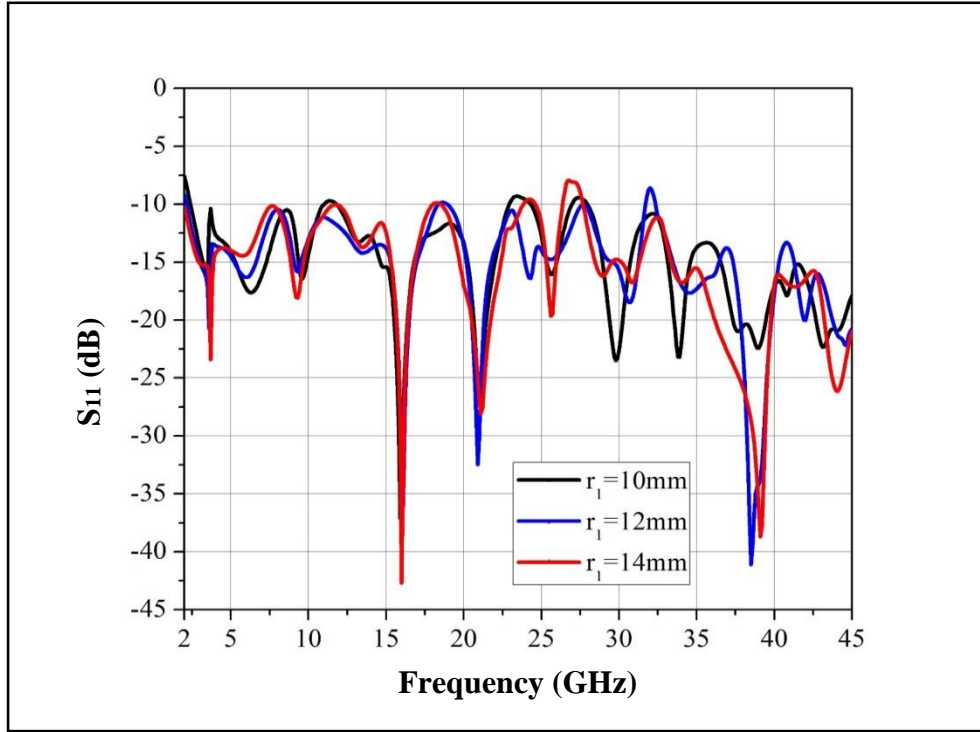


Fig. 4.21 Effect of change in patch dimension (r_1) on the return-loss performance of the proposed UWB antenna-9.

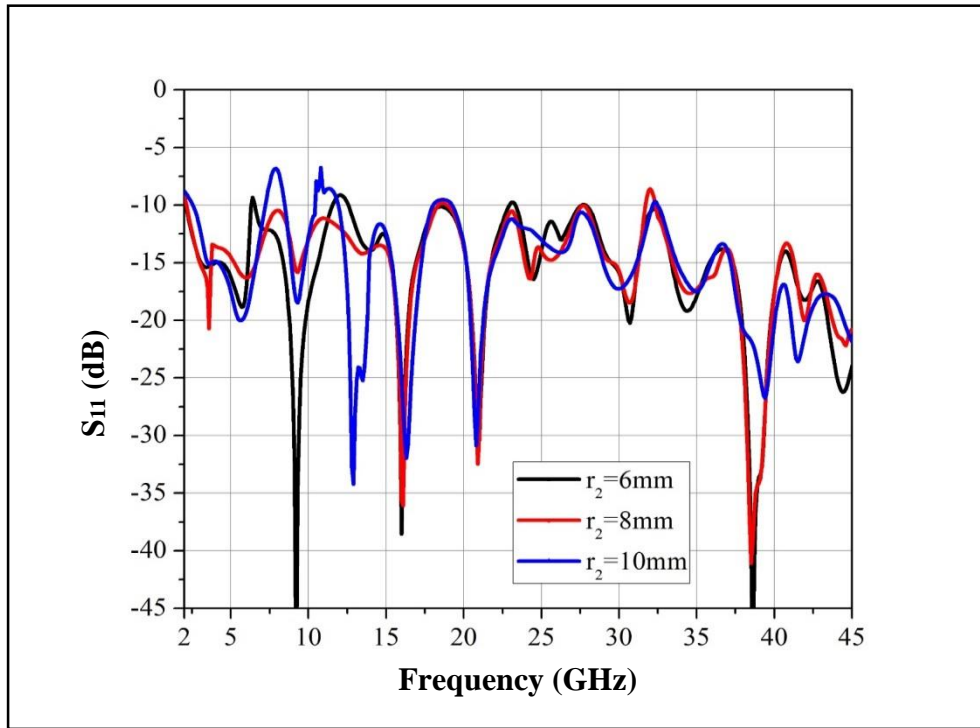


Fig. 4.22 Effect of change in patch dimension (r_2) on the return-loss performance of the proposed UWB antenna-9.

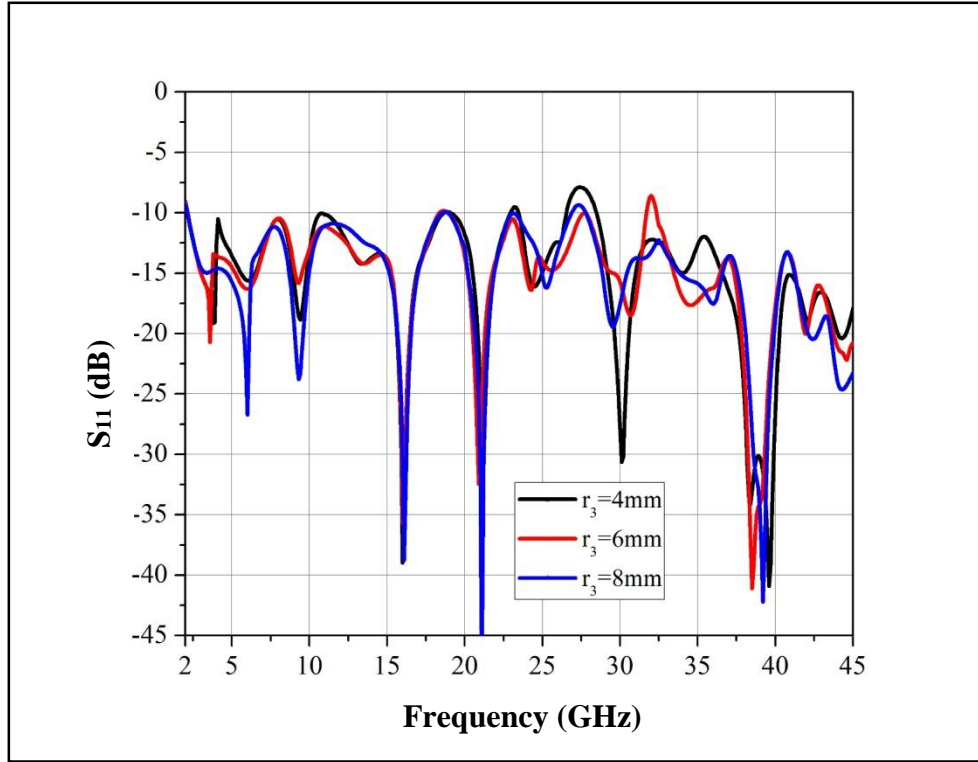


Fig. 4.23 Effect of change in patch dimension (r_3) on the return-loss performance of the proposed UWB antenna-9.

Effect of Ground Plane Size

Figure 4.24 depicts the behaviour of the antenna when the ground plane size (l_g) is varied. The dimension l_g controls the coupling between the ground plane and the patch. It additionally acts as an impedance matching network. The ground size $l_g = 14$ mm is found to be optimal with minimum return-loss and maximum bandwidth.

Effect of Main Feed Width

To feed the antenna, a microstrip transmission line with three different width segments have been used to transform the impedance of the antenna to 50Ω . As per the design formula suggested by Pozar (2012) and Liao (1989), for FR-4 substrate with 1.6 mm height, the width of the feedline for 50Ω impedance should be 3 mm. During optimisation it was found to provide the maximum bandwidth. The effect of change in the width of feed line on the antenna return-loss is shown in Fig 4.25.

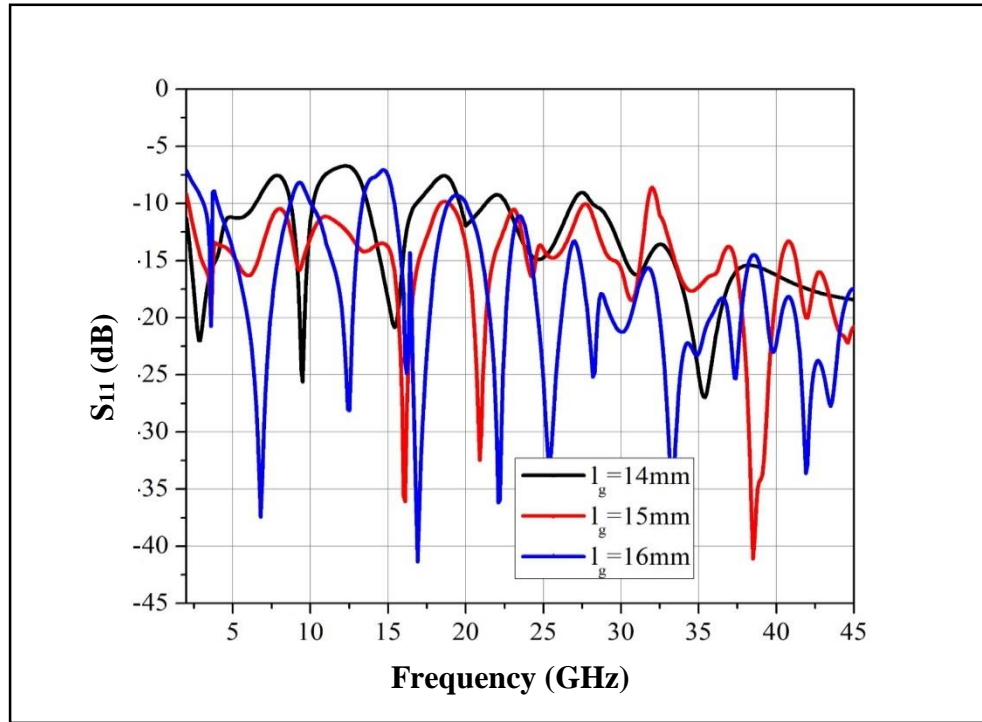


Fig. 4.24 Effect of change in length (l_g) of the ground plane on the return-loss performance of the proposed UWB antenna-9.

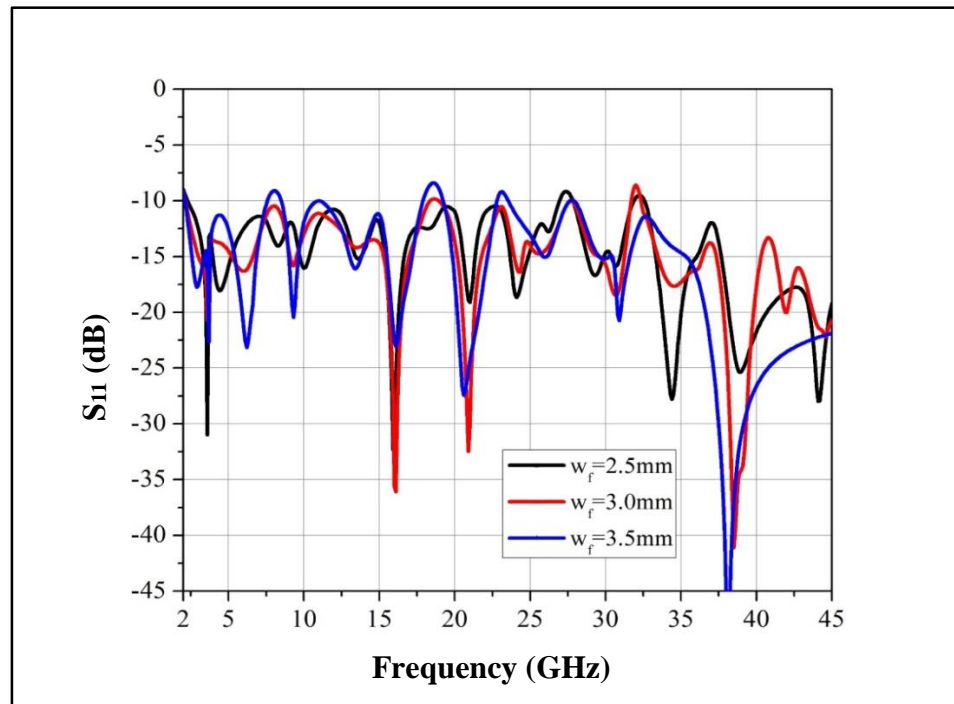


Fig. 4.25 Effect of change in feed width (w_f) on the return-loss performance of the proposed UWB antenna-9.

2.3.4 Radiation Patterns of the Proposed UWB Antenna-9

The three-dimensional radiation patterns of the proposed antenna at different frequencies are shown in Fig. 4.26. At lower band, the E-plane patterns are bidirectional like the dipole antenna and H-plane patterns are omni-directional in principal plane as expected from a vertical dipole. However, as the frequency increases, the radiation patterns become directional. The simulated gain of the antenna is found to vary between 1.9 and 24 dBi as shown in Fig. 4.27.

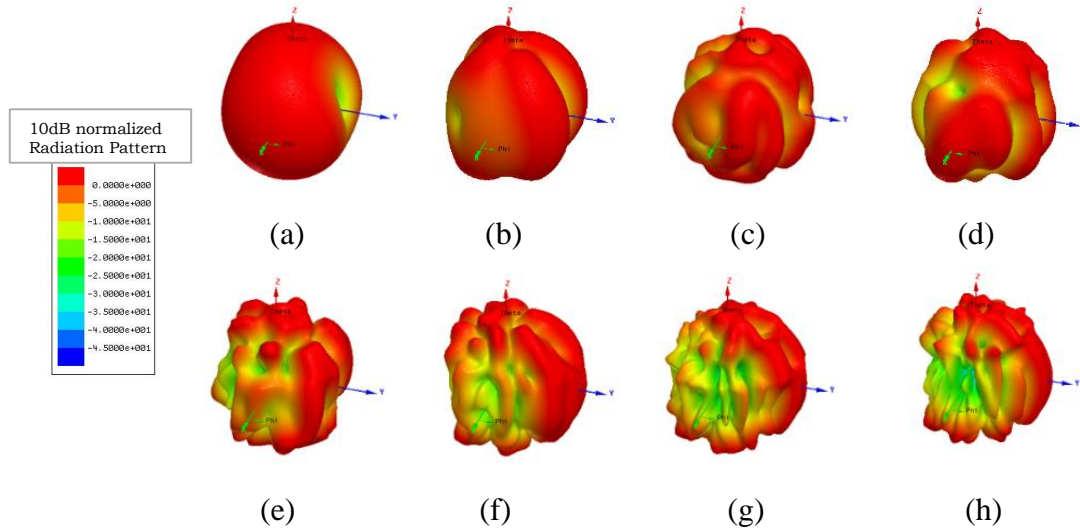


Fig. 4.26 Radiation patterns of the proposed UWB antenna-9: (a) 5, (b) 10, (c) 15, (d) 20, (e) 25, (f) 30, (g) 35 and (h) 45 GHz.

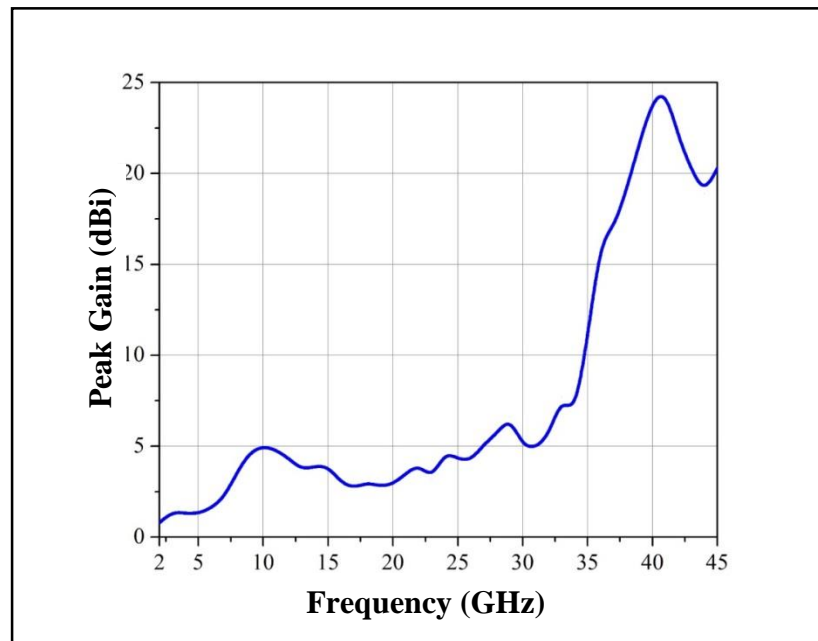


Fig. 4.27 Peak gain of the proposed UWB antenna-9.

In this sub-section, a novel microstrip monopole antenna for ultra-wide band performance is presented. Its operating bandwidth is from 3 to 42.8 GHz which covers much beyond the UWB frequency band authorised by the FCC. The three dimensional radiation patterns show good monopole-like behavior with stable gain varying from 1.9 to 24 dB over the entire frequency band.

2.4 Elliptical Shape Printed Monopole Antenna-10

For all the previous three designs presented in this chapter, we have used circular shape patch antenna. In this design, an elliptical monopole patch fed with five stage microstrip feed line is discussed. The antenna offers impedance bandwidth from 2.7-49 GHz.

2.4.1 Design of the Proposed UWB Patch Antenna-10

In this design, bandwidth has been enhanced using an elliptic planar antenna. The RT/duroid 5880 substrate with thickness $h = 0.787$ mm and relative permittivity $\epsilon_r = 2.2$, $\tan\delta = 0.0009$ is used. Partial ground has been used to achieve better return-loss performance. The geometry of the proposed antenna and the photograph of the proposed antenna are shown as Fig.4.28. Different geometrical parameters of the antenna and corresponding dimensions are listed in Table 4.4.

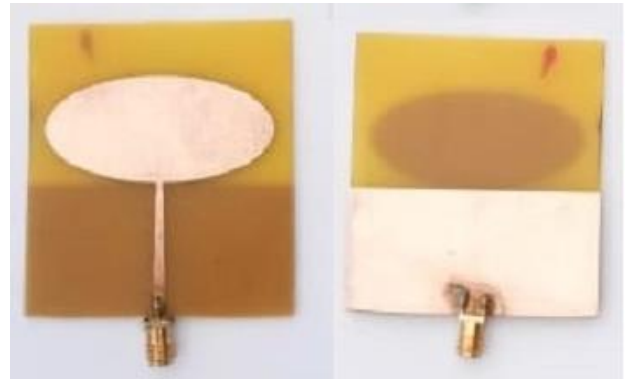
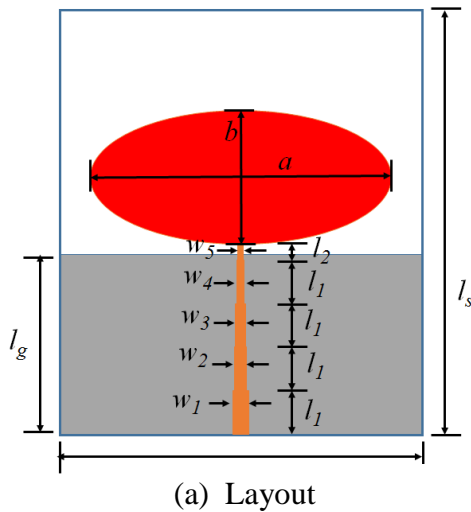


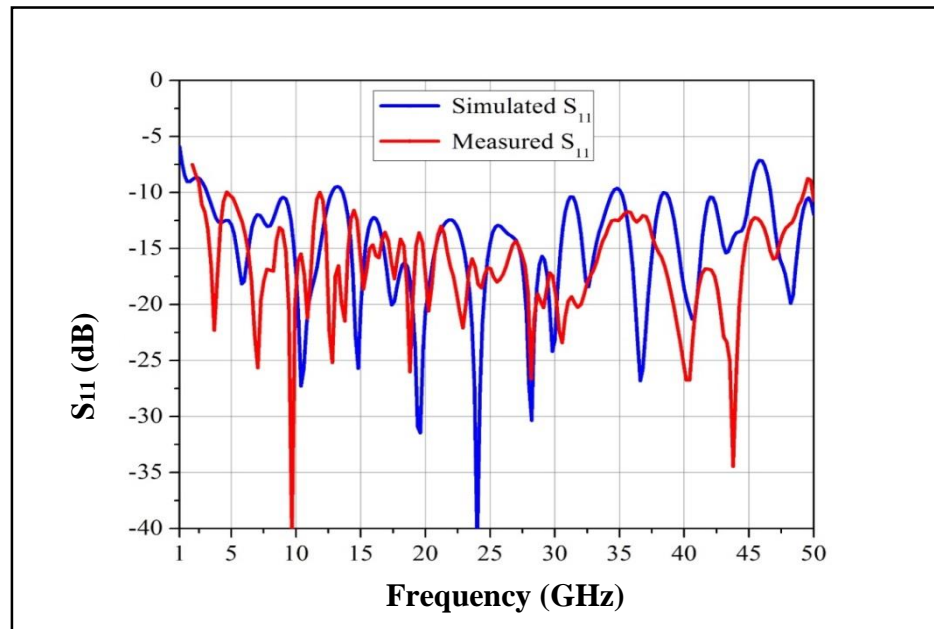
Fig. 4.28 Design of the proposed UWB antenna-10 under consideration.

Table 4.4 Design Parameters of UWB Antenna-10

Design parameter	Value (mm)	Design parameter	Value (mm)
l_s	70	w_3	1.84
w_s	60	w_4	1.56
l_l	7	w_5	1.28
l_2	2.5	l_g	30
w_1	2.4	a	50
w_2	2.12	b	23

2.4.2 Return-loss performance of UWB antenna-10

The proposed antenna was simulated using the HFSS. The simulated return-loss bandwidth covers 3.2 to 45 GHz frequency. The antenna was fabricated and the return-loss was measured using the Vector Network Analyser. The measured return-loss bandwidth covers 2.7-49 GHz frequency band. The simulated and measured return-loss is shown in Fig. 4.29. From the graph, it is evident that the antenna possesses multi-band characteristic in the UWB spectrum.

**Fig. 4.29 Return-loss performance of the proposed UWB antenna-10.**

2.4.3 Parametric Study of the Proposed UWB Antenna-10

In order to study the effect of change in various design parameters on antenna performance, a rigorous parametric study was conducted. The outcomes of the study are discussed below.

Change in Substrate Materials

The size of the antenna is inversely proportional to relative dielectric constant of the substrate material. Thus, the substrate material used for designing a microstrip antenna plays very important role. Also, the loss tangent of the substrate material affects the return-losses at different frequencies. The change in return-loss performance for two different substrate materials, i.e. RT/duroid-3006 (dielectric constant of 6.15, loss tangent of 0.0025) and RT/duroid-5880 (dielectric constant of 2.2, loss tangent of 0.0009) was studied. The results are shown in Fig. 4.30. Based on this study, it was decided to use RT/duroid-5880 as the substrate material.

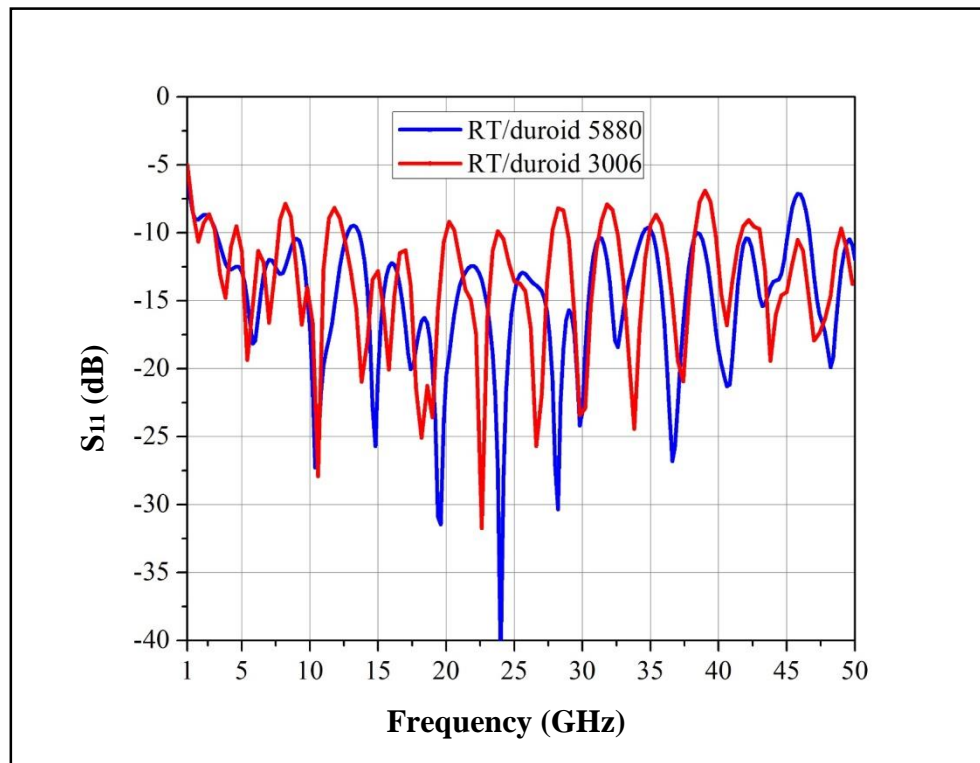


Fig. 4.30 Effect of change in the substrate material on the return-loss performance of the proposed UWB antenna-10.

Change in the Dimensions of Major Axis

The effect of change in dimensions of the major axis (a) of the elliptical patch is shown in Fig. 4.31. It is observed that major axis is very critical parameter for this design and $a = 50$ mm offers the best return-loss performance. For a small variation of a , bandwidth reduces drastically.

Effect of Partial Ground (l_g)

The most critical parameter for this antenna is the length of the partial ground (l_g). The separation in the radiating patch, feedline and ground form a capacitor which affects the impedance matching. It was observed that $l_g = 28$ mm provides better return-loss performance at higher frequencies. As shown in Fig.4.32, the antenna offers maximum impedance bandwidth for $l_g = 30$ mm.

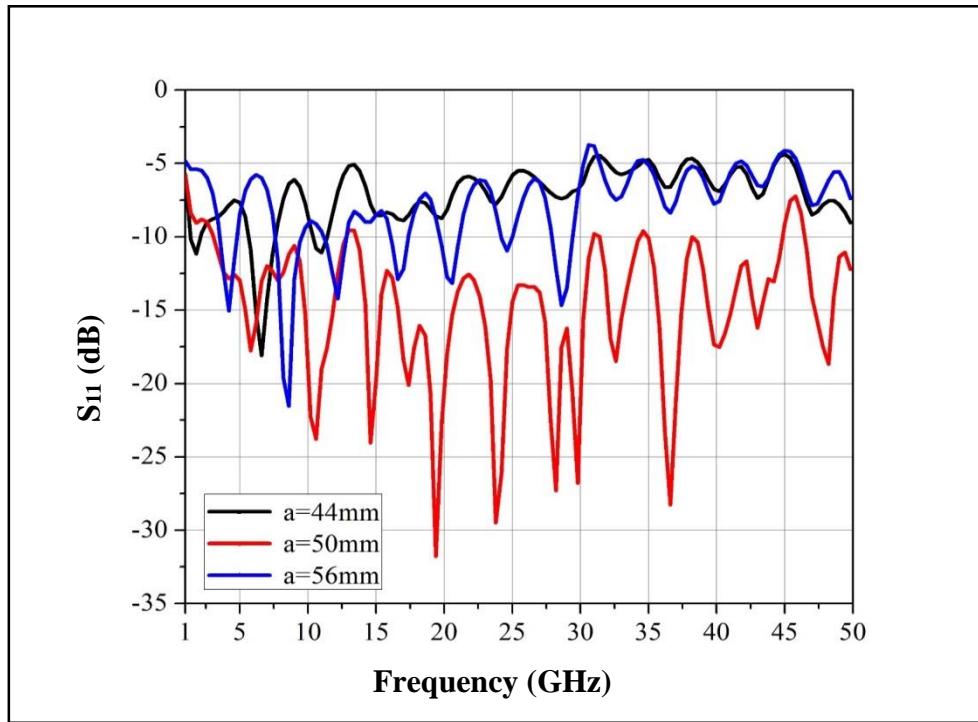


Fig. 4.31 Effect of change in major axis (a) on the return-loss performance of the proposed UWB antenna-10.

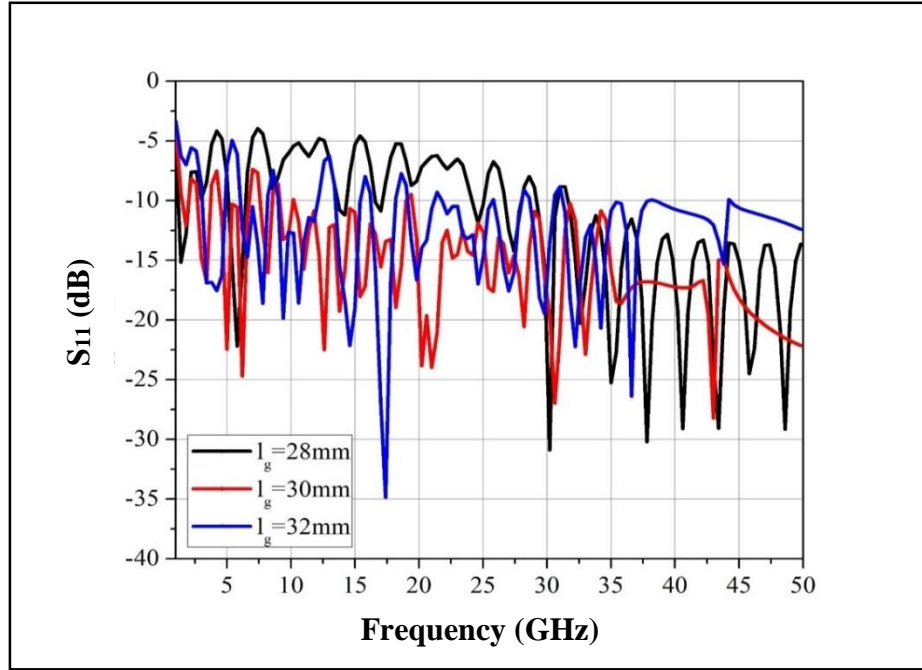


Fig. 4.32 Effect of change in length (l_g) of the ground plane on the return-loss performance of the proposed UWB antenna-10.

2.4.4 Radiation Patterns of the Proposed UWB Antenna-10

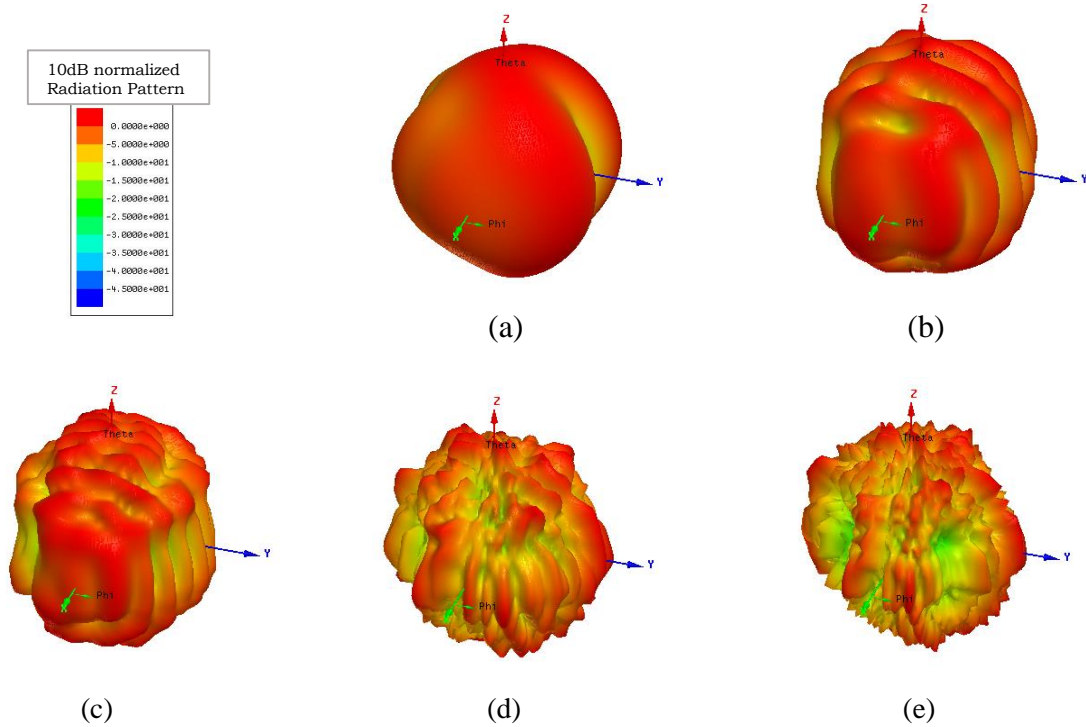


Fig. 4.33 Radiation patterns of the proposed UWB antenna-10: (a) 5, (b) 15, (c) 25, (d) 35, and (e) 45 GHz.

The radiation patterns of the proposed antenna at 5, 15, 25, 35 and 45 GHz are shown in Fig. 4.33. The radiation patterns of the antenna at lower frequencies are different than previously discussed designs. As the frequency increases, the radiation pattern became more directional like a standard monopole antenna. The peak gain of the antenna increases from 1 to 8 dBi up to 40 GHz. However, beyond 40 GHz peak gain increases sharply and at 49 GHz, it attains 27 dBi. A plot of the peak gain versus frequency is shown in Fig. 4.34.

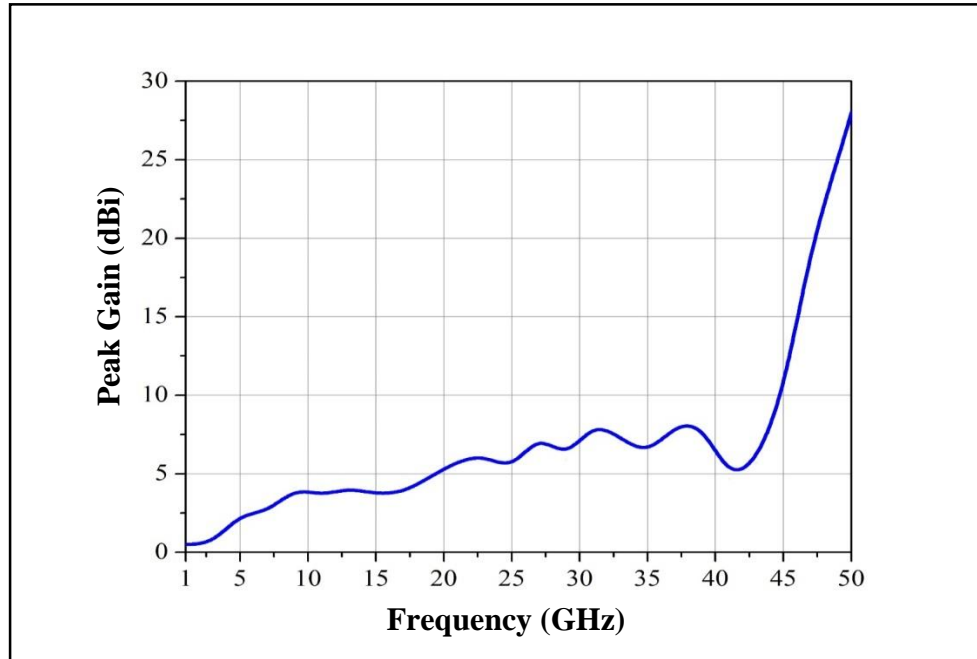


Fig. 4.34 Peak gain of the proposed UWB antenna-10.

In this design, a five-stage microstrip line-fed elliptical monopole patch antenna was elaborated. The proposed antenna provides extreme broadband characteristics in a planar structure. This antenna design is a breakthrough in easy impedance matching and can be directly used for many practical UWB communications.

4.5.Summary

In this chapter, four different UWB patch antenna designs have been examined. The important aspects of all the proposed antennas are summarized in Table 4.5.

Table 4.5 Summary of the Proto Type Patch Antennas: Class III

Design	Substrate	Size (mm²)	Area (mm²)	BW (GHz)
Tri circular patch antenna	FR-4	40×50	2000	2.3-37.6
Circular patch antenna	RT/duroid 5880	40×30	1200	2.2-23.2
Modified circular patch antenna	RT/duroid 5880	40×30	1200	2.2-38
Annular patch antenna	FR-4	35×32	1120	3.0-42.8
Elliptical patch antenna	RT/duroid 5880	70×60	4200	2.7-49

All the antennas can be used for frequency monitoring purpose as well as for signal intelligence, EW, geological and metrological signal, radar navigation, hand-held UWB application, etc. These antennas possess attractive features such as low-profile, low-dimension and simple structure.

SUMMARY AND SCOPE OF FUTURE WORK

This chapter presents the summary of the research work, important conclusions and the future scope of the work.

5.1 Summary and Conclusions

Due to attractive features like light weight, low volume, thin profile configuration, multiband operations, etc. amongst various UWB antenna configurations, the planar microstrip monopole antenna (printed/patch) has been the preferred choice. However, it suffers from limitations such as narrow impedance bandwidth (typically around 2–5%) and low power-handling capability. It has been found that, comparatively, the microstrip monopole configuration has a capability to operate with very large bandwidth. which is useful in UWB applications. Thus, it was decided to study the feasibility of microstrip monopole antenna for spectrum monitoring and other such applications.

The main goal of this work was to explore the design feasibility of the microstrip patch antenna capable of operating from a few GHz to 40 GHz and above with omni-directional radiation patterns and moderate gain to utilise it for spectrum management and other wireless systems.

In this work, the effects of a few main design parameters of microstrip patch antenna, viz., compact size with different shapes and sizes, multi-resonance effect leading to multiband operation, multi-step feed network and partial ground plane with multiple slots have been studied and discussed. Investigations have been carried out using the finite-element method (FEM)-based high-frequency simulation software, HFSSv13. In this thesis, totally ten (10) different UWB microstrip monopole patch antennas with different radiating patch shapes and sizes have been discussed. The return-loss of the prototype antennas was measured using the Vector Network Analyzer, R&S ZVA50, at the Institute of Plasma Research, Gandhinagar. Majority of the designed antennas operate satisfactorily covering the entire

FCC-authorized ultra-wide band except the first one (lower operating frequency 3.5 in place of 3.1 GHz). Four of them are designed for use in UWB applications up to 20 GHz, two up to 30 GHz and four up to 40 GHz and beyond. These designs have been classified as Class-I, II and III antennas and are discussed in Chapters 2, 3 and 4, respectively. A brief summary of all the antennas is presented in Table 5.1.

Table 5.1 Summary of the Proposed Microstrip Monopole UWB Patch Antennas

Sr. No.	Design	Substrate	Size (mm²)	Area (mm²)	Range (GHz)	BW (GHz)
1	Modified rectangular patch antenna	TM-3	16×18	288	3.5-15.2	11.7
2	Half hexagonal circular patch antenna	RT/duroid -5880	50×35	1750	3.1-14.1	11
3	Quarter circular patch antenna	FR-4	35×20	700	3.1-16.3	13.2
4	Goblet shape patch antenna	RT/duroid -5870	24×24	576	3.1-17.1	14
5	Truncated circular patch antenna	RT/duroid -5880	40×35	1400	2-22.2	20.2
6	CPW feed truncated circular patch antenna	FR-4	40×30	1200	2.6-26.5	23.9
7	Tri-circular patch antenna	FR-4	40×50	2000	2.3-37.6	34.3
8	Circular patch antenna	RT/duroid -5880	40×30	1200	2.1-38.6	36.5
9	Truncated annular patch antenna	RT/duroid -5880	40×30	1200	3-42.8	39.8
10	Elliptical patch antenna	RT/duroid -5880	70×60	4200	2.7-49	46.3

All the designs have been simulated and specially optimised for compact size and maximum bandwidth using the HFSS. The most common method to achieve the UWB operation is to provide partial ground in the microstrip monopole configuration, which has been applied in several designs in this work. Other techniques to improve the bandwidth are the use of multi-stepped feed network, narrow slot of different shapes into the radiating patch of the antenna and ground plane below the feed network, which affects the current flow in the patch. Different shapes of radiating patch have been used in different designs and observed that a circular radiating patch provides more bandwidth in comparison to a rectangular one. Elliptical radiating patch with an axis ratio of about 0.4 will provide the highest bandwidth in comparison with the other designs discussed in this thesis.

A CPW-fed patch antenna is difficult to fabricate in comparison to a microstrip feed patch antenna due to limitations in copper-etching accuracies. However, the performance of the CPW-fed patch antenna was observed to be better than the same shape and size microstrip feed patch antenna in terms of bandwidth and radiation patterns at high frequencies.

The radiation patterns of the proposed antennas are found to be near omni-directional at azimuthal plane at low frequencies, which get distorted at higher frequencies. The peak gain of the antennas has been observed to vary between 1 and 8 dBi for initial 90% of the BW and the last 10% shoots beyond 10 dBi.

For all designs, the simulated and measured results were mostly found matching with slight variation in resonance peaks, while maintaining the shape of return-loss graph. These variations may be due to:

- Manufacturing tolerances,
- Undercuts while etching copper at sharp corners,
- Effect of SMA connector at different frequencies, and
- Simulation software limitations, etc.

After studying the proposed microstrip patch antennas, it is concluded that circular and elliptical-shaped patches fed with stepped feed structure and partial ground can provide UWB operations up to several GHz. By proper optimisation and use of slots, improvement

in bandwidth can be achieved as seen in the first design of this work. The bandwidth of the antenna proposed by Jung, Choi and Choi was improved by 59% through proper optimisation and slight modification. All the ten patch antennas are compact and can be easily fabricated, suitable for wireless communication and spectrum-monitoring applications.

Based on different UWB microstrip monopole patch antenna designs, the following general conclusions can be drawn:

- Design of UWB microstrip monopole patch antenna from a few GHz to 40 GHz and beyond is feasible.
- Radiation patterns of the microstrip monopole patch antenna at lower frequencies are omni-directional, like an ideal monopole antenna which becomes directional at higher frequencies.
- The lower cut off frequency is mostly decided by the size of the radiating patch, while the higher frequency is decided by the optimisation of the actual shape, size, feeding techniques and most importantly the dimensions of the partial ground. Improvement in operating bandwidth is feasible by introducing suitable slots in the main radiating patch.
- For the same size of antenna, the shape of the radiating patch and the partial ground plane determine the total operating bandwidth. The operating bandwidth of a circular antenna is observed to be more than a rectangular one, while the maximum bandwidth was achieved by an elliptical radiating patch.
- CPW-fed microstrip antenna can provide better performance in terms of total bandwidth and radiation patterns at higher frequencies in comparison with a microstrip line-fed antenna.

5.2 Future Scope of Work

Different types of planar microstrip patch antennas have been presented in this thesis. Based on the proposed work and experience, the following work may be undertaken in the near future.

- All the ten designs discussed here are single patch antennas with low-to-moderate gain; they also become directional at higher frequencies. Phased array of patch antennas with suitable feed network may provide better gain and radiation pattern. However, designing a suitable UWB feed network will be a challenge.
- In future, new techniques may be explored to reduce the size of the UWB antennas to make them suitable for many future practical applications. Metamaterial is a promising candidate to further reduce the size greatly.
- Large quantum of research work is under progress on wearable microstrip antennas fabricated on curved surface for a particular application, designed for limited band. Design of UWB wearable patch antennas may be particularly useful for portable frequency monitoring applications and can be explored for research.
- In this thesis, default optimisation techniques available with HFSS have been used to optimise antenna performance. However, better optimum results might be possible by using specific algorithms like genetic algorithm (Whitley, 2018) and particle swarm optimisation (Kennedy and Eberhart, 1995), and others.

REFERENCES

- Abed, D., H. Kimouche and B. Atrouz. "Small-Size Printed CPW Fed Aantenna for Ultra-Wideband Communications." *Electronics Letters* (2008): 1003.
- Ahmed, O. and A.R. Sebak. "A Printed Monopole Antenna with Two Steps and a Circular Slot for UWB Applications." *IEEE Antennas and Wireless Propagation Letters* 7 (2008): 411–13.
- Alsath, M. Gulam Nabi and Malathi Kanagasabai. "Compact UWB Monopole Antenna for Automotive Communications." *IEEE Antennas and Propagation Society* 63.9 (2015): 4204–08.
- Anob, P.V., K.P. Ray and G. Kumar. "Wideband Orthogonal Square Monopole Antennas with Semi-Circular Base." *IEEE Antennas and Propagation Society International Symposium. 2001 Digest*. Held in conjunction with: USNC/URSI National Radio Science Meeting (Cat. No.01CH37229) (2001).
- Ansys HFSS 3D Electromagnetic Field simulator for RF and Wireless Design*. 15 Mar 2015.
<<http://www.ansys.com/products/%20electronics/ANSYS-HFSS>>.
- Chair, R., et al. "Miniature Wide Band Half U-Slot and Half E-Shaped Patch Antennas." *IEEE Transactions on Antennas and Propagation* 53.8 (2005): 2645-52.
- Chen, Hong-Twu. "Compact Circular Microstrip Antenna with Embedded Chip Resistor and Capacitor." *IEEE Antennas and Propagation Society International Symposium. Digest. Antennas* (1998): 1356-59.
- Clasen, G. and R. Langley. "Meshed Patch Antennas." *IEEE Transactions on Antennas and Propagation* 52 (2004): 1412-1416.

Coplanar Waveguide Calculator. 6 May 2017. <<https://www.microwaves101.com/calculators/864-coplanar-waveguide-calculator>>.

D'Assuncao, A.G., et al. "Theoretical and Experimental Investigation of Tapered Microstrip Antennas for Wireless Communications." *International Telecommunications Symposium* (2006): 461-63.

DeLisle, Jean-Jacques. *Millimeter Waves Enhance Military Projects*. 11 Aug 2014. <<http://www.mwrf.com/active-components/millimeter-waves-enhance-military-projects>>.

Deschamps, G. A. "Microstrip Microwave Antennas." *Proc. 3rd USAF Symposium on Antennas*. 1953.

Dikmen, Cengizhan M, Çakır Gonca and Çimen Sibel. "Planar Octagonal Shaped UWB Antenna with Reduced Radar Cross Section." *IEEE Transactions on Antennas and Propagation* 62.6 (2014): 2946–53.

Floc'h, J.M. and L. Desclos. "Surface Mounted Monopole Antenna." *Microwave Opt. Technol. Lett.* 16 (1997): 349-52.

Gang, Wen. "A Printed Dipole-Antenna With Tapered Slot Feed For Broad Band Phased Array Antenna." *IET International Radar Conference*. Guilin, China: IET, 2009. 16 Aug 2017.

Garg, R. et al. *Microstrip Antenna Design Handbook*. Artech House, 2001.

Gautam, Anil Kr., Swati Yadav and Vinod Kr. Kanaujia. "A CPW Fed Compact UWB Microstrip Antenna." *IEEE Antennas and Wireless Propagation Letters* 12 (2013): 151–54.

- Ge, Y., K.P. Esselle and T.S. Bird. "A Compact E Shape Patch Antenna with Corrugated Wings." *IEEE Transactions on Antennas and Propagation* 54.8 (2006): 2411-13.
- Guo, Yong-Xin, et al. "A Quarter Wave U-Shaped Patch Antenna with Two Unequal Arms for Wideband and Dual-Frequency Operation." *IEEE Antennas and Propagation Society International Symposium*. 50.8 (2002): 1082-87.
- Gupta, K.C., et al. *Microstrip Lines and Slotlines*. Norwood: , 2nd ed., Artech House, 1996.
- Gutton, H. and G. Baissinot. Flat Aerial for Ultra High Frequencies. Patent French Patent No. 70313. 1955.
- Herscovici, N. "A Wide-Band Single-Layer Patch Antenna." *IEEE Transactions on Antennas and Propagation* 46.4 (1998): 471-74.
- Howell, J.Q. "Microstrip Antennas." *IEEE APS Intl. Symposium Digest*. 1972.
- Wideband Omni-Directional VP Antenna. 18 Jun 2018.
["http://www.alarisantennas.com/product-category/monitoring/."](http://www.alarisantennas.com/product-category/monitoring/)
- Huang, C. Y. and W.C. Hsia. "Planar Elliptical Antenna for Ultra-Wideband Communications." *Electronics Letters* 41.6 (2005): 296-97.
- James, R., P.S. Hall and C. Wood. *Microstrip Antenna: Theory and Design*. Peregrinus on behalf of the Institution of Electrical Engineers, 2015.
- Jang, Y.W. "Broadband Aperture Coupled T-Shaped Microstrip Fed Triangular Patch Antenna." *Microw. Opt. Technol. Lett.* 31 (2001): 262-264.
- Jung, Jihak, Wooyoung Choi and Jaehoon Choi. "A Small Wideband Microstrip-Fed Monopole Antenna." *IEEE Microwave and Wireless Components Letters* 2005: 703-05.

- Kasabegoudar, V.G. and K.J. Vinoy. "Wideband Microstrip Antenna with Symmetric Radiation Patterns." *Microw. Opt. Technol. Lett.* 50 (2008): 1991–95.
- Kasi, Baskaran, Lee Chia Ping and Chandan Kumar Chakrabarty. "A Compact Microstrip Antenna for Ultra Wideband Applications." *European Journal of Scientific Research* 67.1 (2011): 45-51.
- Kennedy, J. and R.C. Eberhart. "Particle Swarm Optimization." *IEEE International Conference on Neural Networks*. Piscataway, NJ, 1995. 1942-48.
- Kim, Ki-Hak and Seong-Ook Park. "Design of the Band Rejected UWB Antenna with the Ring Shaped Parasitic Patch ." *Microw. Opt. Technol. Lett.* 48.7 (2006): 1310-13.
- Kingatua, Amos . *The Role of Millimeter Waves in Ever-Expanding Wireless Applications*. 18 Mar 2018. <www.allaboutcircuits.com/news/the-role-of-millimeter-waves-in-ever-expanding-wireless-applications/>.
- Koohestani, M., M.N. Moghadasi and B.S. Virdee. "Miniature Microstrip Fed Ultra-Wideband Printed Monopole Antenna with a Partial Ground Plane Structure." *IET Microwaves, Antennas & Propagation* 5.14 (2011): 1683.
- Kumar, Girish and K.P. Ray. *Broadband Microstrip Antennas*. Artech House, 2003.
- Lee, K. et al. "Experimental and Simulation Studies of the Coaxially Fed U-Slot Rectangular Patch Antenna." *IEE Proc. Microwaves, Antennas and Propagation* 144.5 (1997): 354.
- Li, Tong, et al. "Bandwidth Enhancement of Compact Monopole Antenna with Triple Band Rejections." *Electronics Letters* 52.1 (2016): 8-10.

- Liao, Samuel Y. *Microwave Devices and Circuits*. Englewood Cliffs, New Jersey: Pentice Hall, 1989.
- Lim, K. S., M. Nagalingam and C.P. Tan. "Design and Construction of Microstrip UWB Antenna with Time Domain Analysis." *Progress in Electromagnetics Research* (2008): 153–164.
- Liu, L., et al. "A Compact Circular Ring Antenna for Ultra-Wideband Applications." *Microw. Opt. Technol. Lett.* 53.10 (2011): 2283–88.
- Liu, Yuan-Fu, Peng Wang and Hao Qin. "Compact ACS Fed UWB Monopole Antenna with Extra Bluetooth Band." *Electronics Letters* 50.18 (2014): 1263–64.
- Lo, Y. et al. "Theory and Experiment on Microstrip Antennas." *IEEE Transactions on Antennas and Propagation* 19.2 (1979): 137–145.
- Long, S.A., L.C. Shen and P.B. Morel. "Theory of the Circular Disc Printed Circuit Antenna." *Proceedings of the Institution of Electrical Engineers*. 1978. 925–28.
- Mokhtaari, Marjan and Jens Bornemann. "Ultra-Wideband Microstrip Antenna with Coupled Notch Circuit." *Proc. of the 5th European Confrence on Antenna and Propagation(EUCAP)*. Rome, Italy, 2011, 1521-1525.
- Mazhar, W., et al. "Compact Microstrip Patch Antenna for Ultra-Wideband Applications." *PIERS Proceedings* (2013): 1100-04.
- Mazhar, Waqas, David Klymyshyn and Aqeel Qureshi. "Log Periodic Slot Loaded Circular Vivaldi Antenna for 5–40 GHz UWB Applications." *Microwave Opt. Technol. Lett.* 59 (2017): 159-63.
- Meinel, Holger H. "Millimeter Wave Applications and Technology Trends." *Annales Des Télécommunications* 47.11-12 (1992): 456–68.

Microstrip line impedance Calculator. 04 Apr 2016. <<http://www.rfwireless-world.com/calculators/Microstrip-line-impedance-calculator.html>>.

Millimeter Waves Enhance Military Projects. 17 Jul 2017. <<https://www.mwrf.com/active-components/millimeter-waves-enhance-military-projects>>.

Mulgi, S.N., et al. "A Compact Broadband Gap Coupled Microstrip Antenna." *Indian Journal of Radio and Space Physics* 33 (2004): 139-141.

Munson, R. "Conformal Microstrip Antennas and Microstrip Phased Array." *IEEE Transactions on Antennas and Propagation* 22.1 (1974): 74–78.

Munson, R. E. Single Slot Cavity Antennas Assembly. U.S.: Patent 3713162. 23 Jan 1973.

Nashaat, Dalia, et al. "Ultrawide Bandwidth 2X2 Microstrip Patch Array Antenna Using Electromagnetic Band-Gap Structure(EBG)." *IEEE Transactions on Antenna and Propagation* 59.5 (2011): 1528-34.

Pozar, D. "Radiation and Scattering from a Microstrip Patch on a Uniaxial Substrate." *IEEE Transactions on Antennas and Propagation* 35.6 (1987): 613-21. 2018.

Pozar, David M. *Microwave Engineering* . Singapore: Wiley & Sons, Inc, 2012.

R&S®ESMD Wideband Monitoring Receiver . Rohde & Schwarz. 2017. <https://www.rohde-schwarz.com/in/product/esmd-productstartpage_63493-9558.html>.

Rafi, G. and L. Shafai. "Wideband V-Slotted Diamond-shaped Microstrip Patch Antenna." *Electronics Letters* 2004: 1166.

- Rambabu, K. , H. A. Thiart and J. Bornemann. “Ultrawideband Printed Circuit Antenna.” *IEEE Transactions on Antenna and Propagation* 54.12 (2006): 3908-11.
- Rambabu, K., et al. “Ultrawideband Printed Circuit Antenna.” *IEEE Journals & Magazines* 54.12 (2006, Volume: 54, Issue: 12): 3908 - 11.
- Richards, W.F. “Microstrip Antennas.” Lo, Y. and S.W. Lee. *Antenna Handbook Theory, Applications, and Design*. Vol. 1. Springer Verlag, 1988. 10.1.
- Richards, W.F., Y.T. Lo and D.D. Harrison. “Improved Theory for Microstrip Antennas.” *Electronics Letters* 15.2 (1979): 42.
- Ritu and Krishan Sherdia. “Microstrip Antenna Design for UWB.” *International Journal of Advanced Research in Computer and Communication Engineering* 2.10 (2013): 3825-28.
- Roy, J.S. and J. Ghosh. “A Multi Frequency Microstrip Antenna.” *Microw. Opt. Technol. Lett.* 46 (2005): 63-65.
- Sadat., S. et al. “A Compact Microstrip Square-Ring Slot Antenna for UWB Applications.” *Progress In Electromagnetics Research*. 2006. 4529-32.
- Sarkar, Debdeep, Vaibhav Kumar Srivastava and Kushmanda Saurav. “A Compact Microstrip-Fed Triple Band-Notched.” *IEEE Antennas and Wireless Propagation Letters* 13 (2014): 396-99.
- Shagar, Arumugam Chellamuthu and Shaik Davood Wah. “Novel Wideband Slot Antenna Having Notch Band Function for 2.4 GHz WLAN and UWB Applications.” *International Journal of Microwave and Wireless Technologies* 3.4 (2011): 451-58.
- Simons, Rainee N. *Coplanar Waveguide Circuits, Components, and Systems*. John Wiley & Sons, 2004.

Singh, L.L.K., et al. "A Novel Versatile Multiband Rectangular Patch Antenna." *Microw. Opt. Technol. Lett.* 52.6 (2010): 1348-53.

Singh, R. K. and Dhaval A. Pujara. "A Novel Design of Ultra-wideband Quarter Circular Microstrip Monopole Antenna." *Microw. Opt. Technol. Lett.* 59.2 (2016): 225-29.

Singh, R. K. and Dhaval A. Pujara. "Design of an UWB (2.1–38.6 GHz) Circular Microstrip Antenna." *Microw. Opt. Technol. Lett.* 59 (2017): 2757-62.

Singh, R. K. and Dhaval A. Pujara. "Design and Development of UWB (3.0–42.8 GHz) Truncated Annular Microstrip Monopole Antenna." *Microw. Opt. Technol. Lett.* 60 (2018): 1581-84.

Singh, R. K. and Dhaval A. Pujara. "Design of Goblet Shape UWB Microstrip Monopole Antenna." *Proceedings of International Symposium on Antennas and Propagation (APSYM 2016)*. 179-182.

Singh, R. K. and Dhaval A. Pujara. "A Novel Circular Ultra-Wide Band Microstrip Antenna Design using Slots, Stepped Microstrip Feed and Partial Ground." *International Symposium on Antennas and Propagation (APSYM 2016)*. 15-17 Dec 2016, Cochin, India.

Sobol, H. "Radiation Conductance of Opencircuit Microstrip." *IEEE Trans. Microwave Theory Technol.* (1971): 885-87.

"Spectrum Monitoring and Compliance." 17 Jan 2017.
<<http://cra.gov.qa/en/document/automated-frequency-management-system-afms>>.

Srifi, Mohamed Nabil, et al. "Planar Circular Disc Monopole Antennas Using Compact Impedance Matching Networks for Ultra-Wideband (UWB) Applications." *Asia Pacific Microwave Conference*. 2009. 782 - 85.

The Role of Millimeter Waves in Ever-Expanding Wireless Applications.
07 Jan 2018. <<https://www.allaboutcircuits.com/news/the-role-of-millimeter-waves-in-ever-expanding-wireless-applications>>.

Tong, Wei and Z. R. Hu. "A CPW Fed Circular Monopole Antenna for Ultra Wideband Wireless Communications." *IEEE Antennas and Propagation Society International Symposium* (2005): 528-31.

Vera, G. A. et al. "Design of a 2.45 GHz Antenna for Electromagnetic (EM) Energy Scavenging." *IEEE Radio and Wireless Symposium* (Mar 2010): 61-64.

Whitley, Darrell . "Introduction to Optimization with Genetic Algorithm." 28 Mar 2018. <<https://www.kdnuggets.com/2018/03/introduction-optimization-with-genetic-algorithm.html>>

Wong, K.L. and H.C. Tung. "An Inverted U-Shaped Patch Antenna for Compact Operation." *IEEE Transactions on Antennas and Propagation* 51 (2003): 1647 – 48.

Wong, Kin-Lu and Jia-Y Sze. "Slotted Rectangular Microstrip Antenna for Bandwidth Enhancement." *IEEE Transactions on Antennas and Propagation* 48.8 (2000): 1149-52.

Wong, Kin-Lu and Wen-Hsiu Hsu. "A Broadband Patch Antenna with Wide Slit." *IEEE Antennas and Propagation Society International Symposium. Transmitting Waves of Progress to the Next Millennium* (2000).: 1414-17.

Wong, Kin-Lu and Yi-Fang Lin. "Small Broadband Rectangular Microstrip Antenna with Chip-Resistor Loading." *Electronics Letters* 33.19 (1997): 1593.

- Wu, Qi, R. Jin and J. Geng. "Ultra-wideband Quas Circular Monopole Antennas with rectangular and Trapezoidal Grounds." *IET Microwaves, Antennas & Propagation* 3.1 (2009): 55.
- Xiao, Shaoqiu, et al. "Bandwidth Enhancing Ultra low Profile Compact Patch Antenna." *IEEE Transactions on Antennas and Propagation* 53.11 (2005): 3443-47.
- Yaccoub, M.H. Diallo, et al. "Rectangular Ring Microstrip Patch Antenna for Ultra-wide Band Applications." *International Journal of Innovation and Applied Studies* 4.2 (2013): 441-446.
- Zhang, M., et al. "A Racket Shaped Slot UWB Antenna Coupled with Parasitic Strips for Band Notched Application." *Progress in Electromagnetics Research Letters* 16 (2010): 35-40.
- Zhiyong, Li, et al. "A Novel Miniature UWB Microstrip-fed Antenna with L-Shape Ground." *Proc. International Symposium on Intelligent Signal Processing and Communication Systems*. 2010. 1-4.